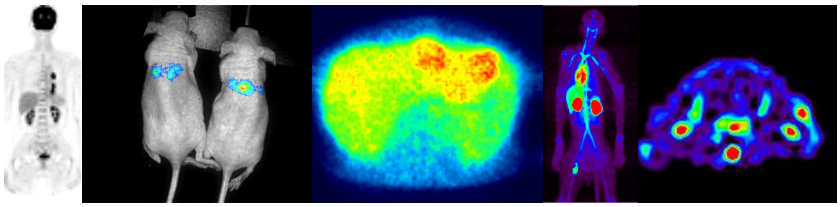

European Society for Molecular Imaging

ESMI FIRST INTERNATIONAL CONFERENCE

MUSEUM NATIONAL D'HISTOIRE NATURELLE

Grand Amphithéâtre du Muséum

PARIS

MAY 17-19, 2006

DiMI Diagnostic Molecular Imaging

European Molecular Imaging Laboratories

ileDeFrance

INSTITUTIONAL AND INDUSTRIAL PARTNERS

The organisers of the conference are grateful for the support of the following partners:

INSTITUTIONAL PARTNERS

EMIL NOE	
DIMI NOE	
CONSEIL REGIONAL ILE DE FRANCE	
CEA – DIRECTION DES SCIENCES DU VIVANT	

INDUSTRIAL PARTNERS

PLATINIUM SPONSORS

BIOSPACE Lab	
GENERAL ELECTRIC HEALTHCARE	
PHILIPS	

GOLDEN SPONSORS

SIEMENS	SIEMENS

SILVER SPONSORS

BRUKER	BRUKER
Mauna kea technologies	MKT Mauna Kea Technologies
SCHERING	SCHERING making medicine work
SKYSCAN	SKYSCAN®
XENOGEN	XENOGEN® Life. Changing.™

SPONSORS

GUERBET	Guerbet
MINERVE	EQUIPEMENT VETERINAIRE MINERVE
VisualSonics	VISUALSONICS

SOMMAIRE

PROGRAMME

Wednesday May 17

16:00-18:00 **ESMI Poster session - INSTN - Saclay**

21:00 **Speakers' Dinner at the restaurant of the Eiffel Tower**

Tuesday May 18

8:30 Registrations - Grand Amphitheatre du Museum

9:00 – 10:15 Inaugural Session
Chair: Andreas Jacobs, Clemens Lowik.

9:00 Welcome - Presentation of ESMI: Structuring the Molecular Imaging Community in Europe and in the World
Bertrand Tavitian, President ESMI, CEA, France.

9:10 Keynote Lecture: Molecular Imaging: A field in development
Ronald Blasberg, Sloan Kettering Institute, USA.

9:50 – 11:20 Molecular Imaging: State of the art and perspectives
Chair: André Syrota, Silvana Del Vecchio.

9:50 Cell Biology and Development
Carsten Schulz, EMBL, Germany.

10:05 Molecular Imaging in Cancer
Juri Gelovani, University of Texas, USA.

10:20 - 10:50 Coffee break

10:50 Molecular Imaging in Cardiology
Markus Schwaiger, University of Munich, Germany.

11:05 Molecular Imaging in Neurodegenerations
David Brooks, Imperial College, UK.

11:20 – 12:05 Molecular Imaging: FP6 Projects for Health
Chair: Frank Roesh, Juri Gelovani.

11:20 EU Cancer research: from FP6 to FP7
Maria Vidal, DG Research, EC, Belgium.

11:35 Presentation of EMIL
Bertrand Tavitian, EMIL Coordinator, CEA, France.

11:50 Presentation of DiMI
Andreas Jacobs, DiMI Coordinator, KUK, Germany.

12:05 – 14:00 Lunch: Pique nique in the Jardin des Plantes

12:05 – 13:00 Press conference

Tuesday May 18 (pm)

14:00 – 15:45 Molecular Imaging: FP6 Projects for Health
Chair: Uwe Haberkorn, Arend Heerschap.

14:00 MI Integrated Project: Integrated Technologies for in-vivo molecular Imaging.
Jorge Ripoll, MI Coordinator, Forth, Greece.

14:15 Presentation of BioCare
Anders Brahme, Karolinska Institute, Sweden.

14:30 Presentation of eTUMOR
Bernardo Celda, University of Valencia, Spain.

Chair: Terry Jones, Andre Merbach.

14:45 The European Institute for Biomedical Imaging Research: An Infrastructure for Multidisciplinary Cooperation
Gabriel .P. Krestin, EAR, the Netherlands.

15:00 Molecular Imaging and the European Association of Nuclear Medicine
Ignasi Carrio, University of Barcelona, Spain.

15:15 Presentation of ISMRM
Chrit Moonen, University of Bordeaux, France.

15:30 COST initiatives in the fields of contrasts agents, radiopharmaceuticals, and molecular imaging.
Silvio Aime, University of Turin, Italy.

15:45 – 16:15 Coffee break

16:15 – 18:00 Molecular Imaging – The public health/societal/economic perspectives
Chair: J. Clark, Adriana Maggi

16:15 Impact of Molecular Imaging for Patients
Bengt Langstrom, University of Uppsala, Sweden.

16:30 Developments in the Industry
- **16:30** Trends in mMRI
  Robert Krieg, Siemens, Germany.
- **16:45** Imagine the future : Molecular Imaging at Philips
  Sjaak Deckers, the Netherlands.
- **17:00** Molecular Imaging, a critical step towards Early Health
  Jean- Luc Vanderheyden, GE healthcare, USA.

17:15 SMEs in the development of Molecular Imaging
- **17:15** Molecular Imaging tools : innovation at high pace
  Marie Meynadier, Biospace Lab, France.
- **17:30** Cellvizio®: a unique technology platform in the Field of *In Vivo* Molecular Imaging.
  Benjamin Abrat, Mauna Kéa Technologies, France.
- **17:45** SkyScan 1178: A fast micro-CT scanner for combination with other imaging modalities
  Elke Van de Casteele, Skyscan, Belgique.

19:00 Visite of the Grande Galerie de l'Evolution

20:00 Cocktail Dînatoire at the Grande Galerie de l'Evolution sponsored by GE Healthcare

Friday May 19

8:30 Registrations - Grand Amphithéâtre du Museum

9:00 – 10:00 Molecular Imaging – a global perspective
Chair: Ron Blasberg, Gitte Knudsen.

9:00 Physics, Chemistry and Biology to achieve a ten-fold increase in signal to background in PET
Thomas Budinger, Lawrence Berkeley Natl Lab, USA.

9:30 Progress and Prospective of Molecular Imaging in Taiwan
Ren-Shyan Liu, Yang- Ming University Medical School, Taiwan.

09:45– 10:15 Coffee break

10:15 – 11:15 Hot Topics in Molecular Imaging
Chair: Robert Muller, Klaas Nicolay.

10:15 MRI of angiogenesis: revealing cellular recruitment, enzymatic activity and gene expression
Michal Neeman, Wiezmann Institute, Israel.

10:35 Dynamic optical imaging of Tumour invasion
Peter Friedl, University of Wuerzburg, Germany.

10:55 In vivo imaging of aptamers
Frederic Ducongé, CEA, France.

11:15 – 12:35 Hot Topics in Molecular Imaging
Chair: Denis Guilloteau, Helmut Maecke

11:15 Looking in Tissues with Fluorescence Molecular Tomography
Vasilis Ntziachristos, Harvard Medical School, USA.

11:35 Imaging of Calcium Signalling
Kelly Rogers, Pasteur Institute, France.

11:55 Perspectives of Molecular MR Imaging in Experimental Neurology
Mathias Hoehn, MPI Cologne, Germany.

12:15 In vivo MRI of songbird brain: neuronal circuitry assessment in extreme model of neuroplasticity
Annemie Van der Linden, University of Antwerp, Belgium.

12:35 Questions and answers

13:00 ESMI General Assembly

13:30 End of the Conference.

CONFERENCES

Molecular Imaging Overview: Where did we start?; Where are we now?; Where will we be in 5+ years?.

Ronald Blasberg

Memorial Sloan-Kettering Cancer Center; New York

Molecular-genetic imaging in living organisms has its roots in the remarkable advances in cell and molecular biology that have occurred during the past two decades. Several different imaging technologies (optical, magnetic resonance, nuclear) developed more or less in parallel, but were initially independent of each other. It is the biological base and the need to optimize the advantages and avoid the disadvantages of the three major imaging modalities that brings the different imaging technologies together. In the US, funding initiatives by the NCI in the late 1990's identified cancer imaging as being one of six extraordinary scientific opportunities that led to the creation of two major programs: the Small Animal Imaging Resources Program (SAIRP) and the In Vivo Cellular and Molecular Imaging Centers (ICMIC) program. Both programs continue to be funded by NCI, and other NIH institutes have created similar funding initiatives. A somewhat corresponding network of European Molecular Imaging Laboratories (EMIL) was established within the EU in 2004, as well as the Diagnostic Molecular Imaging (DiMI) network in 2005.

Current imaging strategies are based on "direct" or "indirect" assessments of molecular-genetic processes, as well as on "bio-marker" or "surrogate" imaging. Direct radiotracer imaging of thyroid function is probably the oldest example of imaging molecular targets, and is founded on the radiotracer principle, first described by George de Hevesy. The tracer technique has been adapted for many applications in physiology and biochemistry, as well as in biomarker/surrogate imaging. More recently, "indirect" reporter imaging in animals (and now in patients) has been developed. Constitutive reporter systems are being used to monitor gene therapy vectors, the efficacy of gene targeting and transduction, the growth, metastases and response of tumor cells to treatment, as well as to monitor adoptive cell-based therapies, including stem cells. Alternatively, reporter systems can function as molecular "sensors" and regulate reporter gene expression in response to endogenous cell processes. These inducible reporter systems are being used to monitor specific intracellular molecular-genetic events and the activity of signaling pathways. This strategy has been widely applied in radionuclide-based and optical imaging, and to a lesser degree in magnetic resonance (MR) imaging.

Optical-based (bioluminescence and fluorescence) reporter and direct imaging systems have been shown to be particularly advantageous in small animals (mice), because of their operational simplicity and relatively low-cost. Although optical imaging has significant limitations related to the scatter and absorption of photons, which limits depth of view and quantification, these issues are now being addressed and some progress has been achieved. The translation of optical imaging strategies to patient studies remains far more problematic. Radiotracer- and MR-based molecular imaging are likely to remain the major modalities that are translated into clinic studies in the foreseeable future.

A novel platform to image kinase activities in cells

Carsten Schultz, Justin Brumbaugh, Christiane Jost, Andreas Schleifenbaum

EMBL Heidelberg, Meyerhofstr. 1, 69117 Heidelberg, Germany

Imaging intracellular enzyme activities by fluorescence resonance energy transfer (FRET) and/or protein translocation has become available for a number of key signaling events. However, the development of efficient sensors is tedious. Therefore, FRET reporters have only been generated for the most prominent enzymes. Here, we report on a novel approach for real-time imaging based on the PKC substrate pleckstrin that opens the possibility to create sensors for a wide array of kinases all sharing the same reporter scaffold. In addition, a single construct can be used to follow two kinase activities simultaneously and responds with opposite FRET readouts for each activity. These designs have become available through close collaboration with structural biologists, namely the NMR group of Michael Sattler at EMBL, who provided crucial structural data for the reporter design.

Animal Models for Molecular Imaging of Cancer.

Juri G. Gelovani, MD, PhD. MD Anderson Cancer Center, Houston, TX.

Molecular-genetic imaging can be defined as the non-invasive visualization of normal, as well as abnormal, cellular processes at molecular–genetic, signal transduction and metabolic levels. Molecular imaging is deeply rooted in chemistry, molecular and cellular biology, genetics, as well as different imaging technologies. Such 'cross-fertilization' of various disciplines has generated a strong driving force for rapid advances in this new and exciting field. Novel molecular-genetic and cellular imaging methods add both spatial and temporal dimensions to the established molecular–biological in situ assays. Versatile and sensitive non-invasive imaging assays that do not require tissue biopsies are becoming extremely important for monitoring different molecular–genetic, signalling and metabolic processes involved in oncogenesis, progression, and maintenance of cancer. Such imaging assays require a multitude of novel target-specific imaging probes labelled with various radionuclides for gamma camera and PET imaging, different magnetic labels for MR imaging, or fluorescent tags for minimally invasive confocal endo-microscopic imaging. Several molecular-genetic reporter systems have been developed for pre-clinical imaging in cancer models in small animals. Reporter genes for multi-modality imaging with fluorescence, bioluminescence, and radiotracer or MR imaging provide a cost-effective solution for monitoring the dynamics of various signal transduction pathways in tumors during tumor development or response to therapy. Animal tumor models bearing these multi-modality reporter systems facilitate the evaluation of novel molecular imaging probes that directly visualize the expression and activity of specific signalling proteins involved in oncogenic and maintenance pathways. Repetitive imaging of these reporter tumor models during the course of therapy provides unique information about the spatial and temporal dynamics of target pathway activity. Already, several molecular imaging methods have been developed for monitoring tumor targeted gene therapies using cell specific, replication-conditional and drug-controlled expression systems. Also, molecular imaging is being rapidly becoming an integral part of different cancer immunotherapies and adoptive cell therapies. It is conceivable, that in combination with novel genomic and proteinomic biomarkers for cancer screening, non-invasive molecular imaging could help early cancer detection and monitoring of anti-cancer therapies by pin-pointing the location of various genetic, signal transduction, and biochemical abnormalities that lead to malignant transformation and preferential survival of malignanices.

Molecular Imaging in Cardiology

Markus Schwaiger, Takahiro Higuchi, Hans-Jürgen Wester

Technische Universität München

Cardiac imaging has matured to an important research and clinical tool in characterizing cardiovascular diseases. The introduction of metabolic tracers in combination with PET have lead to a wide spread clinical acceptance of the delineation of viable myocardium in patients with advanced coronary artery disease. Cardiac innervation can be visualized with tracer approaches evaluating the integrity of presynaptic catecholamine transporters and postsynaptic receptors and may play on clinical role in assessing prognosis of patients with heart failure and arrhythmias.
The experimental use of reporter gene imaging has shown to identify the regional expression of genes in the animal model and can be used in combination with therapeutic approaches to monitor the location and extent of gene expression. The combined application of therapeutic and reporter genes may provide unique tools to monitor gene therapy.
More recently reporter gene imaging has been employed to label stem cells and to use this imaging approach to follow survival and migration of transplanted cells in the animal model.
It is hoped that such probes can be used to monitor the differentiation of cells using tissues specific promoters.
Besides imaging approaches characterizing myocardial tissue, vascular imaging probes have been developed to delineate atherosclerotic plaques. Markers for inflammation such as FDG and MMP inhibitors have shown higher uptake in areas of experimental and clinical plaques.
Future studies have to demonstrate that these promising experimental approaches can be translated in to the clinical environment. Multimodality imaging such as PET/CT and SPECT/CT will provide co registration of signals with high biologic specificity with morphologic information provided by MR or CT imaging.
Molecular imaging in the heart will not be only of diagnostic value, but is hoped to support new therapeutic approaches by monitoring therapeutic effects on vascular biology.

Molecular Neuroimaging

David J Brooks MD DSc FRCP FMedSci

MRC Clinical Sciences Centre and Division of Neuroscience, Faculty of Medicine, Imperial College London

Molecular neuroimaging can play a valuable role in confirming diagnosis of diseases and detecting subclinical dysfunction in at-risk subjects. A number of disease modifying agents are now entering trials as putative neuroprotective agents. Molecular imaging can be used as an objective biomarker to determine the functional consequences of administering such agents. However, while functional imaging can be informative, it cannot yet be used as a surrogate marker of disease outcome.

Peripheral benzodiazepine sites are not normally expressed in the central nervous system unless microglia become activated. 11C-PK11195 PET detects activated microglia in a range of neurological disorders and provides a potential means of measuring the anti-inflammatory effects of neuroprotective agents.

PET has long been used to derive in vivo brain dose-occupancy curves for novel drugs and provide proof of concept. More recently, it has become clear that PET can indirectly detect endogenous neurotransmitter release during pharmacological and cognitive challenges by measuring changes in receptor availability. In the future, PET is likely to be increasingly used to demonstrate the functional effects of novel drugs as well as to determine their binding profiles possibly helping to separate treatment reponders from non-responders.

The European network of excellence EMIL

Bertrand TAVITIAN, CEA / SHFJ, France

The network of excellence EMIL (European Molecular Imaging Laboratories) is the only European network of excellence in molecular imaging for oncology. It was set up and is coordinated by the '*in vivo* imaging of gene expression' group of CEA Orsay.

Included in Priority Thematic Area 1 (life sciences, genomics and biotechnology for health) of the European Commission's 6th Framework Programme for Research and Technological Development (FP6), this five-year project (2004-2009) aims to merge the leading European research teams in molecular imaging, in universities, research centres and small and medium enterprises, to focus on early diagnosis, prognosis and therapeutic evaluation of cancer.

The EMIL network brings together 58 partners representing 43 bodies in 13 European countries, and integrates 6 technological facilities: Orsay (France), Turin (Italy), Cologne (Germany), Leiden (Netherlands), Milan (Italy) and Antwerp (Belgium).

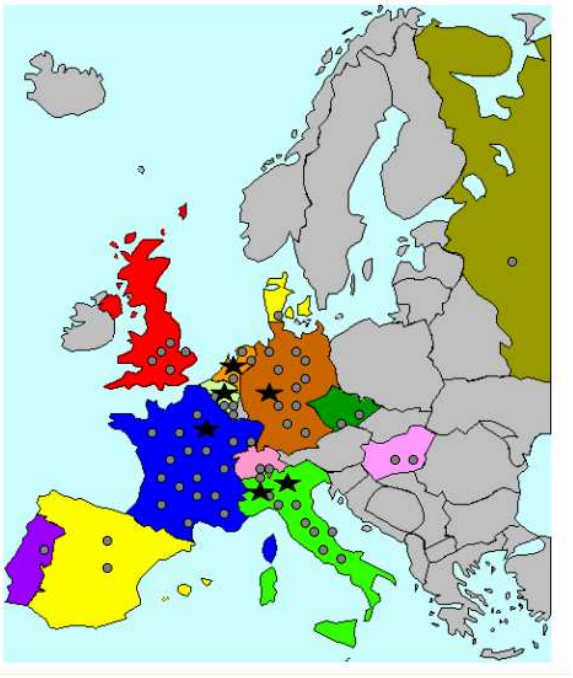

The research and training activities of the EMIL network are based on 9 thematic working groups or 'work packages' (wp), forming a **common activity programme** including:

- Integration activities: creation of a network of technological and training facilities favouring the mobility of researchers and the integration of small and medium enterprises into the EMIL network.
- Dissemination of expertise activities: training, communication, common knowledge management and intellectual property rights.

- Research activities: a common research programme with a horizontal dimension, making use of methodological tools of physics, biology and chemistry necessary for the further development of molecular imaging (instrument techniques, molecular probes, biological engineering), and a vertical integrative dimension, bringing together cancer imaging applications (early diagnostic imaging, development of new therapies, imaging for drug development).

Diagnostic Molecular Imaging: A European Network of Excellence for the development of new molecular imaging strategies aiming to improve the diagnostic and therapy of human diseases

Andreas Jacobs

The DiMI network of Excellence for Identification of new imaging markers for diagnostic purpose had been initiated and has been coordinated by Andreas Jacobs, MD at the Department of Neurology, University of Cologne and Head of the Laboratory for Gene Therapy and Molecular Imaging at the MPI for Neurological Research.
Situated under the first thematic priority “Lifesciences, genomics and biotechnology for health” of the sixth Research Framework Programme, this project runs for a five year period (2005-2010) and aims at bringing together genome-oriented scientists with the various actors of imaging science and clinicians dedicated to formulate novel diagnostic methods based on imaging.

The **main objective of the DiMI project is the creation of a Network of Excellence:**

- to integrate multidisciplinary research aiming towards the development of new probes and novel multimodal non-invasive imaging technology for early diagnosis, assessment of disease progression and treatment evaluation of diseases of the central nervous, cardiovascular and immune system;
- to achieve efficient training of young researchers, dissemination of new common knowledge and integration of SMEs and industry;
- to reach the European leadership role in topics related to molecular imaging for diagnostic purpose especially with respect to the creation of common data platforms, standards and guidelines.

To reach these objectives a unique **multi-disciplinary consortium** has been brought together with all necessary expertise and know-how spanning the fields of physics, instrumentation physics, bioinformatics, chemistry and radiochemistry, biochemistry, molecular biology, as well as various clinical specialties relating to neurosciences, cardiology, radiology and nuclear medicine.

The **DiMI Network integrates 55 groups from thirteen European countries** from the field of molecular imaging. With their intellectual excellence and critical mass the DiMI Network will reach a durable integration into the European Research Area (ERA) and gain European leadership in the creation of common data platforms and relevant standards and guidelines in terms of molecular imaging for diagnostic purposes.

Presentation of the Molecular Imaging Integrated Project

Jorge Ripoll

Institute of Electronic Structure & Laser – FORTH -Heraklion, Crete

An overview of the Integrated Project MOLECULAR IMAGING will be presented, whose goal is to generate and apply novel advanced technology for non-invasive imaging of biomolecular function in living systems ranging from single cells to whole animals. Main areas for technological innovation are i) generation of new biosensors enabling novel ways of functional contrast, ii) improving resolution of microscopic and tomographic imaging systems, and iii) creating new multimodal imaging setups combining different contrast modes.

To achieve this goal the Molecular Imaging project brings together a unique consortium of leading research groups in Europe combining a) engineers, experimental and theoretical physicists (who design new and improved, tomographic and microscopic imaging devices for in vivo-imaging); b) bioorganic chemists and molecular biologists (for the design of new chemical and genetic encoded molecular probes and biosensors); and c) biologists examining fundamental questions at the cell, organ and whole animal level (thereby providing the above research the appropriate and relevant goals for the technological innovation).
Some of the novel research and results obtained in the field of whole animal and cellular imaging will be presented, together with an overview of the project.

BioCare and the Use of PET for In Vivo Predictive Assay and Dose Delivery Imaging in Biologically Optimized Radiation Therapy

Anders Brahme

Medical Radiation Physics, Department of Oncology-PathologyKarolinska Institutet
Box 260, SE 171 76 Stockholm, Sweden

Background. BioCare is an acronym for Molecular Tumor Imaging for Biologically Optimized Cancer Therapy. The project covers a broad range of topics in tumor imaging from design of new detectors to the development of new pharmaca, hypoxia and apoptosis imaging as well as PET-CT-simulation and biological treatment planning based on PET. The presentation will give a very brief overview as well as illustrating some new diagnostic approaches of clinical importance, specially in Radiation Therapy. The fast development of intensity, energy and radiation quality modulated radiation therapy (IMRT and QMRT) during the last two decades with photon and electron beams has resulted in a considerable improvement of radiation therapy, particularly when combined with radiobiologically based treatment optimization techniques. This development and the recent development of advanced tumor diagnostics based on PET-CT imaging of tumor clonogen density and hypoxia opens the field for new powerful radiobiologically based treatment optimization methods. The ultimate step is to use the unique radiobiological and dose distributional advantages of IMRT and light ion beams for truly optimized bioeffect planning where the integral 3-dimensional dose delivery and tumor radiation responsiveness can be monitored early on in the treatment by PET-CT imaging and be corrected by adaptive therapy optimization methods.

Purpose. The main purpose of this paper is, to illustrate some principal areas of development of therapy optimization considering the whole therapy chain from tumor diagnostics and patient fixation through therapy planning and treatment optimization to the repeated treatment setups and dose delivery on a patient that hopefully has a shrinking tumor and may loose weight. Finally, it is the integral dose delivery and the biological effect distribution that matters so the shaping of the optimal incident beams is a truly complex inverse problem, which is hard to solve by such crude approaches as a prescribed point dose to the planning target volume.

Methods. The background indicates that BIologically Optimized Adaptive Radiation Therapy (BioArt) is really the ultimate way to perform high precision radiation therapy using checkpoints on the integral dose delivery and the tumor response, and based on this information, performing compensating corrections of the dose delivery. By using biologically optimized scanned high energy photon or ion beams it is possible to measure in vivo the 3-dimensional (3D) dose delivery using the same PET-CT camera that was used for diagnosing the tumor spread. This method thus opens up the door for truly 3D biologically optimized adaptive radiation therapy where the measured dose delivery to the true target tissues can be used to fine adjust the incoming beams so that possible errors in the integral therapy process are practically eliminated towards the end of the treatment. Interestingly enough all major error sources can be corrected for in this way such as organ motions, treatment planning errors, patient setup and tumor responsiveness errors, as well as dose delivery problems due to gantry, multileaf or scanning beam errors. Since it is possible to quantify the surviving tumor clonogen density after the first week or so of therapy, this information can be used to account for uncertainties in the biological responsiveness of the tumor and really cover all clinical uncertainties at the same time as more accurate dose response data can be derived from the treatment. With the photonuclear or nuclear-nuclear reactions the response of the PET-CT camera is related to the truly delivered integral dose with correct temporal averaging, thus if only small errors are seen, it is sufficient to adjust the last few treatment fractions. Thus, when using PET-CT tumor response monitoring, it is even possible to account for the uncertainty in known historical biological response for the disease of the patient and perform a truly optimized radiation treatment.

Results. Examples of in Vivo dose delivery and radiation resistance measurements using PET & PET-CT imaging are presented. Using recently available biologically based treatment optimization algorithms it is possible to improve the treatment outcome for advanced tumors by as much as 10 – 40% using PET-CT imaging and the BioArt approach with high energy photons and even more with light ions.

Web accessible MR decision support system for brain tumour diagnosis and prognosis, incorporating in vivo and ex vivo genomic and metabolic data (FP6-2002-LIFESCIHEALTH 503094); Acronym: eTUMOUR.

Bernardo Celda, University of Valencia - Spain

Diagnosis and treatment of brain tumours is based on clinical symptoms, radiological appearance, and often a histopathological diagnosis of a biopsy. However, treatment response of histological or radiologically similar tumours can vary widely, particularly for childhood tumours. New technologies are available that may improve tumour classification in terms of diagnosis and prognosis, and may allow individually optimized treatments. ^{1}H Magnetic Resonance Spectroscopy (MRS) is a non-invasive technique for determining tissue biochemicals (the metabolomic profile). ^{1}H MRS can be performed along with clinical MR Imaging but widespread use is hampered by specialised analysis requirements and poor dissemination of the skills needed to interpret the data. The genomic profile of tumours can be determined with DNA microarrays. Early studies have demonstrated differences in gene expression between tumour grades and between tumour types not easily distinguished by morphologic appearance.

We will bring together the expertise required to study the genomic and metabolomic characteristics of brain tumours, with a multi-centre collaboration to acquire statistically significant data, particularly for rare tumour types. Clinical MRS, high-resolution ^{1}H MRS and gene array analysis of biopsies, will be used to investigate how metabolomic and genomic profiles relate to clinically relevant factors such as survival time and treatment response. As well as providing new scientific data on tumour biology, we will develop the technology for this information to be readily and easily used to help radiologists and neurosurgeons in the management and treatment of brain tumour patients. We will build upon expertise obtained with INTERPRET EU project IST-1999-10310, which created a MRS decision support tool (DSS) for tumour diagnosis. A new web-accessible DSS will be developed, incorporating genomic and metabolomic data, and its diagnostic performance validated in a clinical demonstration of added value.

The European Institute of Biomedical Imaging Research (EIBIR)

Prof. Dr. Gabriel P. Krestin, MD, PhD,

Erasmus MC, University Medical Center Rotterdam - The Netherlands

As bio-medical imaging technology moves forward into the 21st century, it has become 'one of the core disciplines of medicine today' as more and more diseases are being diagnosed and treated with these non-invasive technologies and more sophisticated imaging equipment is invented. One of the key problems that European researchers in bio-medical imaging technologies face is a lack of access to existing infrastructures (i.e., HF-MRI, MEG, animal imaging facilities) or even the lack of knowledge of existing infrastructures. Also due to a lack of communication very few joint initiatives are brought together allowing for the pooling of resources throughout Europe to solve common problems and issues.
The European Society of Radiology wishes to join forces with other European Organizations and try to develop a new infrastructure for the excellence of biomedical imaging research in Europe. To achieve this ESR has launched the "European Institute for Biomedical Imaging Research" (EIBIR). This institute will have objectives of;

- building a biomedical imaging research network throughout Europe
- encouraging excellence in basic and clinical imaging research
- creating opportunities for research education.

The EIBIR will promote networking activities within Europe and will ensure the pooling of resources among members to promote a culture of cooperation between them. This will generate critical mass and help coordinate research into new instrumentation, methods, concepts and technologies. EIBIR promotes a multi disciplinary cooperation covering all aspects of bio medical imaging and has support from leading industry players.
The EIBIR will develop a structure that is conducive to networking activities and will be key to spreading good practice, promoting common initiatives and interoperability. The EIBIR will also generate publicity concerning new opportunities for access, provide dissemination of knowledge and training courses for potential users.

Ignasi CARRIO

The International Society of Magnetic Resonance in Medicine (ISMRM) and its Molecular Imaging Activities

Chrit Moonen, President ISMRM

Vision: The ISMRM aspires to be the premier international society working to promote innovation, development, implementation, and communication of magnetic resonance science in medicine and other related fields.

About the ISMRM

- About 5000 members (50% basic scientists, 50% physicians) + 1500 technologists
- International (50% North American, 50% elsewhere)
- One annual meeting (4000 attendees)
- Several scientific workshops and educational outreach meetings each year

ISMRM Molecular Imaging activities at the annual meeting

- Plenary lectures, Scientific sessions and scientific papers on Molecular Imaging from the very beginning of molecular imaging
- Prior to 2000: specific MR contrast agents
- Prior to 2000: biomarkers (perfusion, diffusion, metabolism, macrophage activity) in drug research for preclinical and clinical evaluation
- Post 2003 : dedicated scientific sessions on Molecular Imaging

Specific Molecular Imaging activities :

2003: Organization of scientific symposium in collaboration with the Society of Molecular Imaging

Bordeaux, June 2003: Molecular and Cellular Imaging
Andreas Jacobs, Nicolas Grenier, Vincent Dousset, Michèle Allard, Chrit Moonen
170 attendees

2003: Creation of Study Group « Molecular and Cellular Imaging », first meeting, Kyoto

Meeting 1: Kyoto, Japan, 2004, theme « Stem cell labeling and tracking »
Meeting 2: Miami, May, 2005, theme « Specific MRI contrast agents »

2005: Teaching session « Molecular Imaging », Annual meeting, Miami, 7-13 May

Robert Muller and Silvio Aime, organizers.

COST initiatives in the fields of contrast agents, radiopharmaceuticals and molecular imaging

Silvio Aime

Dipartimento di Chimica IFM - Università di Torino - Torino, Italy

COST (European Cooperation in the field of scientific and technical research) is one of the longest-running instrument supporting cooperation among scientists and researchers across Europe.

COST has been extremely active in promoting collaboration in fields relevant to Molecular Imaging. In particluar I'll present the main results obtained in COST Action D18 ("Lanthanides in Diagnosis and Therapy) and B12 ("Development of new radiotracers for in-vivo assessment of biological function and drug interaction").

Furthermore, the activities planned for the new COSTD38 ("Metal-based systems for Molecular Imaging applicaions" will be presented. Overall these COST initiatives have involved more than 100 research institutions distributed across all Europe attaining an outstanding level of international and interdisciplinary collaboration.

Brengt LANGSTROM

Trends in mMRI

Krieg Robert W.,

Siemens Medical Solutions AG, Germany, 91050 Erlangen, Allee Röthelheimpark 6

Aim

The concept of molecular imaging promises a significant improvement in health care due to better prevention, early detection and more efficient treatment of disease. However this poses a lot of new challenges to technology. Today's nuclear imaging systems still lack appropriate resolution. In addition, FDG today is the only commercially available tracer. MRI mainly lacks adequate sensitivity. Only general purpose contrast media are available.

Methods

MRI scanners continuously improve sensitivity, the trend to higher fields and parallel acquisition techniques support this. The main boost will however come from contrast media with higher relaxivities and higher concentrations in the target tissue. Targeted agents are technically and economically a challenge to industry. Therefore the use Iron Oxide agents with the intrinsic targeting mechanism provided by macrophages pose a compromise to perform molecular imaging already today. Since MI starts in cell cultures and small animals, innovations in imaging technologies will not be achieved on standard clinical scanners. Vendors are challenged to provide adequate solutions. Finally comprehensive MI combines the different parameters coming from MRI and PET. An integration of both methods is necessary.

Results

An overview of the application range of cell and small animal imaging is provided. The translational aspect is also demonstrated on human applications.

Already today SW Tools for the diagnose of malignant lymph node with mMRI are developed. Furthermore MRI is used to speed up the development of molecular drugs, e.g. VEGF inhibitors.

Different examples show the tracking of stem cells with MR into their target tissue.

The question on the further fate of these cells can not be answered with today's MR Technology. PET can then help to demonstrate proliferation of the cells. To a certain extend both methods are complementary but for some questions of tissue characterization both are competing, e.g. the imaging of inflammatory processes in the tissue.

Conclusion

The main trends in mMRI are

- Higher fields and parallel imaging in MRI system technology
- Small animal MRI systems that simplify translation of results to clinical scanners
- Integration of modalities
- Increased work on targeted contrast media.

Thus mMRI already improves healthcare today.

Imagine the future: Molecular Imaging at Philips

Sjaak Deckers, PhD - Philips

In the care-cycle of numerous diseases, the role of diagnostic imaging is expanding. The use of contrast-agents is also increasing in most imaging modalities, also for more disease-specific or targeted contrast agents. Therefore, the interaction between the contrast agent and the device is getting more critical, to tailor the properties and optimize the imaging contrast. Furthermore, using targeted nano-particles containing drug substances, one can even combine imaging with therapeutic applications. In the presentation, an overview will be given of Philips research activities in these domains. Examples of interactions between equipment and agents will be given for various modalities, such as ultrasound and MRI. Philips collaborates with Schering AG, Berlin, to jointly develop devices and contrast agents for optical imaging. The first results of this collaboration, for an optical mammography agent and device, will be described.

“Molecular Imaging, a critical step towards Early Health.”

Jean-Luc Vanderheyden, Global Molecular Imaging Leader

GE Healthcare, 3000 N. Grandview Blvd, W-427, Waukesha, WI 53188,
jeanluc.vanderheyden@ge.com

Advances in chemistry, biology and imaging technology are expanding progress in Molecular Imaging since the unraveling of the Human Genome Project, with the objective of detecting diseases before the patients experience symptoms. In this presentation, we will review the rich history of molecules at both preclinical and clinical stages, identify the key enablers in PET/CT, SPECT, MRI and fluorescence imaging, and determine how their use will shape the future of healthcare by moving from a model of treating late disease to one of early health, where disease is diagnosed and treated earlier. The link between understanding the predisposition to developing disease, the ability to diagnose and monitor using molecular imaging technologies, and tailoring therapies to individual patients will be demonstrated using concrete examples in Alzheimer's disease, cardiology and oncology.

Molecular imaging tools: innovation at high pace

Marie Meynadier, PhD CEO.

Biospace lab, Paris

Life sciences, chemistry and physics have combined in the recent years to allow and fuel the development of molecular imaging in drug development. This cross-fertilization and tight interactions between emerging enterprises and academia result in an extremely fast pace of product development that includes breakthrough as well as incremental innovation. In this dynamical environment, Biospace has developed a comprehensive portfolio of molecular imaging equipment in vitro, in vivo and now in actio that bring to the lab the full value of real time imaging

Cellvizio®: a unique technology platform in the Field of *In Vivo* Molecular Imaging.

Benjamin ABRAT

Mauna Kea Technologies – Paris

Molecular imaging has become a major focus for many labs and companies and has the ambition to change Medicine. The development of Cellvizio® technology platform (Mauna Kea Technologies, Paris, France), a fibered confocal fluorescence microscope, makes it possible to obtain *in vivo* and *in situ* cellular images both at the Pre-clinical and at the Clinical stages.
Primarily used on animals in a range of applications such as neuroscience, cancer research, or cardiology, Cellvizio® has already been translated into the clinic : Mauna Kea Technologies obtained the CE Label and the FDA approval in 2005 for its Cellvizio®-GI, dedicated to gastroenterology.
Cellvizio® imaging platform can be combined with almost any other imaging modalities (Endoscopy, MRI, PET, SPECT, Ultra-Sound, …) and is ready to be used with most fluorescent molecular probes.

SkyScan 1178: A fast micro-CT scanner for combination with other imaging modalities

Elke Van de Casteele, Skyscan, Belgium.

The SkyScan 1178 is an ultra-fast micro-CT system for high throughput in-vivo scanning of small laboratory animals. The X-ray scanner contains two source-detector pairs positioned at 90 degrees plus half the opening angle of the source. In this way the projection data can be acquired twice as fast as with 1 source-detector pair. The instrument can be used with one computer for scanning control and reconstruction or with a cluster of 4 workstations for speeding up the reconstruction time. The typical scanning+reconstruction cycle for full volume (512x512x512 pixels cube) is 53 seconds. During scanning the source-camera assembly is turning around the animal, which remains statically in the carbon-composite bed. The instrument has an integrated physiological monitoring system for in-vivo small animal scanning, including colour real-time imaging of the animal during investigation, gating from breathing and heart beats, body temperature measurement and stabilization, etc. Furthermore an extra adaptation block for mounting of the bed in another imaging system is included.

Physics, Chemistry and Biology to achieve a 10-FOLD increase in signal to background in positron tomography

Thomas F. Budinger,
Professor, Univ. Calif. Berkeley; Senior Scientist,

Lawrence Berkeley national laboratory

The evolution of positron tomographs from ring shaped gantries to organ specific geometries has occurred over the past 44 years with an improvement of resolution from 15 mm to 2.6 mm for human imaging systems and to 1 mm for animal systems. But the potentials of PET for molecular imaging require an improvement in the signal to background in order to image gene expression and low abundance targets. Though physical principles of solid angle improvement and more efficient scintillators are well understood, background and noise reduction through discovery of new scintillators and through chemical ligand design can result in an overall increase of the signal to background by factors of 10 to 200. The detector energy resolution of 3 percent can result in reductions of background from scattered annihilation photons by a factor of 5, and time-of-flight deployment can reduce the uncertainty in signal accuracy by a factor of 5. The photofraction of a practical scintillator must be higher than a few percent in order to maintain detection efficiency. For example, the new scintillator lanthanum bromide has capabilities for time-of-flight but materials of low atomic numbers lead to a photofraction squared of only 2 %. This is 6 – 10 times less than current PET tomography materials.

Chemical ligand discovery that emphasizes good affinity (i.e., low off rate relative to on rate) for specific targets is the principal emphasis of must radiopharmaceutical development programs. However good affinity is only one aspect of PET ligands. The current specific activities of PET compounds using F-18 is 1,000 times lower than the ideal due to F-19 contamination. A method to increase the specific activity by 180 will be shown for an assemblage by loading F-18 in the MS2 capsid vehicle. But even this improvement in specific activity is not enough to allow imaging of gene expression. What is needed is an amplification method using prodrug approaches, cytosol enzymes with high activity that trap ligands and aptamer approaches. But a concerted effort in computational chemistry to reduce background accumulation might be of the greatest importance for imaging low abundance targets, once specific activity increase and amplification schemes are deployed.

In sum, signal to background improvements that will enable a wide variety of new molecular imaging studies ranging from childhood behavioral chemistry to enzyme pathway investigations are expected from:

- Gantry designs to improve sensitivity.
- Detector materials to increase sensitivity and reduce background.
- Computational chemistry to achieve specificity in ligand design
- Macromolecule and nanoparticle engineering for specific activity and amplification.

Acknowledgements: The theme of this presentation was developed with suggestions from Stephen Derenzo, Ronald Huesman, and William Moses in instrumentation and from innovations by Matt Francis, John Gerdes, Jacob Hooker, James O'Neil, and Scott Taylor.

Molecular Imaging in Taiwan

Ren-Shyan Liu, MD

Molecular and Genetic Imaging Core, National Research Program for Genomic Medicine
National PET/Cyclotron Center, Taipei Veterans General Hospital
National Yang-Ming University Medical School, Taipei, Taiwan

There were only few sporadic research activities of molecular imaging in Taiwan before 2002 when the governmental financed Molecular-Genetic Imaging Core (MAGIC) and Functional and Micro-Magnetic Resonance Imaging Core (FMIC) were established for technical R & D and service for the National Research Program for Genomic Medicine (NRPGM). In the past 4 years, MAGIC has established the facilites and technologies for gene expression imaging and in vivo assessment of specific biomarkers of the diseases in small animal models by the following core laboratories: radiochemistry lab, cell and tissue autoradiography lab, biophotonic imaging lab, viral and non-viral gene construction, transfection and animal model preparing lab, microPET lab, microSPECT lab and medical physics lab. The specific aims of MAGIC are to establish an integrated multimodality technical core which may conduct the researches for novel technologies of in vivo imaging sciences, such as radiolabeling of novel agents for targeting of gene, gene-related products, metabolic substrates and antibodies, tissue specific reporter gene system, multiple-gene reporter system, cell trafficking, and multimodality images registration and analysis. FMIC has a 4.7T, a 7T and a 9.4T MRI facilities. FMIC is dedicated to provide state-of-the-art MRI equipments, comprehensive MRS technical support including experimental design, targeted technology development, imaging data analysis and education for research in MRI and MRS and their biomedical applications. The works conducted by MAGIC and FMIC in the past 4 years have gone about as planned. Up-to-date 3 more institutions have established the in vivo molecular imaging facilities and 2 are undergoing development.

MRI of Angiogenesis: Revealing Cellular Recruitment, Enzymatic Activity and Gene Expression

Michal Neeman, Dorit Granot, Keren Ziv, Vicki Plaks, Liora Shiftan, Galit Mazooz, Gila Meir, Batya Cohen

Department of Biological Regulation, the Weizmann Institute of Science, Rehovot 76100 Israel.

Background: Tumor angiogenesis is a multiplayer process requiring concerted action of multiple cell types, growth factors, receptors and enzymes. Each step in the process provides a potential target for therapeutic intervention.

Aim: The aim of our work is to reveal the regulatory network controlling vascular remodeling in vivo. For that aim we developed multiple complementary imaging tools for assessment of specific steps in angiogenesis.

Methods: Intrinsic changes in MRI relaxation rates induced by functional changes in blood vessels as well as changes in relaxation induced by exogenously administered contrast media were developed for monitoring changes in vessel permeability and vasoreactivity, lymphatic drain, recruitment of labeled cells and in situ labeling of cells with genetically encoded markers, as well as deposition and degradation of extracellular matrix components.

Results: Dynamic analysis of tumor angiogenesis by molecular imaging provides essential information for sketching the regulatory network of the role of vessels in tumor progression and metastasis. Thus, MRI was able to map non-invasively the process of vascular maturation and the associated recruitment of host stroma cells and extracellular matrix changes in fibrin crosslinking and degradation of hyaluronan. Recent developments towards in vivo imaging of gene expression demonstrated the ability to detect endothelial specific activation of genes using MRI reporters.

Conclusions: Molecular imaging of angiogenesis complements anatomical, functional, and cellular imaging in providing multiparametric dynamic evaluation of the growth of tumor vessels and its impact on tumor progression. Such tools are essential for mapping the regulatory network of angiogenesis and provide the basis for development and monitoring of patient tailored therapy.

Acknowledgements:
This work was supported by NIH R01 CA75334, The Israel Science Foundation, The Minerva Foundation and Varian Biosynergy.

References:
1. Dorit Granot, Leoni A. Kunz-Schughart and Michal Neeman. Labeling Fibroblasts with biotin-BSA-GdDTPA-FAM for multi-modality Tracking of Tumor Associated Stroma by fluorescence and MR imaging. MRM, 2005 54:789-797.
2. Galit Mazooz, Tevie Mehlman, Thung-Shen Lai, Charles. S Greenberg, Mark W. Dewhirst, Michal Neeman Development of MRI Contrast Material for In vivo mapping of tissue Transglutaminase activity. Cancer Res. 2005 Feb 15;65(4):1369-75.
3. Batya Cohen, Hagit Dafni, Gila Meir, Alon Harmelin, and Michal Neeman, Ferritin as an endogenous MRI reporter for Molecular Imaging of Gene Expression. Neoplasia, 2005 Feb;7(2):109-17.
4. Liora Shiftan, Tomer Israely, Miriam Cohen, Veronica Frydman, Hagit Dafni, Robert Stern and Michal Neeman, MRI visualization of hyaluronidase in ovarian carcinoma, Cancer Research, 2005 10316-10323.
5. Liora Shiftan and Michal Neeman, Kinetic Analysis of Hyaluronidase Activity using a Bioactive MRI Contrast Agent, Contrast Media and Molecular Imaging, in press 2006.

Dynamic optical imaging of tumor invasion

Peter Friedl

Rudolf Virchow Center for Experimental Biomedicine and Department of Dermatology, University of Wuerzburg, 97080 Wuerzburg, Germany

We have used multimodal optical confocal and multiphoton imaging of invasive tumor cells in 3D collagen matrices as well as GFP- and RFP-expressing tumoral xenografts during invasion in the mouse dermis to show different patterns of tumor cell migration and dissemination in tissues. Invasion patterns range from single cells and single-cell strands, as well as collective invasion of multicellular solid protusions allowed by expansive growth. During molecular intervention using protease inhibitors or integrin antagonists, invasion was unexpectedly not abrogated but rather converted to a different migration program, i.e. from mesenchymal to amoeboid movement or from collective to nonetheless efficient individual-cell dissemination. Thus, time-résolve high-resolution optical imaging combined with targeted intervention has revealed transition programs in tumor invasion and metastasis and the underlying tumor escape with relevance to therapeutic combination regimens.

Aptamers for *in vivo* imaging

F. Ducongé[1], C. Pestourie[1], L. Cerchia[2], K. Gombert[1], J. Boulay[3], Y. Aissouni[3], D. Libri[3], V. De Franciscis[2] and B. Tavitian[1].

[1]CEA/DSV/DRM Service Hospitalier Frédéric Joliot, INSERM ERM 103, Orsay, France ; [2]Instituto per l'Endocrinologia e l'Oncologia Sperimentale "G. Salvatore" del CNR, Napoli, Italy ; [3]Centre de Génétique Moléculaire, C.N.R.S., Gif sur Yvette, France.

Aptamers are nucleic acid structures selected by an iterative selection procedure (basically named SELEX) to promote catalytic activity or interaction with a molecular target of interest (proteins, small compounds…). They are often compared to nucleic acids-based antibodies. With respect to antibodies, aptamers present several advantages for *in vivo* applications: 1- Aptamers do not appear to trigger an immune response, which is one of the major limitations of antibodies for *in vivo* use. 2- Their smaller size (8–15 kDa in comparison to 150 kDa) could promote a better tissue penetration. 3- Aptamers may be chemically synthesized for relatively low prices, better batch-to-batch reproducibility and easier incorporation of chemical modifications, conferring plasmatic resistance to their degradation or improved pharmacokinetic.

In order to produce aptamers that are efficient in vivo, SELEX must be performed against proteins in their native conformation, a condition that may be difficult to achieve for membrane proteins. This could explain why only a few aptamers have been selected against membrane proteins, in contrast to soluble targets. We validate a whole-living cell SELEX protocol to target the transmembrane receptor tyrosine kinase (RTK) RET (REarranged during Transfection) in its natural environment.

RET is mutated in multiple endocrine neoplasia type 2A and 2B syndromes and in familial medullary thyroid carcinoma. The C634Y mutation in the extracellular domain causes constitutive activation of the receptor. We found one aptamer, named D4, which bound specifically to RET and blocked RET dimerization-dependent signalling pathways induced either by GDNF or by the C634Y activating mutation. The aptamer also inhibits RET-dependent changes in cell phenotype: the growth of neurites from PC12 cells expressing the wild-type RET receptor and activated with GDNF is blocked by D4, as are changes in morphology seen in NIH-3T3 cells following expression of the constitutively active RET^{C634Y} receptor. Interestingly, D4 did not bind to a recombinant extracellular RET fragment, highlighting the strength of our approach.

We are now evaluating the aptamer D4 and some derivatives for in vivo molecular imaging of RET^{C634Y} expressing tumours.

Research is carried out in the frame of the European-funded EMIL programme (LSHC-2004-503569) and supported by the CEA-CNRS *Imagerie du petit animal* programme and a grant no. 3527 from the Association pour la Recherche sur le Cancer.

Looking in tissues with Fluorescence Molecular Tomography

Vasilis Ntziachristos

Fluorescence imaging is a powerful modality that is increasingly used for gene-expression profiling, probing protein function and elucidating cellular pathways. Fluorescence generated in in-vitro assays can be easily quantified using fluorometers or charge coupled devices (CCD). Similarly, fluorescence of superficial structures has been imaged in vivo using intravital, confocal or multiphoton microscopy. Quantification and imaging of fluorescence in deeper tissues however has been more elusive. This talk describes current progress with methods developed for in-vivo fluorescence imaging and tomography that allow for accurate and quantitative observations. We further demonstrate how three-dimensional imaging can be applied to imaging fluorescent proteins and of exogenously administered fluorescent probes with molecular specificity in-vivo through entire animals. Finally, clinical translation and applications are discussed.

Non-invasive *in vivo* imaging of Ca^{2+} signaling in live animals

Rogers KL[1], Picaud S[1], Roncali E[2], Boisgard R[2], Colasante C[1], Stinnakre J[1], Tavitian B[2], Brûlet P[1]

[1]Unité d'Embryologie Moléculaire, CNRS URA 2578, Institut Pasteur, Paris, France, [2]Laboratoire d'imagerie de l'expression des gènes, INSERM ERM 103, CEA, Service Hospitalier Frédéric Joliot, Orsay, France

A major challenge in biology is to monitor chemical transduction of external signals into cellular activity, in a physiological context. We describe a technique based on whole animal bioluminescence imaging where changes in local calcium concentrations [Ca^{2+}] can be non-invasively recorded in live animals. Transgenic mice expressing the mitochondrially targeted calcium sensitive bioluminescent probe, GFP-aequorin, were imaged using a highly sensitive photon counting system for whole animals. We will show that mitochondrial [Ca^{2+}] can be repeatedly detected during muscle contraction induced by motor-nerve stimulation over hours and with a high time resolution. Dynamic patterns of calcium distribution can also be visualized in the intact animal during epileptic seizures. Furthermore, increases in [Ca^{2+}] can even be followed in freely moving animals. Non-invasive detection of calcium signaling with temporal resolution on a similar time scale as signal transduction processes in the living animal offers a unique way to study un-anaesthetised and un-restrained animals in their physiological environment.

Perspectives of Molecular MR Imaging in Experimental Neurology

Mathias Hoehn

In-vivo-NMR-Laboratory, Max-Planck-Institute for Neurological Research, Cologne, Germany

During the past few years, high spatial resolution MR imaging has created a niche developing strategies for highly sensitive in vivo cell tracking. The major area of application has been to implantation of stem cells after cerebral lesions, with the aim of monitoring the cells' dynamics and interaction with the host tissue. This has already led to several exciting studies about stem cell migration towards the lesion. These early projects were concerned with the highly resolved localization of the cells which had been labeled with iron oxide nanoparticles.

Presently, efforts are undertaken to extend the visualization from *localization* to *function*. For this purpose, so-called "responsive contrast agents", consisting of gadolinium chelates, are custom-designed. They are then incorporated in their inert state into the cells. Upon expression of a pre-defined enzyme, this enzyme will activate the contrast agent, resulting in a hyperintense image contrast. Thus, enzyme activity, and, in consequence, gene expression of the implanted cells is imaged.

As the purpose of most of the cell implantation experiments is the investigation of their regenerative potential, it is of great interest to study functional brain recovery with fMRI, following such tissue replacement therapy. For this end, recent advances have resulted in an animal model studying the somatosensory cortical activation profile, while making the model compatible with repetitive anesthesia sessions for longitudinal studies over many weeks. Such studies are of importance as they allow to evaluate, before cell implantation, chances of spontaneous recovery, which is a potential confounding factor for the evaluation of therapeutical success. Extreme spatial and temporal resolution of the fMRI data permit to resolve even individual cortical layers during the activation process. Finally, application of diffusion tensor imaging (DTI), hand in hand with manganese enhanced MR imaging, provide morphological interpretation of the functional recovery processes by imaging the structural intactness or damage of thalamo-cortico fiber connections after stroke.

In vivo MRI of songbird brain: neuronal circuitry assessment in extreme model of neuroplasticity

Annemie Van der Linden
Bio-Imaging Lab, University of Antwerp, Groenenborgerlaan 171, 2020 Antwerp, Belgium.

The neural substrate for song behaviour (i.e. song learning and singing) in songbirds is called the song control system. This system displays a remarkable seasonal plasticity whereby not only the volume of several key song control nuclei change in size, but also the density of the connections between them changes as a function of seasonal and hormonal influences and capacity for song learning. Moreover the songbird brain displays adult neurogenesis to a degree that finds no match in any mammalian brain. Some of the volume changes in the song control nuclei are the result of incorporation of new neurons. Other volume changes are the result of increased dentritic branching or changes in cell or extra cellular space volumes. These features make the songbird brain into one of the best documented models to study neuroplasticity and adult neurogenesis (1). However until recently this unique model has been deprived of in vivo (molecular) imaging tools which are commonly used in human, primate and small rodent neuro research.

The current presentation aims at providing an overview of how MRI succeeded in visualising, characterising and quantifying seasonal neuroplasticity in the songbird brain (2-9). Using Manganese Enhanced (ME) MRI we could monitor and quantify changes in the volumes of different song control nuclei. Using Diffusion Tensor MRI (DTI) with the resulting parameters (FA=Fractional Anisotroptry, MD=Mean Diffusion, λ_r=Radial diffusivity, $\lambda_\parallel$=Axial diffusivity) enabled us to quantify seasonal changes in the connections and the volumes of different song control nuclei. MR Imaging studies were done repetitively in spring and in summer and the data could be related to behavioural data on seasonal changes in song production. Because the Song Control System is so well studied it represents a valuable model for testing and validation of in vivo MRI tools assessing changes in neuronal circuits. The same tools will then find an excellent application in the study of neurodegeneration driven neuronal circuit alterations especially in models of Parkinson and Huntington disease.

References:

(1) Zeigler HP. Behavioral Neurobiology of Birdsong. New York: New York Academy of Sciences; 2004.
(2) Van der Linden A., M. Verhoye, V. Van Meir, I. Tindemans, M. Eens, P. Absil and J. Balthazart. (2002) : In vivo manganese-enhanced magnetic resonance imaging reveals connections properties of the songbird vocal control system. *Neuroscience, vol 112: 467-474.*
(3) Tindemans I., Verhoye M., Balthazart J., Van der Linden A. (2003) : In vivo dynamic ME-MRI reveals differential functional responses of RA- and area X-projecting neurons in the HVC of canaries exposed to conspecific song. *The European journal of neuroscience , 18, p. 3352-3360*
(4) Van der Linden A., van Meir V., Tindemans I., Verhoye M., Balthazart J. (2004) : Applications of manganese-enhanced magnetic resonance imaging (MEMRI) to image brain plasticity in song birds *NMR in biomedicine , 17:8, p. 602-612*
(5) Van Meir M., Verhoye M., Absil P., Eens M., Balthazart J., van der Linden A. (2004) : Differential effects of testosterone on neuronal populations and their connections in a sensorimotor brain nucleus controlling song production in songbirds: a manganese enhanced-magnetic resonance imaging study *Neuroimage , 21, p. 914-923*
(6) Van Meir V., Boumans T., De Groof G, Van Audekerke J., Smolders A., Scheunders P., Sijbers J., Verhoye M., Balthazart J., Van der Linden A. (2005) : Spatiotemporal properties of the BOLD response in the songbirds' auditory circuit during a variety of listening tasks. *Neuroimage. 1;25(4):1242-55. IF= 6.192*
(7) I.Tindemans, T. Boumans, M. Verhoye, A. Van der Linden. (2006) :IR-MEMRI in vivo visualization of oscine neuroarchitecture including the main forebrain regions of the Song Control System. NMR Biomed. 2006 Feb;19(1):18-29.
(8) V. Meir,D. Pavlova, M. Verhoye, R. Pinxten, J. Balthazart, M. Eens, A. Van der Linden (2005) : In vivo imaging of the seasonal volumetric and functional plasticity of song control nuclei in relation to song output in a female songbird, Neuroimage. 2006 Mar 8; [Epub ahead of print]
(9) De Groof G., Verhoye M., Van Meir V., Tindemans I., Leemans A., Van der Linden A. (2005) : In vivo diffusion tensor imaging (DTI) of brain subdivisions and vocal pathways in songbirds. Neuroimage. 2006 Feb 1;29(3):754-63. Epub 2005 Oct 19.

POSTERS

ANIMAL MODEL

Investigations of magnetically labelled macrophages with MRI

A. Hartung [1,2], K.-H. Herrmann [1], M.R. Lisy [2], I. Hilger [2],M.E. Bellemann [3], W.A. Kaiser [4], J.R. Reichenbach [1]

[1] *Medical Physics Group, Institute for Diagnostic and Interventional Radiology, Friedrich-Schiller-University, Jena, Germany;* [2] *Experimental Radiology, Institute for Diagnostic and Interventional Radiology, Friedrich-Schiller-University, Jena, Germany;* [3] *Department of Biomedical Engineering, University of Applied Sciences, Jena, Germany;* [4] *Institute for Diagnostic and Interventional Radiology, Friedrich-Schiller-University, Jena, Germany;*

Background: Macrophages are involved at essentially all stages of the immune response. They are also effectors and regulators of the inflammatory response. Therefore, labelling of macrophages is highly relevant for diagnostic and therapeutic evaluation and may facilitate detection of inflammations by using MR molecular imaging [1].

Aim: To label macrophages using biological superparamagnetic iron oxide particles and to determine their properties in both *in vitro* and *ex vivo* experiments.

Methods: Bacterial magnetosomes (Ø 42 nm) were obtained from the Max-Planck Institute for Marine Microbiology (Bremen; Germany) and were used as MR contrast agent. To investigate the relaxivities of these magnetosomes, samples with different iron concentrations (0 – 0.129 mmol/l) where prepared in repeat determination and fixated in 2% agarose gel. To investigate the iron uptake three solutions of J774A.1-macrophages were incubated with magnetosomes. Samples of cell counts ranging from 0 - 2000 cells/µl were diluted from each of the solutions in repeat determination and fixated in 2 % agarose gel. A clinical 1.5 T Scanner (Sonata, Siemens Erlangen) was used for MRI. T1-, T2- and T2*-relaxation times were investigated with a Turbo-FLASH sequence (TE/TR/FOV/d/α = 2.73 ms/4000 ms/50 mm/5 mm/8°, NEX = 4, matrix 64, TI=17 5–3000 ms), a single echo spin-echo sequence (TR/TE/FOV/d/α = 3000 ms/11;30;60; 120 ms/60 mm/5 mm/90°, matrix 192×256) and a multi-echo gradient echo sequence (12 echoes, TR/ FOV/d/α = 3000 ms/ 60 mm/5 mm/21°, 128 matrix, TE = 4.52–80 ms, NEX = 10) , respectively, by using a small loop coil (Ø 30 mm). ROI analysis was performed to determine the relaxivities R1, R2 and R2* of pure magnetosomes and relaxation rates 1/T1, 1/T2 und 1/T2* of cells with magnetosomes. To approve the labelling of macrophages with magnetosomes in an animal model, peritonitis was induced in two mice, one of which received an iv injection of magnetosomes (10 mg/kg) after 90 min. MRI was performed 6 h after inducing the peritonitis. The mice were sacrificed with ether before imaging. The small loop coil was used to acquire dual-echo gradient echo images of both mice (TR/TE/d = 60 ms/19; 50 ms/1 mm, NEX = 2).

Results: R1-, R2- und R2*-relaxivities of pure magnetosomes in 2 % agarose gel were 3.2 ± 0.4 $[mM \times s]^{-1}$, 526 ± 56 $[mM \times s]^{-1}$ and 1198 ± 342 $[mM \times s]^{-1}$, respectively. Cells with magnetosomes showed only a slight effect on T1, similar to pure magnetosomes, and a change of relaxation rate 1/T1 was only observed with 2000 cells/µl. So far, signal increase (T1 effect) caused by SPIOs has only been observed for vessels and edemas [2-4] and is not to be expected in agarose fixed probes. Distinct stronger effects were observed for 1/T2 and 1/T2*. MR images of the mouse which received an injection of magnetosomes showed signal decrease in the area of the peritoneum, whereas no signal changes were observed in the mouse without injection.

Conclusion: These *in vitro* measurements and *ex vivo* MR imaging of mice demonstrate that mac-rophages can be successfully labelled by using magnetosomes. The largest effects were observed in the T2*-weighted sequence. Further investigations *in vitro* an *in vivo* are needed to investigate the feasibility of this effect in our model.

References:

[1] M. Rudin. Molecular Imaging-Basic Principles and Applications in Biomedical Research, Imperial College Press, 2005; pp 468-470. [2] G. Simon *et al*. RöFo 2006; 178: 200-206. [3] A. Lutz *et al*. Radiology 2004; 233: 149-157. [4] G. de Lussanet *et al*. Radiology 2003; 229: 429-438

Influence of a cholic acid diet on the hepatobiliary function in mice using pinhole single photon planar scintigraphy

Goetz C1, Choquet P1, Monassier L2,3, Breton E1, Elfertak L2, Auwerx J2, Constantinesco A1

1 Service de Biophysique et Médecine Nucléaire, CHU de Hautepierre 67098 Strasbourg
2 Institut clinique de la Souris, 67404 Illkirch
3 Laboratoire de Neurobiologie et Pharmacologie Cardiovasculaire, Faculté de Médecine 67085 Strasbourg

Background: Bile acids are well known for their essential role in dietary lipids absorption and cholesterol catabolism. Recently, bile acids were found to play a major role controlling their homeostasis acting as general metabolic integrators [1].

Aim: To evaluate influence of cholic acid on in vivo hepatobiliary function in adult mice comparing a control group of (n = 6) CD1 to a group of (n = 6) CD1 treated by an enriched cholic acid diet using planar hepatobiliary scintigraphy.

Methods: A dedicated small animal gamma camera with 1.5 mm pinhole, 170x170 mm field of view was used (Gaede Medizinsysteme Gmbh, Freiburg, Germany). 0.2ml and 150 MBq of Tc99m-tBIDA tracer (Mebrofenin, CIS-Bio International, Gif/Yvette, France) were injected intravenously using a caudal catheter to both groups under isoflurane anesthesia. Multiple anterior abdominal images were acquired at a rate of 1 image/minute during 30 minutes. Hepatobiliary transit times were measured from regions of interest placed over the mice liver. Temporal parameters standing for the kinetics of mebrofenin collecting into hepatocytes and kinetics of biliary excretion were obtained from the background noise corrected hepatogram. The vascular deconvolved hepatogram permitted calculation of the hepatic extraction fraction HEF and halflife constant standing for the kinetics of the tracer transit through the hepatocytes as well as for its biliary excretion [2]. Compartmental analysis was finally used to measure the hepatic uptake and excretion half-lives of the tracer for both groups [3].

Results: No difference was found in HEF between the two groups. However all temporal parameters from corrected and deconvolved hepatogram, or resulting from the compartmental analysis, show statistically significant differences with the threshold of 5% between the two groups.

Conclusions: The cholic acid supplemented group is characterized by a slower uptake of the tracer into the hepatocytes and by an overall faster biliary excretion. Although the molecular mechanisms underlying bile acids homeostasis are imperfectly known yet, the in vivo results obtained indicate that cholic acid modify the biliary salts kinetics according to current molecular biology assumptions [1].

References:

[1] Watanabe M, Houten SM et al; *Nature. 439*:484-489 (2006)
[2] Brown PH et al.; *Journal of Nuclear Medicine. 29*:623-630 (1988)
[3] Juni JE et al.; *Radiology. 177*:171-175 (1990)

Fluc-rhabdomyosarcoma cancer model for quantitative and long-term *in vivo* follow-up using Bioluminescence imaging.

Marleen Keyaerts, MD[1]; Karine Breckpot, PhD[2]; Olive Tchouate[1]; Tomas Bos[3]; Vicky Caveliers, PhD[1]; Philippe R. Franken, MD, PhD[1]; Kris Thielemans, MD, PhD[2]; Axel Bossuyt, MD, PhD[1]; Tony Lahoutte, MD, PhD[1].

[1]*Department of Nuclear Medicine, In Vivo Cellular and Molecular Imaging Center (ICMIC), Academic Hospital Vrije Universiteit Brussel AZ-VUB, Brussels, Belgium*

[2]*Laboratory of Molecular and Cellular Therapy, Department of Physiology and Immunology, Medical School of the Vrije Universiteit Brussel (VUB), Brussels, Belgium.*

[3]*Department of Haematology and Immunology, Vrije Universiteit Brussel (VUB), Brussels, Belgium.*

Background: Oncologic animal models that can be readily evaluated and that are predictive of the human response are critically important for the advancement of more effective therapies and for enhancing our understanding of cancer cell biology. However, the study of animal models has been limited by the difficulty of accurately assessing disease burden.

Recently, *in vivo* models for cancer research have greatly improved by the development of sensitive and non-invasive imaging strategies to quantitatively assess tumour burden. The use of luciferase-expressing cells enables *in vivo* bioluminescence imaging to quantify viable tumour cells.

Aim: to establish a stable and sensitive *in vivo* rhabdomyosarcoma model using lentiviral transduction of the luciferase reporter gene and quantification by bioluminescence imaging.

Methods: The rhabdomyosarcoma cell line R1M was transduced using vesicular stomatitis virus glycoprotein (VSV.G) pseudotyped, triple helix containing, self-inactivating lentiviral vectors (MOI 30), which encode two reporter genes, i.e. the firefly luciferase (Fluc) gene and truncated nerve growth factor (tNGFR) gene, separated by an internal ribosomal entry site (IRES). Flow cytometry was used to evaluate the transduction efficiency (percentage of tNGFR positive cells) and viability of the R1M cells. The use of a Intensified Cooled Charged-coupled Device camera (Photon Imager, Biospace, Paris, France) allowed us to assess Fluc expression after administration of luciferin both *in vitro* as well as in live animals.

Results: The transduction efficiency after lentiviral transduction was evaluated 3, 13, 32 and 44 days after transduction by flow cytometry, revealing high (>95% tNGFR positive cells)) and stable transduction of the R1M cells, without hampering their viability or *in vitro* growth. We evaluated the light signal produced by these Fluc positive cells *in vitro* using serial dilution ranging from $5x10^5$ to 120 cells in a black 96-well plate. ROI analysis showed a good correlation ($r^2 = 0,97$) between photon emission and number of cells imaged, detectable up to 120 cells/well. Preliminary *in vivo* results in nu/nu mice show high photon emission immediately after subcutaneous inoculation of $1,5x10^5$ R1M-Fluc cells.

Conclusion: We have developed a stable expression of Fluc in the R1M rhabdomyosarcoma cell line using lentiviral transduction. The high signal intensity allows quantification of xenograft viability starting immediately after inoculation. This enables the study of complex cellular processes and the efficacy of therapeutic strategies by non-invasive Bioluminescence Imaging.

Imaging brain inflammation with [11C]-PK-11195 in a rat model of focal cerebral Ischemia

Rojas S1, Martin A1, Arranz MJ1, Purroy J1, Pareto D2, Gispert JD2, Llop J2, Millan O2, Planas AM1
1 IDIBAPS, 2 IAT; Barcelona, Spain

Background: 11C-PK11195 is used in PET imaging studies for in vivo tracing brain inflammatory reactions, as it binds to the peripheral benzodiacepine receptor (PBR). Yet, the extent and features of the microglial reaction necessary to induce a positive PET signal with 11C-PK11195 are not well characterized.

Aim: Here we aimed to study in vivo the progression of the post-ischemic inflammatory reaction by PET with 11C-PK11195 following transient focal cerebral ischemia in the rat at different time points from 1 to 7 days.

Methods: Ischemia was induced by 1-hour intraluminal occlusion of the middle cerebral artery in Sprague-Dawley rats (n=30). Following PET image co-registration with a rat brain atlas or T1-3D MRI for anatomical identification, we defined regions of interest for each animal according to the infarcted tissue evaluated postmortem. In the tissue we examined microglia and macrophages with several markers (lectin, OX42, OX6, CD57), and the time course of PBR mRNA expression by real-time RT-PCR.

Results: The results showed increase of PBR mRNA at 4 and 7 days in the ipsilateral hemisphere, and a clear 11C-PK11195 PET signal in the region of infarction at 7 days. At this time microglia acquired a morphology resembling macrophages (arrows) and the reaction was well confined in an area surrounded by the astroglial scar. We found an increased 11C-PK11195 signal in the non-affected tissue at 4 days, which was attributed to the presence of ramified reactive microglia in the absence of macrophages. This is compatible with a transient, diffuse and moderate microglial reaction in non-ischemic areas. At 24h the signal intensity in the infarct region was smaller than in sourrounding regions and reactive microglia was scarce within the core of infarction.

Brain infarct at 7 days | Reactive microglia/macrophages at 7 days | $_{11}$C-PK11195 signal at 7 days

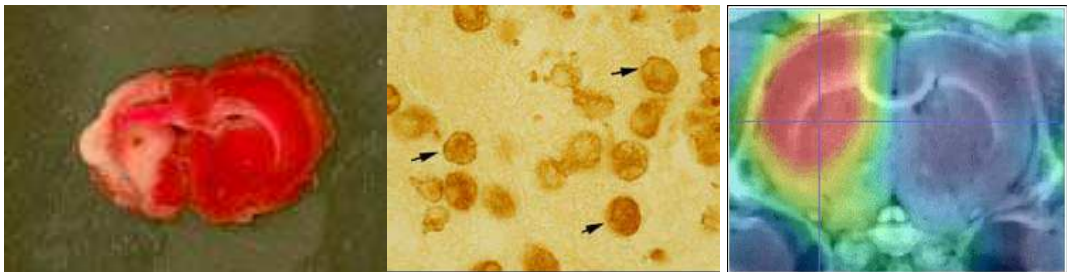

Conclusions: The results show that 11C-PK11195 is an excellent marker of confined regions of lesion with abundant reactive microglia. Nonetheless, the ischemic zone was less clearly identified at early stages after injury due to still low density of reactive microglia within the infarct, and to a transient inflammatory reaction in areas of the brain not affected by ischemia.

Acknowledgement: *This study was funded in part by the EC-FP6-project DiMI, LSHB-CT-2005-512146, and FIS (FS041104-O).*

In vivo evidence for reduced brain volumes in APP/Au mouse models favors the hypothesis of intraneuronal Aß toxicity in AD

Vanhoutte G[a], Van Broeck B[b,c], Van Dam D[d], De Deyn P[d], Van Broeckhoven C[b,c], Kumar-Singh S[b,c], Van der Linden A[a].

[a]*Bio-Imaging Laboratory, University of Antwerp, Groenenborgerlaan 171, 2020 Antwerpen, Belgium*

[b] *Neurodegenerative Brain Diseases Group, Department of Molecular Genetics, Flanders Interuniversity Institute for Biotechnology, University of Antwerp, Universiteitsplein 1, 2610 Antwerpen, Belgium*

[c] *Laboratory of Neurogenetics, Institute Born-Bunge, University of Antwerp, Universiteitsplein 1, 2610 Antwerpen, Belgium*

[d] *Laboratory of Neurochemistry and Behaviour, Institute Born-Bunge, University of Antwerp, Universiteitsplein 1, 2610 Antwerpen, Belgium*

Background: Amyloid ß (Aß) is known to deposit extracellularly as amyloid plaques in brains of Alzheimer's disease (AD) patients. However, recent publications [1,2] counter this prevailing hypothesis of AD pathogenesis via aggregated extracellular Aß toxicity and suggest that prior to the development of extracellular plaques, Aß will deposit intraneuronally and plays a pivotal role in the early pathogenesis of AD.

Aim: As there exists enough evidence to conclude that, in AD, Aß accumulates within neurons, the remaining question is whether intraneuronal Aß42 accumulation merely reflects increased production with resultant increased extracellular neurotoxicity or whether intraneuronal Aß42 can also directly damage neurons from within. To that end a new APP/Au transgenic mouse model was developed based on a novel APP mutation (T714I) discovered in an Austrian family (APP/Au) [3]. In this aggressive type of AD, the pathology coincided with abundant non-fibrillar diffuse plaques and intraneuronal Aβ composed of Aβ42, while Aβ40 was nearly absent [4]. To study the pathogenic mechanism *in vivo*, the APP/Au transgenic mice were submitted to behavioral studies and volumetric MRI measurements in a longitudinal manner. In comparison with age-matched APP wild-type (APP/Wt) controls we searched for changes in cognitive behavior and changes in brain volumes along with changes in accumulation of amyloid.

Methods: Cognitive performance was assessed in APP/Au and APP/Wt mice at the age of 8-9 months with hidden-platform Morris Water Maze and passive avoidance tasks (n=14 each). High resolution magnetic resonance images of a 3D volume of 20*20*20 mm^3 were acquired using T_2 weighted RARE sequence (7T Pharmascan, Bruker) while mice were under isoflurane anaesthesia (0.5-1%) at the age of 12 months (n = 6 each) and 20 months (n = 5 each). Using Amira software (TGS, Richmond, TX), we estimated at the 2 time points the volume of the total brain and the hippocampal formation through manual segmentation.

Results: Total brain volumes of APP/Au mice were significantly reduced at both time points

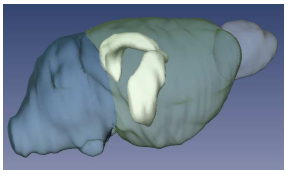

(472.14 ± 18.16 mm^3 vs. 514.73 ± 18.88 mm^3; *P=0.006* and 447.59 ± 20.92 mm^3 vs. 499.55 ± 16.60 mm^3; *P = 0.003*). For the hippocampus no significant volume differences were found. The figure presents the hippocampal volume coloured white within the total brain volume which also shows the separation of the cerebellum (blue), cerebrum (green) and bulbus olfactorius (light blue). The decrease in total brain size was attributable to cerebral volumes while volumes of olfactory bulb and cerebellum were not altered. No cognitive problems were observed on Morris Water Maze and passive avoidance tasks.

Conclusions: This is the first MR report on smaller total brain volumes in an AD mouse model. Moreover, from the APP/Au mice, we can conclude that intraneuronal accumulation of Aβ is an important factor in the pathogenesis of AD as our results indicate a reduced brain volume in the transgenics as a clear sign of neurodegeneration. It is indeed reasonable to suspect that massive amyloid accumulations exist at the expense of cellular viability an eventually impair the ability of neurons to maintain synaptic contact which will generate neurodegeneration. The absence of any cognitive impairment is in agreement with normal hippocampal sizes. However, intraneuronal inclusions by 6 months of age started to appear predominantly in hippocampal regions. This strengthens the hypothesis that intraneuronal inclusions characterize an early event in the AD pathogenesis and can occur before behavioral or volumetric changes can be uncovered.

References:

[1] Glabe C; *J Mol Neurosci*. 17(2):137-45 (2001)
[2] Gouras GK et al.; *Neurobiol Aging*. 26(9):1235-44 (2005)
[3] Van Broeck B et al.; submitted to *Neurobiol Aging.* (2006)
[4] Kumar-Singh S et al.; *Hum Molec Genet*. 9(18):2589-98 (2000)

White and grey matters changes in a rat model for Huntington's disease discerned with in vivo DTI

Van camp Nadja[1] Blockx Ines[1], Lluisa Camon[2], Nuria de Vera[2], Verhoye Marleen[1-3]*Leemans Alexander*[3], Martinez Emili[2], Sijbers Jan[3], Planas Anna[2], Van der Linden Annemie[1]
[1]*Bio-Imaging Lab, University of Antwerp, Belgium;*
[2] *IDIBAPS, Barcelona, Spain;*
[3]*Vision Lab, University of Antwerp, Belgium*

Background: Huntington's disease (HD) is an autosomal neurodegenerative disorder characterized by diffuse brain atrophy, although the most substantial neuronal loss occurs in the caudate and putamen. It has been shown in carriers of HD that regional cerebral atrophy and white matter changes already occur during the preclinical phase. Diffusion tensor imaging (DTI) provides information about anatomical connectivity and brain microstructural morphology and has been shown to specifically trace neurodegenerative changes such as axonal degeneration, demyelization, cell swelling in demyelization disorders and Alzheimer disease.

Aim: In this study we applied high resolution DTI on the Quinolinic Acid (QA) lesion rat model of Huntington's Disease 6 weeks after lesioning to investigate grey and white matter changes in this aniomal model.

Methods: Female Wistar rats were stereotaxically injected in the left striatum (referred to Bregma: AP:+0.2 mm, L: +2.8 mm, V:-4.5 mm) with Quinolinic acid (HD model, n=6; 240 nmol/ 1 µl) or vehicle (SHAM, n=6; PBS adjusted to pH 7.4).
Six weeks after surgery high resolution MRI DTI was performed successfully on 6 HD (231±4g), 4 SHAM (255±9g) and 4 control animals (225±8g). High resolution (voxel size: 0.117µm x 0.117µm) DTI (SE DTI: TR/TE = 2200/43ms, 14 averages, b= 800 s^2/mm, diffusion sensitizing gradients along 7 directions) of the entire rat brain (coronal slices with slice thickness of 0.43mm) was performed on a 7T Bruker system under 1.5-2% isoflurane anesthesia. As the measurements took 8 hours, rats were intensively monitored and their temperature was kept constant at 37,2±0,1℃ and bre athing rate at 57±3 breaths per minute. DTI maps were first calculated using in house developed Matlab routines. Images were accurately coregistered using non-linear warping allowing voxel-wise statistical mapping of tensor invariant differences between the control and HD groups (Fig 1-2B).

Results & Conclusions: Rat models of HD clearly showed enlarged ventricles ipsilateral to the lesion side; whereas SHAM operated animals did not show clear anatomical or structural changes. Figure 1 shows the mean First Eigenvector FA (FEFA) map of the HD (left) and control group (right) showing morphological changes at the affected striatum (white arrow).

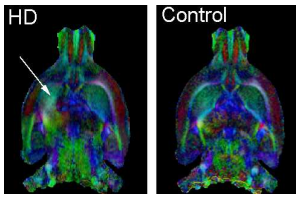

Figure1: FEFA map in HD (left) and controls (right)

Statistical analyses between the control and HD groups showed that the mean and radial diffusivity (RD) but not the Fractional Anisotropy (FA) increased significantly in both the striatum (str) and cortex (ctx) ipsilateral to the lesion side, as a consequence of degeneration of the striatial and cortical neurons in response to the QA exitotoxicity (Fig 2). In addition, FA was significantly decreased in the external (ec) and internal capsule (ic) ipsilateral to the lesion side (Fig2B: FA). As the radial diffusivity was significantly increased (Fig2B: RD). These white matter changes are probably related to demyelization.

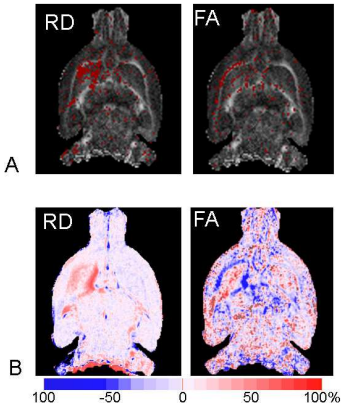

Figure 2A, Statistical mapping of RD and FA: red spots show significant changes between controls and HD; 2B, percentual differences between the control and HD group, blue means decreased RD (left) or FA (right), red indicates increased values in HD as compared to controls.

This study was funded in part by the EC - FP6-project DiMI, LSHB-CT-2005-512146 and SBO IWT Flanders.

Evidence of invasion by labeled stroma stem cells of hydrogel-foam scaffold

Bogaert A.[1], Potier E.[3], Méric P.[1], Petite H.[3], Rivière C.[2], Gillet B.[1]
1 laboratoire de RMN biologique, ICSN, CNRS, Gif sur Yvette.
2 Laboratoire des milieux désordonnés et hétérogènes, CNRS, Paris;
3 Laboratoire de biomecanique et biomateriaux osteo-articulaires UMR7052, CNRS, Paris

Background: Stem cell therapy of skeletal tissues involves the transplantation of stem cells to the tissues that have been damaged by injury or disease. The preferred source of skeletal stem cells is the bone marrow because it contains adult stem cells, which can be easily driven towards a bone phenotype. These cells are placed in a biomaterial scaffold used to promote cells adhesion, proliferation and differentiation as well as encourage vascular invasion and ultimately new bone formation *in vivo*.

Aim: In order to be detected by MRI (which is a non-invasive method, appropriated to follow their evolution *in vivo*) stem cells were labeled by anionic superparamagnetic nanoparticles.
The final aim of this study is to follow the cell therapy efficiency. The aim of this presentation, which is the first step of the total study is to differentiate this labeled stem cells from the biomaterial scaffold, and to follow their evolution in function of time.

Methods: The used cells were human marrow stromal stems cells, obtained from bone marrow of human shinbone. The used nanoparticles are anionic and are internalized by endocytosis. The labeling was carried out by incubation of the stems cells in a “proliferating” state, during 20 min at 37℃ in a citrated 5mM RPMI solution of these nanoparticles. This labeling was checked by measuring the iron content by magnetophoresis and EPR.
Acrylonitrile-sodium methallylsulfonate copolymer (commercially called AN69) exhibits an excellent biocompatibility. The AN69 was used in the form of hydrogel-foam, in order to investigate the possibility of forming three-dimensional scaffolds for bone-tissue engineering. The mean porosity of these hydrogel-foams was (200µm, 500µm, 1mm, without porosity = « full »)
The experiments were carried out on a “Wide bore” 9.4 T vertical magnet VARIAN Inova equipped with gradient coils (2T/m), and using a 8 mm diameter “loop-gap” coil.

Results: Measurements on cell culture after labeling by nanoparticles have shown that labeling did modify neither the cell viability nor their ability to proliferate.
T2 and T1 measurements on « full » AN69 sample, allowed to optimize experimental parameters for studying variable porosity hydrogel-foams. Three porosity types were selected, and seeded with labeled cells at different concentrations, then fixed (PAF 0.1%).

Conclusions: MRI study and 3D reconstruction were used to choice the optimum experimental conditions to track the cell evolution in the AN69 during experiments of dynamic cell. Cell concentrations of 10^6 and 10^5/ml and porosity types of 1mm and 500µm will be chosen for in vivo studies on animal model.

In Vivo Imaging of Dendritic Cell Traffic to the Lymph node

Liora Shiftan and Steffen Jung
Department of Immunology, Weizmann Institute of Science.

Background: Dendritic cells (DC) are short-lived, highly phagocytic cells, which serve as the "gate-keeper" to alarm the immune system in case of pathogen encounter. Tissue DC, which engulf antigen in combination with pathogen signatures “mature” by shutting off their phagocytic potential, start to express surface MHC and costimulatory molecules and migrate via the afferent lymphatics to the lymph nodes (LN). Once they arrive in the nodes, they have become antigen presenting cells with unrivaled potency to stimulate or “prime” naïve T cells.

Aim: To use Magnetic Resonance Imaging (MRI) to study parameters controlling DC maturation and migration dynamics en route to the LN.

Method: Paramagnetic Streptavidin (SA)-beads (1-4 micron) were injected to the hind limb of BALB/c mice. Phagocytic DC were marked for MRI by uptake of these beads. Uptake was further boosted and specified by using receptor-mediated endocytosis (1). Cells were followed using MRI 24h and 48h after the injection. From the MR images R_2 values were calculated.

Results: As revealed by the *in vitro* DC culture, the analysis of excised lymph nodes, and in the *in-vivo* scans, DC engulfed the beads very efficiently. Importantly, only in the mouse that received the beads in conjunction with LPS (a potent immuno-stimulatory pathogen signature) beads could be detected in the tissue-draining LN. In contrast, in mice that received the beads without LPS the bead deposit remained exclusively at the site of injection.

Conclusions: Our results suggest that the SA-coupled magnetic beads do not stimulate DC maturation, but addition of LPS mobilizes DC to migrate to the LN. The beads used in this study are too big to move on their own to the LN (2). Since DC are the only cells known to internalize particles and migrate, we conclude that the dots that we detected in the LN are DC-associated. In future experiments we will couple the paramagnetic beads to stimulatory entities (anti-CD40) as well as fluorescent dyes in order study DC maturation, transit and selection of specific targeted LN, using MRI and 2 photon microscopy.

References:

1. Ahrens, E. T., M. Feili-Hariri, H. Xu, G. Genove, and P. A. Morel. 2003. Receptor-mediated endocytosis of iron-oxide particles provides efficient labeling of dendritic cells for in vivo MR imaging. *Magn Reson Med 49:1006*.
2. Sai T. Reddy , Annemie Rehor, Hugo G. Schmoekel, Jeffrey A. Hubbell , Melody A. Swartz In vivo targeting of dendritic cells in lymph nodes with poly(propylene sulfide) nanoparticles. J Control Release. 2006 Mar 8;

Diagnosis of peritonitis using near infrared optical imaging of *in vivo* labeled macrophages

Marcus-René Lisy, Ph.D.; Elisabeth Schüler cand. Med.; Ingrid Hilger, Ph.D.; Werner A. Kaiser M.D., M.S.
Institute for Diagnostic and Interventional Radiology, Friedrich-Schiller-University Jena, Erlanger Allee 101, D-07747 Jena, Germany

Purpose: To noninvasively detect early stages of peritoneal inflammation with fluorooptical methods by *in vivo* labeling of macrophages using a near infrared fluorescent dye.

Methods and Materials: Uptake of the near infrared fluorochrome DY676 (Dyomics, Jena, Germany) by mouse macrophages *J774A.1* has been tested in vitro. Peritonitis was induced in 6 NMRI-mice by intraperitoneal injection of 3 mg zymosan A. After intravenous injection of 55 nmol fluorochrome per kg body weight, imaging was performed using the whole body small animal near infrared fluorescence (NIRF) imaging system (bonSAI, Siemens, Erlangen, Germany) at short exposure times of 0.5 s. *In vivo* data were confirmed by *ex vivo* investigation of isolated peritoneal macrophages with NIRF imaging and confocal laser scanning microscopy.

Results: Fluorochrome was found to be taken up by macrophages and stored within intracellular compartments. Qualitative and quantitative analysis of NIRF images of whole mice with peritonitis revealed a significant increase of fluorescence intensities in the ventral cavity by factor 4.6 from 188 ± 41 arbitrary units in control animals to 869 ± 151 arbitrary units in diseased mice that have received fluorochrome intravenously. Ex vivo imaging of opened mice and confocal laser scanning microscopy of isolated peritoneal macrophages evidenced involvement of those cells in imaging.

Conclusions: Diagnosis of peritonitis by near infrared optical imaging of *in vivo* labeled macrophages is feasible, indicating that early stages of inflammation could be detected by the proposed diagnostic method.

MicroPET-based Imaging of Endogenous Gene Expression in Transgenic APP23 Mice

Galldiks N[1,4], Heneka MT[5], Winkeler A[1,3], Rüger MA[1,3], Bauer B[2], Küstermann E[2], Hoehn M[2], Heiss WD[1-4], Jacobs AH[1-4]
[1]Laboratory for Gene Therapy and Molecular Imaging, [2]MPI for Neurological Research, [3]Center of Molecular Medicine (ZMMK), Departments of Neurology at the Universities of [4]Cologne and [5]Münster, Germany. Andreas.Jacobs@pet.mpin-koeln.mpg.de

Background: APP23 transgenic mice develop Aβ deposits in neocortex and hippocampus which stimulate local inflammation in Alzheimer's disease (AD). Noradrenergic depletion by Locus coeruleus (LC) degeneration due to neurotoxin *N*-(2-chloroethyl)-*N*-ethyl-2-bromobenzylamine (DSP4) potentiates Aß-induced cortical inflammation. Although known for several decades that LC degeneration occurs early in AD, the contribution of LC degeneration to AD pathogenesis remains unclear.

Methods: MicroPET imaging was performed in non-treated APP23 mice (n=4) and in APP23 mice with DSP4-treatment (n=4) 1, 3.5 and 7 months after treatment, respectively, with 2-[^{18}F]fluoro-2-deoxy-D-glucose ([^{18}F]FDG) for the assessment of cerebral metabolic rate of glucose (CMRGlc), with [^{11}C]flumazenil ([^{11}C]FMZ) to study neuronal integrity, and with [^{11}C]N-methyl-4-piperidyl-acetate ([^{11}C]MP4A) to evaluate acetylcholine-esterase (AChE) activity. Tracer injections were performed under halothane anaesthesia by intravenous application of 200µCi [^{18}F]FDG, [^{11}C]FMZ and [^{11}C]MP4A, respectively. During tracer uptake mice were conscious. Subsequent neuroimaging was performed under ketamine/xylazine anaesthesia 30min after tracer-injection. Maximum a posteriori (MAP) reconstruction was performed without scatter and attenuation correction. Data were evaluated by regions of interest (ROI) analysis and cortex-to-cerebellum ratios were calculated. To ensure proper ROI placement, microPET images were coregistered with high resolution magnetic resonance brain images (7Tesla).

Results: 1 month after DSP4 treatment FMZ-binding and AChE activity was significantly reduced in DSP4-treated APP23 mice in comparison to mice without treatment ($p<0.05$; t-test). 3.5 and 7 months after DSP4-treatment FMZ-binding and AChE activity remained significantly decreased, and additionally, the CMRGlc was significantly reduced in DSP4-treated APP23 mice in comparison to mice without treatment ($p<0.05$; t-test).

Conclusions: MicroPET-based imaging of endogenous gene expression allows non-invasive quantification of disease-related imaging markers in APP23 mice. With appropriate imaging markers microPET shall allow rapid phenotyping of mouse models for neurodegenerative disease as well as assessment of therapeutic effect. MicroPET data support hypothesis that LC degeneration may contribute to the pathogenesis of AD.

Multi-modal Imaging of C17 Cells

Klein M, Waerzeggers Y, Winkeler A, Li HF, Himmelreich U, Hoehn M, Heiss WD, Jacobs AH

Laboratory for Gene Therapy and Molecular Imaging, Max-Planck-Institute for Neurological Research, Cologne, Germany

Introduction: Neuronal stem cells (NSC's) or primary neural progenitor cells (NPC's) have the ability to specifically migrate towards sites of CNS injury like tumors (1), neuroinflammation or stroke (2). These cells are also able to integrate into the host cytoarchitecture and can be engineered to disseminate bioactive molecules and viral vectors (3). Because of this exceptional migratory potential these NSC's or NPC's seem to be highly attractive experimental tools for vector-mediated gene therapy of cerebral glioma (4). However, before designing a clinical study-protocol, non-invasive monitoring of the used genetically engineered progenitor cells and of their therapeutic potency have to be addressed in preclinical studies.

Aim: The purpose of this study is multi-modal, non-invasive monitoring of C17 progenitor cells, C17 progenitor cell migration and of C17 progenitor cell mediated gene therapy of intracranial gliomas using PET, MRI and BLI.

Material and methods: For PET-imaging of ex-vivo labeled C17-TIG cells, cells were incubated with ^{124}I-FIAU (0.5 mCi, 4 h), washed and implanted into subcutaneous growing human Gli36dEGFR gliomas in nude rats (n=4) at different concentrations (10^4,10^5,10^6). Unlabeled C17-TIG cells (10^6 cells; n=3) served as negative control. To serve targeted application of cells into viable tumor tissue, location and viability of tumors were assessed by means of MRI and multimodal micro-PET imaging (^{18}F-FDG, ^{11}C-MET or ^{18}F-FLT).
For multi-modal imaging of C17 progenitor cell migration, C17-LITG cells ($2x10^5$ cells) were injected into the left striatum of nude mice (n=4), contra lateral to injected Gli36dEGFR cells. To find the optimal migration conditions glioma cells ($1x10^5$ cells) were injected prior (7d) or simultaneous with the progenitor cells. For imaging cell migration, serial BLI and ^{18}F-FHBG-PET images were conducted. Glioma growth was verified with ^{18}F-FLT PET and MRI.

Results: Prelabeled C17-TIG cells were visualized directly after implantation at all cell concentrations with the intensity being proportional to the number of implanted cells. ^{124}I-FIAU signal intensity decreased over time more rapid than the decay of radiotracer. 24 hours after injection the remaining radioactivity was 18,0 % (42,0 %; 60,1 %) of the expected value for 10^4 (10^5; 10^6) cells. ^{18}F-FHBG PET detected 10^7 cells of both cell lines 24 hours after transplantation in a single animal.
First BLI migration experiments showed evidence of C17 cell migration towards ic gliomas. This slight migration could be visualized by BLI, while the tumor could be seen by PET and MRI. No PET signal could be obtained from the migrating cells, most likely due to the undisturbed blood brain barrier in this area. Other experiments, where the C17 LITG cells were implanted into a preexisting tumor, showed PET-signals, too.

Conclusion: ^{124}I-FIAU pre-labeled C17-TIG cells can be visualized by PET, the detection level being 10^4 cells. The relatively fast decline of ^{124}I-FIAU signal intensity suggests cell death, cell wash out or cell migration from the injection site. Signs of intratumoral cell migration could not be observed with µPET, however C17 cell migration towards ic gliomas could be visualized by BLI.

References:

1. Aboody K, Brown A, Rainov NG, Bower KA, Liu S, Yang W, Small JE, Herrlinger U, Ourednik V, Black PMcL, Breakefield XO, Snyder EY. (2000) Neural stem cells display extensive tropism for pathology in adult brain: evidence from intracranial gliomas. *Proc. Natl. Acad. Sci.* 97:12846-12851
2. Hoehn M, Kustermann E, Blunk E, Wiedermann D, Trapp T, Wecker S, et al (2002) Monitoring of implanted stem cell migration in vivo: a highly resolved in vivo magnetic resonance imaging investigation of experimental stroke in rats. *Proc. Natl. Acad. Sci.* 99:16267-72
3. Snyder EY, Deitcher DL, Walsh C, Arnold-Aldea S, Hartwieg EA and Cepko EL (1992) Multipotent neural cell lines can engraft and participate in development of mouse cerebellum. *Cell* 68:33-51
4. Benedetti S, Pirola B, Pollo B, Magrassi L, Bruzzone MG, Rigamonti D, Galli R, Selleri S, Di Meco F, De Fraja C, Vescovi A, Cattaneo E and Finocchiaro G (2000) Gene therapy of experimental brain tumors using neural progenitor cells. *Nature Med.* 6:447-450

Primary mesenchymal stem cells in small animal models

S. Grüner, S. Schindler, S.Tokalov, Y. Deuse, G. Wolf, N. Abolmaali
ZIK OncoRay, Medical Faculty Carl Gustav Carus, TU Dresden, 01307 Dresden, Germany

Background: Bone marrow (BM) mesenchymal stem cells (MSCs) are adult pluripotent cells that are considered to be an important resource for cell-based diagnostics, particularly for MR imaging, and for therapy [1, 2]. The analysis of MSCs frequency in BM tissue of aging animals and development of their best growth conditions is important for an optimized applicability in research and may become essential for understanding the future clinical potential of MSCs.

Aim: The purpose of this study was to optimize protocols to accomplish a primary MSCs culture from rats.

Methods: Animal experiments were performed with rats of different weight: 92±5 g (19 rats), 147±3 g (18), 210±3 g (10), 268±8 g (9) and 381±22 g (6) and were approved in accordance with institutional guidelines and the German animal welfare regulations. BM was removed from both femurs and tibias. Mononuclear cells (MNCs) were enriched from other BM cells using density gradient centrifugation. Additionally, the capability of MSCs to attach to fibronectin-coated culture flasks was utilized to separate them from the non attaching hematopoietic cells. Different culture medias like low-glucose Dulbecco's Modified Eagle Medium (Invitrogen, Germany), low-glucose Dulbecco's Modified Eagle Medium + VEGF, Endopan and Panserin 401+Panexin D (all PanBiotech GmbH, Germany), EBM®-2 (Cambrex, USA) and Endothelial Cell Growth Medium MV2 (Promocell, Germany) were tested to determine the best growth conditions for MSCs. Cell viability, the expression of several FITC stained surface antigens (CD4, CD11a, CD11b, CD25, CD31, CD44, CD45, CD90, CD105) as well as cell cycle analyses (PI staining) were performed using flow cytometry (CyFlow, Partec, Germany).

Results: As expected from the maturity of the immune system and the age of the rats, flow cytometry analysis revealed significant ($p<0.01$) proportional reduction of MNCs in the BM as compared to other white cell lineages. Comparing the youngest and the oldest rats, the percentage of MNCs and of granulocytic cells changed from 65%±1 to 48%±3 and from 33±1% to 49±3% (r=0,67). MNCs revealed fibroblast-like morphology of MSCs in 3-5 days of culture. Endopan promoted the best proliferation of MSCs (20±5% of them were in S phase in 2 weeks of culture), while the other media tested had less or even no effects on cell growth. MSCs were unique in their phenotypes and they were positive for CD44, CD90, CD105, and negative for typical hematopoietic and endothelial markers: CD4, CD11a, CD11b, CD25, CD31 and CD45. So far, the survival time of this primary cell culture is 4 months.

Conclusions: The relative ease of isolating MSCs from bone marrow and the great plasticity of the cells with unique growth, phenotypical and cytochemical characteristics make them an attractive cell type for the development of new cell-based diagnostics, in particularly MRI, and therapeutic strategies using small-animal models. Also the diverse responses of MSCs to different culture media provide a clue for the selection of optimal multiplication and maintenance of MSCs.

References:

[1] Le Blanc K, Pittenger MF; *Cytotherapy* 7: 36-45 (2005)
[2] Hung CJ. et al.; *Clin. Cancer Res.* 11: 7749-7756 (2005)

MRI-based Experimental Tools to Asses Brain Function in Regenerative Therapies

Ramos-Cabrer P, Justicia C, Wiedermann D, Hoehn M
In-vivo-NMR Laboratory, Max-Planck-Institute for Neurological Research, Cologne

Background: Regenerative therapies are expected to play an important role in the recovery of brain functional losses following stroke. The non-invasive assessment of functional recruitment of tissue grafts into existing neuronal networks and its influence in the recovery of functional losses are essential aspect of these therapies.

Aim: To describe a recently developed longitudinal fMRI protocol for the rat (1,2), in combination with electrophysiological measurements and behavioral test, to study functional outcome of the animals at different time points after stroke, and to use these tools to study spontaneous recovery on untreated animals (required to establish a baseline for future studies with stem cells).

Methods: Wistar rats (n=22) submitted to 60 min occlusion of the middle cerebral artery. Under medetomidine anesthesia, T2, CBF and BOLD-fMRI longitudinal studies were performed for each animal one week before, and 2 days, 1, 2, 3, 4 and 7 weeks after MCAO. All experiments were conducted at 7T. Functional BOLD imaging was achieved acquiring multislice SE-EPI images during electrical forepaw stimulation. Both forepaws were alternatively stimulated (2 mA constant current pulses) with a block paradigm (5x[45s rest + 15s stimulation] periods). Somatosensory evoked potentials (SSEPs) were recorded in the same experimental sessions, placing subcutaneous electrodes over both S1 cortical areas of the brain. Images were analyzed using Image J and STIMULATE software.

Results: Before MCAO, normal BOLD and SSEP recordings were obtained during forepaw stimulation for all animals. Following the ischemic insult, three different situations were observed: 1) a group of animals showed unaltered BOLD and SSEP signals. 2) A second group showed normal recordings in the healthy brain hemisphere but presented a transient loss of BOLD signal in the affected hemisphere, accompanied by a distortion (amplitude and latency) of the SSEPs. In this group normal activity (as determined by both BOLD and SSEP) was regained in the affected hemisphere 2 to 3 weeks after MCAO. 3) A third group suffered a total and permanent loss of both BOLD and SSEP signals in the affected hemisphere.

Conclusions: The usefulness of the described protocol has been proved. In this 7 weeks longitudinal study, only function recovery but no signs of reorganization (i.e. shift of functional representation fields) was observed. The observation of abnormal electrical activity in S1, together with a lack of BOLD, two to three weeks after stroke, provides an early indication of late functional recovery following focal cerebral ischemia in the rat.

References:

[1] Weber R, et al; *Neuroimage* 29:1303-10 (2006)
[2] Ramos-Cabrer et al; *NMR Biomed*. 18:440-6 (2005)

A novel in vivo animal model for human myeloma based on Bioluminescence Imaging (BLI) of tumor cell growth and response to experimental therapy

Rozemuller H[1 *], van der Spek E[2 *], H. Bogers-Boer L[2], Zwart MC[1], Bloem AC[1], Lokhorst HM[2], and Martens ACM[1]
[1]Department of Immunology, University Medical Center Utrecht , Utrecht, The Netherlands.[2] Department of Hematology, University Medical Center Utrecht , Utrecht, The Netherlands.

Background: Preclinical testing of new therapeutic strategies or new cytotoxic drugs for the treatment of multiple myeloma (MM) requires animals models that closely resemble human disease and that allow quantitative evaluation of the applied therapy. Although human myeloma cells can engraft in immune deficient mice, they show a random distribution and it is not possible to monitor tumor growth nor response to experimental treatment because adequate methods for repeated sampling of the tumors are lacking.

Aim: The aim of our study was to explore the use of bioluminescence imaging (BLI) technology in combination with luciferase gene marking to follow homing and outgrowth of luciferase marked human myeloma cells and to develop this into an animal model for preclinical testing of potentially new treatment modalities.

Methods: Human MM cells (i.e. U266 or RPMI-8226/S cells), both of human origin, were injected i.v. into RAG2γ double knock-out mice. These mice are immune deficient because they lack T-, B and NK cells and the mice easily accept human cells (van Rijn et al., Blood 2003, Rozemuller et al., 2004). Human MM cells were transduced with a GFP-Firefly luciferase (fLuc) fusion gene. When luciferase converts the substrate luciferin, photons are emitted that can be registered by using sensitive CCCD cameras. The absolute number of photons that are produced correlates (in our application) with the total or local tumor mass.

Results : Mice were injected i.v. with GFP-fLuc $2x10^6$ cells MM cells (U266 or RPMI8226/S) and then imaged weekly using BLI. Engraftment and outgrowth occurred in all mice but it was limited to the bone marrow compartment, thus resembling human MM. FACS analyses and histology revealed the presence of human CD45, CD138, CD38 and GFP positive myeloma cells in a variety of examined bone specimen. Infiltration into other organs was not observed. Within 2 weeks after injection significant BLI signals were detectable. Per mouse 5-10 foci showed luciferase activity, predominantly in the pelvic region, skull, limbs and the spine. After 9-12 weeks all mice were killed due to excessive tumor growth. Growth curves that were made on the basis of subsequent BLI images revealed exponential growth of the total tumor mass per mouse as well as for the individual foci of MM growth in each mouse. All curves show similar growth kinetics with an average population doubling time of approximately 5-6 days. The range in which tumor growth can be monitored with BLI (and as a consequence also the response to treatment) spans 3-4 decades. The BLI signals could postmortem be confirmed by flow cytometry of GFP+ cells in affected bones. Therapeutic intervention with total body irradiation led to a two log reduction in tumor load reflected in a tumor growth delay of 5-6 weeks. This was the case for the total tumor load per animal as well as for the individual foci of multiple myeloma growth.

Conclusions: Our results illustrate the major advantage of using BLI for quantitative evaluation tumor growth and for evaluation of the effect that a given treatment has on the tumor progression. Thus, we have developed a novel in vivo model to study the characteristics of homing and outgrowth of MM and we show that it can be used for quantitative evaluation of the efficacy of the therapeutic intervention applied.

CANCER

Preclinical SPECT/CT Analyses of Radiofolates Combined with Chemotherapeutics

Müller C[1], Hohn A[1], Schibli R[1,2]
[1]*Center for Radiopharmaceutical Science ETH-PSI-USZ, Villigen, Switzerland*
[2]*Dept. of Chemistry and Applied Biosciences ETH Zurich, Zurich, Switzerland*

Background: The folate receptor (FR) is overexpressed on a variety of tumors. Therefore, folate-based radiotracers can be used to specifically detect FR-positive neoplastic tissues[1]. However, the tumor (tu) uptake of radiofolates is relatively low whereas the accumulation in FR-positive kidneys (ki) is high due to substantial expression of FR in the brush-border membrane. This gives rise to unfavorable high dose burden to renal tissue and generally low tu/ki ratios respectively.

Aim: The aim of this study was to enhance FR-assisted tumor uptake in order to improve the tu/ki ratios of radiofolates. This should be achieved with chemotherapeutic like antifolates, which interfere with the cell's folate metabolism. Results have shown that FR is unregulated in cells, which were treated with antifolates [2]. We reasoned to administer the antifolate pemetrexed (PMX) in tumor bearing mice. Differences between animals with and without PMX administration should be assessed via *in vivo* SPECT and *ex vivo* biodistribution experiments.

Methods: For these studies the novel SPECT tracer ^{99m}Tc-PAMA-folate recently synthesized in our laboratories was used[3]. Female athymic nude mice bearing KB-cell xenografts (human nasopharyngeal cancer cell line expressing FR) were used. PMX (400 □g/mouse) and ^{99m}Tc-PAMA-folate (0.3-500 MBq) were administered via the tail vein. PMX was injected at different time points (15 min, 30 min, 1h, 2h) prior to administration of ^{99m}Tc-PAMA-folate. Combined SPECT/CT imaging experiments were performed with the 'X-SPECT™'-system (Gamma Medica Inc.).

Results: The tumor uptake of ^{99m}Tc-PAMA-folate in mice without administration of PMX reached a maximum of 2.33 ± 0.36 %ID/g at 4 h p.i. At the same time activity in the kidney was high 17.3% ± 0.3 %ID/g resulting in a tu/ki ratio of only 0.12 ± 0.02. Mice pre-injected with PMX did not display enhanced tumor. If the PMX was pre-injected 1 h before ^{99m}Tc-PAMA-folate the amount of radioactivity in the tumor was 2.21 ± 0.34 %ID/g (4 h p.i.). However, a significant reduction of radioactivity in the kidneys was observed (1.14 ± 0.18 %ID/g, 4 h p.i.). This gave rise to an unprecedented high and favorable tu/ki ratio of 1.99 ± 0.51. At the same time other tu/organs and tu/tissue ratios were almost identical with those in the control animals. SPECT analyses (24 h p.i. of ^{99m}Tc-PAMA-folate) confirmed the *ex vivo* data: In mice receiving PMX the radioactivity in the kidney was virtually absent but tumors were clearly visible. High-resolution SPECT-scans using a 1 mm pinhole collimator revealed inhomogeneous distribution of the radiotracer in the tumors (with and without PMX) as well as predominant accumulation in the renal cortex (without PMX only).

Conclusions: Administration of PMX reduced significantly the specific unwanted accumulation in the renal tissue but did not result in an increased tumor uptake of ^{99m}Tc-PAMA-folate. Thus, application of radiolabeled folate derivatives in combination with antifolate could potentially reduce significantly the dose burden to critical organs such as kidneys in humans. These findings are very important for better cancer tissue localization in abdominal regions as well as for folate based radionuclide therapy in the future.

References:

[1] Leamon CP, Low PS; *Drug Discovery Today*. 6:44-51 (2001).
[2] de Nonancourt-Didion M et al.; *Cancer Letters.* 171:139-145 (2001).
[3] Müller C et al.; *Eur. J. Nucl. Med.* in press.

In vivo targeting of EGFR expressing tumour cells using ^{99m}Technetium labelled anti-EGFR nanobody™ and pinhole SPECT

Tchouate G.O[1], Huang L[2], Caveliers V[1], Gallez C[1], Vanhove C[1], Keyaerts M[1], Revets H[2], De Baetselier P[2], Bossuyt A[1], Lahoutte T[1]

[1]Division of Nuclear Medicine, In Vivo Cellular and Molecular Imaging Center, University Hospital Vrije Universiteit Brussel (AZ-VUB) and [2]Department of Molecular and Cellular Interactions, Flanders Interuniversity Institute for Biotechnology, Vrije Universiteit Brussel, Belgium.

Background: Nanobodies™ are the smallest intact antigen-binding fragments of naturally occurring camelid heavy-chain antibodies that are fully functional. Their small size (15kDa), high solubility, stability and pharmacokinetic profile favour their use as imaging agents. The aim of this study was the assessment of the uptake of radiolabelled Nanobody™ directed against EGFR by tumour cells expressing different levels of EGFR.

Materials and methods: An EGFR-specific Nanobody™ (heavy-chain antibody fragment) was labelled through its hexahistidine-tag with ^{99m}Tc-tricarbonyl intermediate $[^{99m}Tc(H_2O)_3(CO)_3]^+$ which was synthesized using the commercial available Isolink® labelling kit. In vivo targeting properties of ^{99m}Tc-antiEGFR was evaluated in nu/nu mice bearing A431 skin carcinoma (n=7) and DU145 prostate carcinoma xenograft (n=6) that express approximately $2x10^6$ and $2x10^5$ EGFRs per cell respectively. Pinhole-SPECT was performed 3 h post intravenous administration of average 120 MBq (75-163) ^{99m}Tc-antiEGFR. The acquisitions were performed using a dual-headed gamma camera (e.cam^{180}, Siemens) mounted with pinhole collimators (1,5mm pinhole opening). The images were acquired over 360° in 64 steps of 30s. Images were reconstructed using an iterative algorithm (PHOSPHOUR, Vanhove C.).
Image quantification was performed using AMIDE Medical Image Data Examiner software. Ellipsoid regions of interest were drawn around the tumour and the total body. Tumour uptake was calculated as the ratio of the counts in the tumour divided by the injected dose and normalised for the tumour volume (%ID/cm^3 tumour). Tracer retention was calculated by dividing the total body counts at 3h by the injected dose.

Results: The biodistribution of the tracer showed marked renal activity in all mice (n=13). Tumour uptake of the radiolabelled Anti-EGFR was higher in A431 xenografts (n=7) expressing high level of EGFR and than those bearing DU145 carcinomas cell line (n=6) with low EGFR expression. The average uptake was 5,02+/-1,25 and 1,88+/-0,93%/cm^3 respectively ($p<0,01$). The retention of the tracer in A431 and DU145 xenografts at 3hours post injection was 86%+/-6,03 and 67,2+/-5,83 respectively($p<0,01$).

Conclusion: Radiolabelled antiEGFR Nanobodies™ are potential probes for the visualisation of EGFR expressing tumour in vivo. The uptake is related to the expression level of the receptor.

References:

1. MacDonald A., Chisholm G.D. & Habib F.K. (1990) Production and response of a human prostatic cancer line to transforming growth factor-like molecules, Br. J. Cancer. 62(4):579-584.
2. Haigler H., Ash J.F., Singer S.J., Cohen S. (1978) Visualization by fluorescence of the binding and internalization of epidermal growth factor in human carcinoma cells A-431, Proc. Natl. Acad. Sci. USA 75(7):3317-3321.
3. Revets H, De Baetselier P, Muyldermans . Nanobodies as novel agents for cancer therapy. Expert Opin Biol Ther. 2005 Jan;5(1):111-24.
4. Christian Vanhove, Michel Defrise, Philippe R. Franken, Hendrik Everaert, Frank Deconinck, Axel Bossuyt Interest of the ordered subsets expectation maximization (OS-EM) algorithm in pinhole single-photon emission tomography reconstruction: a phantom study. Eur J Nucl Med. 2000 Feb;27(2):140-6.

Feasibility, reliability and potency of recurrent *in vivo* imaging for non-invasive follow-up of experimental hepato-cellular carcinomas (HCC) in rats by combination of hepatocyte-selective contrast agent and micro-CT detection

Youssef C[1], Bouhadjar M[1], Osswald AB[1], Balboni G[2], Mutter D[1], Marescaux J[1], Soler L[1], Aprahamian M[2]

[1] IRCAD, 1 place de l'hôpital 67000 Strasbourg, France and [2] U701 Inserm, DKFZ, Heidelberg, Germany

Aim: The primary goal of this study was to establish proof that a simple recurrent procedure combining micro-CT scanning and iodinated triglyceride (ITG) packed in the lipophylic core of synthetic chylomicron remnants as a contrast agent is a convenient and reliable imaging tool for *in vivo* follow up of the course of HCC under emerging therapeutic managements.

Methods: Orthotopic liver tumours were generated in ACI rats by injection of 2.10^5 Morris Hepatoma cells (from the DKFZ tumour cell library) within either left lateral or medial hepatic lobe. The ITG contrast agent, trade-named Fenestra® (Alerion Biomedical Inc., San Diego, CA), was delivered 9-h prior imaging by a single intra-peritoneal injection (4.5 ml/Kg). It targets normal hepatocytes via its affinity for apolipoprotein-E receptors. Tumour appears thus as a defect within the liver mass on CT-scans performed with a microCAT II (Imtek Inc., Knoxville, TN). Imaging was performed under breath gating to avoid abdominal movements, improving image quality. Indeed, voxel resolution of the reconstructed image can reach 120 μm^3.

Experiments and Results: The accuracy of tumour size measurements was assessed by a two-step experiment. At first, tumour volumes were calculated ($V = [x.y.z]\square/6$) in one hand from values collected via the 3D set of Amira software (Data Analysis and Geometry Reconstruction v. 2.3, San Diego, CA) on CT scan coronal, axial and sagital slices of the tumours at their maximal dimensions and, in the other hand from direct measurements of the same tumours after euthanasia. A perfect linear correlation ($r^2 = 0.998$, $P<0.001$) was observed between the two methods. Then, we compared tumour volumes calculated from CT scan slices to those obtained from the 3D CTscan image through two original softwares developed by the IRCAD: the 3D-VPM software that gives a clearly delineated 3D volumetric image of the HCC visualized within the hepatic gland, and the 3D-VSP software, providing a numerical volumetric value computed from the number of voxels include in the tumours. This comparison gave also a perfect correlation ($r^2 = 0.997$, $P<0.001$).
The ability of *in vivo* imaging to achieve a non-invasive follow-up of HCC was at last assessed on 16 rats. They were randomly affected to one of the two following: untreated control group and one group submitted to conventional HCC chemotherapy (750 µg/Kg IV of Doxorubicine at 2-week intervals up to a total amount of 3 mg/Kg) as treatment reference. Recurrent CTscans were performed at 2-week intervals from day 7 post tumour induction until death. In this way, each animal of both groups provided sequential information on tumour progression and animal survival. At day 35, mean tumour size reached 4.8 ± 1.2 cm^3 in controls *vs.* 1.9 ± 1.2 cm^3 in treated HCC ($P<0.05$). Medial survival was 58 days for the control group vs. 73.9 days for the treated one ($P<0.05$) and actuarial survival was significantly improved (log rank test, $P< 0.05$).

Conclusion: Long-term follow up of HCC by the mean of *in vivo* molecular imaging using micro CTscan and high affinity liver contrast provides two kinds of long-term information - speed of tumour progression/regression in experimental conditions close to clinic and changes in actuarial survival - constituting a reliable tool for testing new CHC molecular therapies such as anti-angiogenic or anti-growth factor drugs.

Comparison of 99mTc-HYNIC-TOC and 99mTc-HYNIC-TATE suitability for somatostatin receptor scintigraphy in patients with proven GEP-NET tumours.

B.Janota[1], R.Mikolajczak[1], Jerzy Walecki[2], Jarosław Ćwikła[2]
1. Radioisotope Centre Polatom, Swierk, Poland
2. Department of Radiology, Central Clinical Hospital of the Ministry of Internal Affairs and Administration, Warsaw, Poland.

Aim: The aim of our study was to compare the imaging abilities of the new technetium-99m labeled somatostatin analogs, ^{99m}Tc-hydrazinonicotinyl-Tyr^3-octreotide (^{99m}Tc-HYNIC-TOC [^{99m}Tc-TOC]) and ^{99m}Tc-hydrazinonicotinyl-Tyr^3-octreotate (^{99m}Tc-HYNIC-TATE [^{99m}Tc-TATE] in somatostatin receptor scintigraphy (SRS) in patients with confirmed GEP-NET tumours. HYNIC-TOC and HYNIC-TATE were synthesized in our laboratory on solid phase using the Fmoc strategy, followed by the development of kit formulation. The differences in sstr receptor affinity and rate of internalization “in vitro” were the basis for investigation whether the substitution of Thr(ol) in HYNIC-TOC by Thr in HYNIC-TATE had significant influence on “in vivo” results.

Methods: 12 patients (5 male, 7 female; mean age 55years, range 38–75) all had histologically proven GEP-NET, neuroendocrine carcinoma low malignancy (NECLM, WHO type II). Every one had no active treatment during examination. All had routine SSTR due to tumour staging or restaging. Eleven had active disease confirmed in further anatomical and functional imaging, biochemistry and clinical follow-up, one had no active disease.
Each patient received a mean activity of 480-520 MBq ^{99m}Tc-TOC and ^{99m}Tc TATE. Both scintigraphy examinations were performed 2-3 h after injection of radiotracers using standard WB and SPECT techniques in each case. The time interval between the studies using each tracer ranged from 7 to 28 days (mean interval, 12 days). Results: ^{99m}Tc-TOC and ^{99m}Tc TATE showed an equivalent scan result in 11 patients (92%), single case showed discrepancies due to underestimated spread of disease using ^{99m}Tc TATE compared to ^{99m}Tc TOC. In each case the semiquantitative region-of-interest analysis was performed including target to background (lung) ratio T/B. Following structures were analysed: tumour (most active lesion), liver and kidney. In each case mean and median value of uptake were calculated. Mean tumour T/B ratio for TATE -7,25 and for TOC 8,92, liver T/B 4,19 (TATE) and 5,86 (TOC) and kidney 5,88 (TATE) and 4,71 (TOC). Significant difference was noted only within liver (p=0,008 Wilcoxon Matched Pair test) and tendency to higher uptake within kidney (p=0,071 Wilcoxon Matched Pair test). There was no significant difference within tumour.

Conclusion: This study in homogenous group of patients, all with GEP-NET (NECLM) revealed a significant difference between uptake of tracer within liver with no significant difference within tumour and kidney uptake. Both tracers seem to be very promising for detection of sstr positive GEP-NET tumours.

Key Words: ^{99m}Tc HYNIC-TOC, ^{99m}Tc-HYNIC-TATE, somatostatin, scintigraphy

Optical Molecular Imaging of the Female Breast: Value of CT-Laser-Mammography (CTLM) as an Adjunct to Mammography (MG) in the Differentiation of Benign and Malignant Breast Lesions.

D. Flöry, C.C. Riedl, S. Jaromi, M. Fuchsjaeger, C. Reiner, T.H. Helbich;
Department of Radiology, University of Vienna, Vienna, Austria

Purpose: Optical molecular imaging of the female breast allows breast cancer detection using measurements of tissue haemoglobin concentration as a surrogate marker for tumor angiogenesis. The purpose of this study was to evaluate CTLM, a novel optical molecular imaging technology, as an adjunct to MG in the differentiation of benign and malignant breast lesions.

Materials and Methods: In a prospective study, CTLM scans (CTLM scanner Model 1020 by IMDS, Inc. FL), and MG of 410 patients with 421 breast lesions were obtained. Histopathological diagnosis (biopsy, n=143 and/or surgery, n=278) was performed in all cases. The CTLM images were read as an adjunct to MG. ROC curves were calculated for each modality and the combined approach.

Results: Of 421 lesions, 191 (45.4%) were malignant and 230 (54.6%) were benign including 100 invasive ductal carcinoma (IDC), 30 invasive lobular carcinoma (ILC), and 48 ductal carcinoma in situ (DCIS). CTLM was true positive in 127/191 (66.5%) malignant lesions and true negative in 145/230 (63.0%) benign lesions. Sensitivity was higher for invasive cancer (73.0%) than DCIS (47.9%). ROC curves revealed a larger area under the curve (AUC) for the combined approach (0.777) as for MG (0.759) and CTLM (0.646) alone. Sensitivity and specificity for MG were 98.4%, and 22.5% respectively. Missed carcinomas were DCIS in 25 cases and (39.1%), and grade one or two invasive cancer in 26 cases (40.6%).

Conclusion: Our results indicate that optical molecular imaging of the female breast with CTLM is feasibly. CTLM has potential adjuctive value to MG in the differentiation of breast lesions. The majority of missed cancers were noninvasive cancers and high-grade invasive carcinomas.

Optical molecular imaging of the female breast: Imaging findings with CT-Laser Mammography (CTLM) in human breast lesions.

D. Flöry, C.C. Riedl, S. Jaromi, M. Fuchsjaeger, C. Reiner, T.H. Helbich;
Department of Radiology, University of Vienna, Vienna, Austria

Background: Optical molecular imaging of the female breast allows breast cancer detection using measurements of tissue haemoglobin concentration as a surrogate marker for tumor angiogenesis. CT-Laser mammography (CTLM) is a new tomographic breast imaging modality that uses near-infra-red laser light of 808 nm wavelength for breast imaging.

Aim: The purpose of this study was to describe morphological findings in human breast lesions with CTLM.

Materials and Methods: In a prospective study, CTLM scans (CTLM scanner Model 1020 by IMDS, Inc. FL), and MG of 410 patients with 421 breast lesions were obtained. Histopathological diagnosis (biopsy, n=143 and/or surgery, n=278) was performed in all cases. CTLM images were read by radiologists with knowledge of the position of the lesions but who were blinded to histology and morphological findings from mammography. It was assessed whether there was increased absorption, a sign of malignancy, on CTLM and the appearance (volumes or linear branching) and shape (round or irregular) of the lesions. Missed carcinomas were assessed for type and histological grade.

Results: Of 421 lesions, 191 (45.4%) were malignant and 230 (54.6%) were benign including 100 invasive ductal carcinoma (IDC), 30 invasive lobular carcinoma (ILC), and 48 ductal carcinoma in situ (DCIS). Increased absorption was seen significantly more often in malignant (66.5%) than in benign breast lesions (37.0%, $p < 0.05$). Invasive ductal cancer showed most often increased absorption (76.0%), followed by invasive lobular carcinoma (63.3%) and DCIS (47.9%). Common morphological characteristics of increased absorption were “volumes” (91.8% of benign and 89.0% of malignant lesions) with round shape (71.2% of benign and 63.9% of malignant lesions). Missed carcinomas were DCIS in 25 cases and (39.1%), and grade one or two invasive cancer in 26 cases (40.6%).

Conclusion: Common morphological characteristics of increased absorption were “volumes” with round shape. The majority of missed cancers were noninvasive cancers and high-grade invasive carcinomas.

Optical Molecular Imaging of Cancer Using Targeted Contrast Agents

Ebert B[1], Jakob J[2], Licha K[3], Hauff P[3], Perlitz C[3], Klamm U[2], Kemmner W[2], Haensch W[2], Voigt J[1], Moesta KT[2], Schirner M[3], Macdonald R[1]
[1]*Physikalisch-Technische Bundesanstalt, Abbestr. 2 – 12, D-10587 Berlin, Germany*
[2]*Department for Surgery and Surgical Oncology, Charité, Campus Berlin-Buch, Germany*
[3]*Schering AG, Research Laboratories, Berlin, Germany*

Background: Early detection and therapy of cancer and pre-cancerous lesions is essential for disease free and overall survival. Sensitive planar fluorescence imaging in reflection geometry is a widespread technique in the context of molecular imaging to improve sensitivity and specificity of cancer screening[1,2]. Diffuse optical imaging without contrast agents in general has not sufficient sensitivity and specificity for the detection of cancer, yet contrast enhanced optical imaging with targeted or non-specific[3] fluorescent probes may improve the diagnostic capability of optical cancer detection techniques.

Aim: To study the feasibility of a neoangiogenesis-targeted optical imaging approach for the detection of spontaneous breast cancers in transgenic mouse model cancer lesions by wide beam reflectance fluorescence imaging *in vivo*.

Methods: Studies were carried out in females of the transgenic mouse strains WAP-T/TNP. The mice developed spontaneously a total of 20 palpable tumours of mammary glands (diameter
2 mm to 10 mm) within 3 to 9 month after lactation. As a conjugated molecular probe an indotricarbocyanine dye coupled to an anti-EDB-FN single chain antibody fragment was used. Following conjugated-dye injection, all tumours were detectable based on a clearly enhanced fluorescence signal at the tumour site. Fluorescence images were obtained in reflection geometry using a pulsed solid state laser system for wide beam excitation and an intensified CCD camera for observation. Dye accumulation was detected immediately after injection and up to 48 h post injection.

Results: All 20 tumors were clearly demarcated 6 h after injection of the specific contrast agent. The highest contrast was reached about 30 min after injection. The urogenital tract was demarcated as well due to renal elimination of the contrast agent. On contrary, application of the free (i.e. non-specific) dye did not lead to significant contrast. Tumours and mammary glands without contrast agent were also poorly or even not demarcated. Histological examination demonstrated invasive epithelial tumours of the mammary gland at the sites with enhanced fluorescence, which were similar to invasive ductal carcinoma. Approaches to determine the concentration of contrast agents in tissue covered by skin will be discussed.

Conclusions: Optical molecular imaging using specific contrast agents was applied for sensitive detection of breast cancer, which reveals potential for breast cancer screening based on fluorescence mammography. Indotricarbocyanine dye anti-EDB-FN antibody single chain fragment conjugates demarcate small tumours (2 mm) in transgenic animal models. The presented transgenic murine lines are suited as experimental model to study molecular changes connected with ductal carcinomas in situ (DCIS) and its progression to cancer.

References:
[1] Becker A et al.; *Nature Biotechnol.* 19:327-331 (2001)
[2] Licha K et al.; *J Biomed Optics.* 10:41205-41211 (2005)
[3] Fischer T et al.; *Acad Radiol.* 13:4-13 (2006)

Imaging of early tumor response to tyrosine kinase inhibitors by microSPECT

A. Zannetti[2], F. Iommelli[1], A. Papaccioli[2], J. Sommella[2], P. Ferraro[1], A. Baiano[1], M. Salvatore [1], S. Del Vecchio[1]
[1]University "Federico II", [2]CNR-Istituto di Biostrutture e Bioimmagini. Naples, Italy.

Aim: The aim of our study was to detect early tumor response to tyrosine kinase inhibitors in animal tumor models by non-invasive SPECT imaging with 99mTc-MIBI. Our previous studies showed indeed an increase of 99mTc-MIBI uptake in cultured tumor cells upon exposure to staurosporine.

Methods: A panel of tyrosine kinase inhibitors including gefitinib (ZD 1839, Iressa, EGFR inhibitor), imatinib (STI571, Gleevec, Bcr-Abl inhibitor), ZD6474 (VEGFR-2 inhibitor) has been selected and tested in cultured tumor cell lines and human xenografts. MCF-7, MDA-MB231 and T47D (wild type and Bcl-2 transfected) breast cancer cells, A549 and SKLU-1 lung cancer cells and A431 epidermoid cancer cells were incubated with increasing concentrations of gefitinib, imatinib and ZD6474 and tested for 99mTc-MIBI uptake by 60 min incubation. Then control and Bcl-2 overexpressing T47D cells were subcutaneously injected into opposite flanks of individual nude mice. Imaging studies by microSPECT and biodistribution analysis were then performed with 99mTc-MIBI before and after gefitinib treatment (150 mg/Kg/d p.o. for 3 days).

Results: Gefitinib treatment caused a 2-fold increase of 99mTc-MIBI uptake in all cancer cell lines tested. As compared to untreated control, Bcl-2 overexpressing breast cancer cells showed the highest enhancement of 99mTc-MIBI uptake after treatment with gefitinib, imatinib and ZD6474. All tumor xenografts could be detected after 3 days of gefitinib treatment by microSPECT whereas no tracer uptake was observed in the same tumors at the baseline scan. Consistently, a 2-fold increase of 99mTc-MIBI uptake determined as % ID/g was also found in treated tumors as compared to untreated controls.

Conclusion: Our findings indicate that early tumor response to tyrosine kinase inhibitors can be detected by 99mTc-MIBI scan.

Optimization of dendritic cell labeling for MR tracking in cancer patients after vaccination

P. Verdijk, T.W.J. Scheenen, A.A. Veltien, J.W.M. Bulte, P. Walczak, W.J. Lesterhuis, I.J.M. de Vries, C.J.A. Punt, A. Heerschap, C.G. Figdor

Background: Dendritic cells (DCs) are the professional antigen presenting cells of the immune system. Recent clinical studies indicate that mature DCs are effective cancer vaccines when loaded with tumor antigens[1]. To induce an effective immune response, these cells should migrate to the lymph nodes (LN) to interact with naïve T cells. Monitoring cellular migration in vivo is important to improve the efficacy of DC-based therapies[2]. Recently we demonstrated that DCs labeled with superparamagnetic iron oxide (SPIO) can be imaged and tracked in melanoma patients after intranodal injection[3].

Aim: To demonstrate in detail that DCs can be efficiently labeled with SPIO without affecting DC function and that low numbers of SPIO-labeled DC can be imaged in vitro on a 3T MR whole body scanner using clinically applicable parameters.

Materials and Methods: Autologous DCs were cultured from monocytes obtained from peripheral blood[3] and labeled with the clinically approved SPIO formulation Endorem® by adding various amounts of SPIO to the DC culture one day before adding the maturation factors. Iron contents of DCs were determined by Prussian Blue staining and Ferrozin-based spectrophotometric iron assay. The phenotype, T cell stimulatory function and migratory behavior were determined of both SPIO-labeled and unlabeled DCs. MR imaging of phantoms, containing SPIO-labeled DC in 6% gelatin was performed at 3T and 7T.

Results and Discussion: DCs were effectively labeled with SPIO by adding the particles to the immature DC culture one day before maturation. The iron content per cell increased in a linear fashion with increasing concentrations of SPIO in culture. As at the highest concentration of SPIO (400 μg/ml) the cell viability was decreased, 200 μg/ml of SPIO was chosen as the optimal dose. At this concentration, phenotypic characterization of DC by flowcytometry for DC maturation markers showed that SPIO did not influence DC differentiation and maturation. Furthermore, both the allogeneic and autologous T cell stimulatory capacity of DCs was not changed by the addition of SPIO and the migratory capacity of SPIO-labeled cells was still intact. Cell densities of 100/μl could still be observed in GRE images of phantoms. Using a threshold of 50% signal decrease in a GRE image, which is appropriate for in vivo conditions and signal to noise, we estimate to be able to detect 10^3 DCs/μl if present throughout some adjacent voxels.

Conclusions: DC labeling with SPIO was efficient and did not affect DC function and migration at a concentrations of 200 μg/ml in the medium. Therefore, labeling DC with SPIO particles is a clinically safe method (without the need of adjunct transfection agents) for monitoring cell migration of cell vaccines. Low densities of SPIO-labeled DC can be imaged on the 3T spectrometer, demonstrating its potential for in vivo tracking of SPIO-labeled cells at a therapeutic dose.

References :

1. Schuler G, et al. Curr Opin Immunol 15:138-147, 2003
2. Figdor CG et al. Nat Med 10:475-480, 2004
3. De Vries IJ, et al. Nat Biotechnol. 23:1407-1413, 2005.

PET guided Chemotherapy - Monitoring Metabolic Effects of Temozolomide Chemotherapy in Malignant Gliomas and of Long-Term Adjuvant Chemotherapy in Patients with Glioblastoma

[1]Norbert Galldiks, [2]Lutz W. Kracht, [1]Lothar Burghaus, [2]Roland Ullrich, [2]Kristina Kesper, [1,2]Wolf-Dieter Heiss, [3]Karl Herholz, [1,2]Andreas H. Jacobs
[1]Department of Neurology, University of Cologne, Germany, [2]Max Planck-Institute for Neurological Research, Cologne, Germany, [3]Wolfson Molecular Imaging Centre, University of Manchester, UK

Background: One general trend in oncology is to monitor biological effects of chemotherapy. [^{11}C]methionine (MET)-PET may be a helpful tool to differentiate responders from non-responders and may provide valuable information for making treatment decisions, especially in non-responders. Therefore, MET-PET might have the potential to predict clinical outcome.

A further focus of interest is the monitoring of metabolic effects in glioblastomas (GBM) when adjuvant temozolomide (TMZ) chemotherapy is been administered longer than 12 cycles; recent TMZ adjuvant chemotherapy recommendations suggest up to 6-12 cycles in the standard dosage after maximal resection of the GBM and concomitant radio-/TMZ-therapy.

Patients and Methods: Sequential MET-PET studies were performed before and after the 3rd cycle of TMZ chemotherapy in 15 patients with malignant gliomas, and in 12 patients also after the 6th cycle. Long term-outcome was assessed by calculating the time-to-progression (TTP) in months.
Additionally, we observed two patients with GBM treated with adjuvant TMZ therapy up to 20 and 27 cycles, respectively. Due to a stable clinical status TMZ was discontinued and reduced, respectively. Three MET-PET follow-up scans in both patients were performed until the change of adjuvant therapy regimen, and, to image these effects, two additional MET-PET scans were performed afterwards in both patients. Additionally, to measure proliferative activity of the GBM two [^{18}F]fluoro-L-thymidine (FLT)-PET scans was performed in one patient after the change of adjuvant therapy regimen.

Results: The median TTP was significantly longer in malignant glioma patients with decline of methionine uptake than in patients with increasing methionine uptake (23 vs. 3.5 months; p=0.01, log rank test).
After discontinuation and dose reduction of adjuvant TMZ therapy in two patients with GBM the metabolic activity of the tumor as measured by MET- and FLT-PET increased.

Conclusions: First, a reduction of MET uptake during TMZ treatment predicts favorable clinical outcome. Secondly, MET- and FLT-PET is able to monitor metabolic effects of long-term adjuvant TMZ therapy more than 12 months in patients with GBM after discontinuation and dose reduction, respectively. PET imaging offers a new method to follow the biological activity of malignant glioma and has to be studied in a larger patient group to establish its clinical value.

Design and preclinical evaluation of melanoma targeting agents for internal radionuclide therapy.

Chezal JM, Papon J, Labarre P, Denoyer D, Bayle M, Miot-Noirault E, Chavignon O, Teulade JC, Madelmont JC, Moins N.
UMR 484 INSERM- Université d'Auvergne- Centre Jean Perrin, Clermont-Ferrand, France.

Background : Targeted internal radionuclide therapy would be an effective alternative for disseminated melanoma treatment. *N*-(2-diethylaminoethyl)-4-iodobenzamide (BZA) and compounds of the series exhibit a specific affinity for melanoma tissue giving them a potent application for gamma imaging (^{123}I) or radionuclide therapy (^{131}I or ^{125}I).[1, 2] The *ortho*-iodinated analog (BZA_2) is developed as a specific melanoma imaging agent for SPECT.[3] The melanoma affinity is due to a cellular internalization and a binding to melanin pigment. [4-7]

Aim : A pharmacochemical study has been done in order to discover new derivatives with a longer retention time in the tumour of melanoma B16 bearing mice and so, promising agents for the targeting of radionuclides in melanoma for therapy. New molecules synthesized were BZA analogs varying by (i) methylene chain and amino alkyl substituents, (ii) aromatic ring.

Methods : Design of compounds, synthesis, labelling by ^{125}I and study of their biodistribution in B 16 F0 melanoma bearing C57BL6 mice after intravenous injection (0.1 µmol, 0.74–0.92 MBq/animal; 10 animals / compound). Mice were sacrificed, quickly frozen in liquid nitrogen at different times after administration (1, 3, 6, 24 or 72 hours) and cryosectioned into slices of 40 µm at -22°C. The radioactivity contained in the slices was analyzed using an AMBIS 4000 detector. The radioactivity was quantified in different organs including tumour and expressed as percentage of injected dose/g of tissue (%ID/g). For comparison of tumour (T) uptake with other tissues, ratios of radioactive concentrations (T/organ) were determined illustrating the image contrast. Dosimetry parameters for a ^{131}I utilization were extrapolated using MIRD program. Finally, first tests of the effects of ^{131}I-UMR 12 on the tumour growth in melanoma bearing mice were performed.

Results : For number of the studied molecules, a tumour fixation was observed and four compounds BZ18, UMR3, UMR7 and UMR12 exhibited an original pharmacokinetic profile: high, specific and durable tumour concentration with a rapid clearance from non-target organs. For BZ18, UMR3, UMR7 and UMR12 respectively, the tumour concentration after 72 h was 4, 3.4, 7.4 and 15.6 fold compared to BZA and in term of dosimetry, for ^{131}I labelled, the tumoural absorbed dose was 1.9, 1.4, 3.7, and 4.9 fold. Such profiles made these compounds promising for an application to internal radionuclide therapy and particularly UMR 12 which was first selected.
Moreover, i.v. administration of ^{131}I-UMR12 to melanoma bearing mice showed a marked decrease in tumoural growth comparatively to controls and a lengthening of median survival time.

Conclusions : These data are promising for an application to internal radionuclide therapy, namely ^{131}I-UMR12. Our study of antitumoural efficacy is undergoing with different experimental protocols and on different melanoma animal models (grafted tumour and /or metastases). The cellular internalisation of UMR 12 has to be confirmed and the evaluation of ^{125}I-UMR 12, Auger electrons emitting is planned.

References :

[1] Michelot et al ; *J. Nucl. Med.,* 1993; 34: 1260-1266.
[2] Moins N et al; *Nucl Med Biol,* 2001; 28: 799-808.
[3] Moins N et al; *Eur. J. Nucl. Med.*, 2002, 29: 1478-1484.
[4] Labarre P et al ; Melanoma Res., 2002; 12: 115-121.
[5] Guerquin-Kern et al; *BioMedical Engineering On Line*, 2004, 16p.
[6] Mansard S et al; *Nucl. Med. Biol.*, 2005; 32: 451-458.
[7] Chehade F et al ; *J. Nucl. Med.,* 2005; 46: 1701-1706.

Peptide dye and peptide quantum dot conjugates for optical molecular imaging

Grötzinger C and Wiedenmann B
Department of Hepatology and Gastroenterology, Charité - Universitätsmedizin Berlin, Germany

Background: Optical imaging using near-infrared fluorescent contrast media promises to be one of the most successful developments in molecular imaging techniques.[1] Peptide dye conjugates combine ease of synthesis with high affinity and specificity of the conjugate.[2,3] In contrast to antibody conjugates, they are much smaller, have higher diffusion rates in tissues and can be easily modified. As a new development, fluorescent nanoparticles known as quantum dots have been introduced into imaging as a alternative, brighter and more stable fluorophore.

Aim: To explore the capabilities of peptide dye and peptide quantum dot conjugates for molecular imaging on a cellular level and to use confocal laser microscopy to visualize binding and internalization.

Methods: We have made use of several peptide dye conjugates with emission in the visible and near infrared spectrum to visualize binding, internalization and trafficking of somatostatin and other neuropeptide hormones in neuroendocrine tumor cells and sections of human neuroendocrine tumors.

Results: Using the 633 nm emission line available in many confocal laser scanning microscopy systems we have been able to excite fluorescence of near-infrared carbocyanine dyes and visualize binding and internalization of octreotate in neuroendocrine tumor cells in vivo and after fixation. This endocytosis was compared with endocytosis of the receptor labelled with GFP. Similarly, we were able to monitor binding of these conjugates to fresh frozen sections of tumor tissue and to compare this binding pattern with binding of radiolabelled conjugates in autoradiography and receptor staining. Resuls obtained with chemical dye conjugates were comparable with quantum dot conjugates. Using a confocal laser scanning microscope, advantages of quantum dots were not as pronounced as reported in other experimental setups.

Conclusions: Although most conventional laser scanning setups are not equipped with lasers in the near infrared spectrum, due to their excitability at 633 nm near-infrared dyes and conjugates thereof can easily be visualized, even in living cells. Quantum dot conjugates may be excited at variable wavelenghts but in our system show little improvement over chemical dyes. One of the great challenges will be to enhance overall sensitivity to allow for ex vivo tissue monitoring of dye conjugates after systemic application.

References:
[1] Weissleder R, Ntziachristos V.; Nat Med. 9, 123-8 (2003)
[2] Licha K et al.; Bioconjug Chem. 12, 44-50 (2001)
[3] Becker et al.; Nat Biotechnol. 19, 327-31 (2001)

Monitoring of Suicide Gene Therapy for Experimental Gliomas by Molecular Imaging.

[1]Miletic H, [2]Fischer Y, [3]Litwak S, [4]Waerzeggers Y, [4]Rueger MA, [4]Himmelreich U, [4]Li H-F, [4]Winkeler A, [1]Deckert M, [3]Neumann H, [2]von Laer D, [4]Jacobs AH
[1]Department of Neuropathology, University of Cologne, Germany
[2]Georg-Speyer-Haus, Frankfurt am Main, Germany
[3]Neural Regeneration Unit, Institute of Reconstructive Neurobiology, University Bonn LIFE & BRAIN Center and Hertie Foundation, Bonn, Germany
[4]Laboratory for Gene Therapy and Molecular Imaging, MPI for Neurological Research with Klaus-Joachim-Zülch-Laboratories of the Max Planck Society and the Faculty of Medicine of the University of Cologne, Germany

Background: We developed two new gene therapeutic strategies for experimental glioma: (i) we isolated multipotent adult progenitor cells, a highly proliferative subpopulation of mesenchymal stem cells, from the rat bone marrow. We demonstrated migration of these stem cells within experimental glioma and upon expression of the suicide gene HSV-tk an efficient therapeutic bystander effect with 66% of long-term survivors [1]. (ii) We developed lentiviral vectors pseudotyped with lymphocytic choriomeningitis (LCMV) glycoproteins (GP) and showed a specific tropism of these vectors for glioma cells [2]. Treatment of rat experimental glioma with LCMV-GP pseudotypes carrying HSV-tk resulted in 90% of long-term survivors.

Aim: The aim of the present study is to monitor (i) the distribution of HSV-tk expressing stem cells and the transduction of tumor cells by LCMV-GP pseudotyped lentiviral vectors carrying HSV-tk and (ii) the therapeutic effects of both strategies by positron emission tomography (PET) and magnetic resonance imaging (MRI).

Methods: $8x10^4$ rat 9LDsRed glioma cells were implanted into the right striatum of Fischer rats. After 5 days stem cells expressing HSV-tk-eGFP or LCMV-GP pseudotypes carrying HSV-tk-eGFP were injected into the tumor (stem cells and vectors) and at the tumor border (vectors only). Animals in the therapeutic group and in the control groups without vector or stem cell injections received 30 mg/kg ganciclovir (GC) i.p. Further control groups received vectors or stem cells and were not treated with GC. MR and PET-imaging was performed for (i) localization of tumours (MRI; [^{11}C]MET); (ii) assessment of tissue-dose of vector-mediated gene expression and localization of stem cells ([^{18}F]FHBG-PET); and (iii) induced therapeutic response (MRI and [^{11}C]MET-PET). Therapeutic efficiency was quantified by differences in (i) tumour volume; (ii) [^{11}C]MET-accumulation and (iii) histology.

Results: Stem cells and vector transduced tumor cells were detected by [^{18}F]FHBG-PET imaging 7 days and 4 days after implantation, respectively. During GC therapy, tumor size in the therapeutic groups was reduced compared to control groups. At the end of treatment tumors were not detectable in vector-treated animals and only residual tumors were visible in stem cell-treated animals by [^{11}C]MET-PET and MRI. The imaging data strongly correlated with histology.

Conclusions: The present study demonstrates, that stem cell-based and vector-mediated gene therapies for malignant glioma using the suicide gene HSV-tk can be monitored successfully by molecular imaging:

(1) stem cells and vector-transduced tumor cells can be detected by [^{18}F]FHBG-PET before application of the prodrug.
(2) the therapeutic effects identified by [^{11}C]MET-PET and MRI strongly correlate with histology

References:

[1] Miletic H et al. (2006) Cancer Research, submitted.
[2] Miletic H et al. (2004) Human Gene Therapy 15:1091-100.

Multi-Modality Imaging of regulated gene expression *in vivo*

[1,2]A. Winkeler, [4]M. Sena-Esteves, [5]L.E.M. Paulis, [1]L. Li, [1,3]M. Klein, [1]P. Monfared, [1,3]M.A. Rueger, [1,2,3]A.H. Jacobs.
[1]Max-Planck-Institute for Neurological Research, [2]Center for Molecular Medicine and [3]Department of Neurology at the University of Cologne, Cologne, Germany, [4]Department of Surgery, Children's Hospital of Philadelphia, Philadelphia, USA, [5]Department of Biomedical Engineering, Eindhoven University of Technology, Eindhoven, The Netherlands.

Objective: To investigate non-invasive assessment of inducible gene expression in an intracranial tumour model *in vivo*.

Background: Non-invasive imaging of gene expression can be performed by positron emission tomography (PET) as well as optical imaging (OI). We previously demonstrated that regulated gene expression mediated by inducible HSV-Amplicon vectors (HET6C-*tk39,* HET6C-*luc*) can be non-invasively imaged by the use of a fluorescence gene (*rfp)* in cell-culture, a PET reporter gene (*HSV-1-tk39*) and an optical imaging gene (*firefly luciferase, fluc*) in a subcutaneous tumour model *in vivo*.

Methods: To non-invasively assess regulated gene expression *in vivo* with OI, we used a bi-directional Tet-regulated HSV-Amplicon vector controlling gene expression of two optical imaging genes (HET6C-*fluc*). The non-invasive monitoring with PET was performed with an identical vector expressing *HSV-1-tk39* instead of *fluc*. The fluorescence gene *rfp* as well as the bioluminescence gene *fluc* or the PET reporter gene *tk39* were placed under doxycycline-responsive elements. To compare regulation *in vivo* Gli36□EGFR (human gliomas) tumours were grown intra-cranially in nude mice. After tumor localisation by MRI, a mixture of HET-luc and HET-tk39 virus was injected. Subsequently a series of multi-modal imaging was performed with a bioluminenscence camera and microPET to image luciferase and tk39 expression, in presence or absence of doxycycline (dox).

Results: *In vivo*, HET6C-*fluc* regulated gene expression could be non-invasively assessed by Bioluminescence Imaging (BLI) in 5 mice**.** The maximal ratio of induction after dox-treatment was 14.9-fold. In contrast to these results Positron Emission Tomography (PET) HET6C-*tk39* regulated gene expression could not be imaged with ^{18}FHBG-PET. Up to know the tumour signal did not exceed background in the induced state. However, recent results with ex-vivo infected glioma cells showed that imaging regulated gene expression in the intracranial tumour system in general is possible.

Conclusions: For the first time intracranial regulation of exogenous gene expression from *in vivo* infected cells is imaged with non–invasive BLI whereas visualisation of regulation with ^{18}FHBG-PET is, up to now, only possible with *ex-vivo* infected cells. The lack of monitoring regulation with PET in *in vivo* infected cells may be due to lower sensitivity of this system.

Supported in part by MSWF 516-400 002 99, ZMMK-TV46 and DFG-Ja 981/1-2, EC - FP6-project DiMI, LSHB-CT-2005-512146 and EMIL, LSHB-CT-2004-503569

Towards non-invasive assessment of endogenous regulation of gliomas

[1,3]P. Monfared,[1,2]A. Winkeler,[1,3]M. Klein, [1,3]H. Li,[1]G. Schneider, [1,2,3]A.H. Jacobs.
[1]Max-Planck-Institute for Neurological Research, [2]Center for Molecular Medicine and [3]Department of Neurology at the University of Cologne, Cologne, Germany

Background: The transcription factor E2F1 is deregulated in the majority of human tumours via a number of different mechanisms. Previous study describes an E2F1-responsive adenoviral vector for brain tumours that promises to target cancer cells more specifically than the standard approach (1). A recent study showed that p53 dependent gene expression can be imaged *in vivo* by positron emission tomography (PET) (2). We propose to image alterations of the level of E2F1 non-invasively *in vivo*.

Aim: To proof, whether distinguished levels of free E2F1 in glioma cells can be detected in response to an exogenous stimulus (BCNU) by using an imaging marker gene under control of an E2F1 responsive promoter element.

Methods: To assess expression levels of free E2F1 in the human U87dEGFR glioma cells, E2F1 protein was immunoprecipitated after incubation with BCNU (2.5, 8.25, 25 µM). Free E2F1 as well as p53 and p21 expression was evaluated by Western blot. To generate a reporter system a retroviral vector was constructed which places the firefly luciferase (*luc*) and the PET marker gene *tkgfp* under control of an E2F1 responsive element. As been described by Doubrovin, transcriptional regulation was assured by mutating the enhancer of the 3'-LTR of the retroviral vector.

Results: E2F1 protein levels significantly increased in the response to BCNU treatment (4-times). In addition, p53 and p21 expression increased in the same manner. Currently, stable expressing E2F1re*luc*IRES*tkgfp* expressing human U87dEGFR glioma cells are evaluated in culture and *in vivo*. Our preliminary results are showing that the activity of E2F1 endogenously in tumor cells can be detected and significantly increased after BCNU treatment.

Conclusions: The changes in free E2F1 expression in BCNU treated cells should be sufficiently enough to drive various expression levels of the imaging marker genes, which should allow a non-invasive assessment of E2F-1 regulation *in vivo*.

References:
1- Parr, M.J. et al. *Nat.Med* 10, 1145-1149.(1997)
2- Doubrovin, M. et al. *Pro.Natl.Acad.Sci.USA* 98, 9300-9305. (2001)

Induction of gene expression by focused ultrasound in induced rat tumours

Claire ROME, Matthieu LEPETIT-COIFFE, Bruno QUESSON, Josette ARSAUT, Franck COUILLAUD, Chrit T.W. MOONEN
Laboratory for Molecular and Functional Imaging
ERT 5543 CNRS/ University Victor Segalen Bordeaux
146 rue Leo Saignat, Case 117
33076 Bordeaux, France

Gene therapy requires tight control of both spatial and temporal expression of the therapeutic transgene. Heat-shock promoters, especially the human *hsp70* promoters, have been proposed for gene therapy strategies because they are both heat-inducible and efficient. A noninvasive physical approach which permits local temperature control was developed in our laboratory. Automatic execution of a predefined temperature-time evolution is performed using MRI-guided focused ultrasound (MRI-FUS) with real-time feedback control in a whole-body clinical MRI system (1.5T Philips Intera MR System). In the present work, this procedure was used for the control of gene expression driven by the *hsp70B* promoter following a preliminary account (Guilhon et al., 2003).
A stable clonal modified C6 glioma cell line was used to induce subcutaneously implanted tumors in young rats (3-weeks-old). The cell line was engineered in such a way to contain the green fluorescent protein (GFP) gene under the control of the human *hsp70B* promoter. *In vivo,* selective areas within the generated tumors were submitted to a 5-min weak and constant temperature elevation using the MRI-FUS system. Treated animals were sacrificed 6 h following the heating procedure. Tumors were resected, snap-frozen and cut into 20-µm slices for histology, fluorescence imaging and immunohistology. Preliminary results show that cells in heated region are alive. Imaging analysis show so local induction of GFP expression in regions heated.

Guilhon E, Quesson B, Moraud-Gaudry F, de Verneuil H, Canioni P, Salomir R, Voisin P, Moonen CT, 2003. Image-guided control of transgene expression based on local hyperthermia. Mol Imaging 2 (1); 11-17.

Multimodality molecular imaging of tumor angiogenesis using quantum dots

Mulder WJM 1, Strijkers GJ 1*, Castermans K 2, van Beijnum JR 2, oude Egbrink MGA 3, Chin PTK 4, Storm G 5, Griffioen AW 2, Nicolay K 1

*1Biomedical NMR, Department of Biomedical Engineering, Eindhoven University of Technology, the Netherlands; 2Angiogenesis Laboratory, Maastricht University & Hospital, the Netherlands; 3Department of Physiology, CARIM, Maastricht University, the Netherlands; 4Laboratory of Macromolecular and Organic Chemistry, Eindhoven University of Technology, the Netherlands; 5Department of Pharmaceutics, UIPS, Utrecht, the Netherlands; *presenting author*

Background: Quantum dots (QDs), semiconductor nanocrystals in a size range of 2 to 6 nm have gained much interest the last few years for biological imaging purposes [1]. Angiogenesis, the formation of new blood vessels, is involved in many pathological processes, including cancer [2]. In the angiogenic cascade different cell surface receptors, including the αvβ3-integrin, are expressed at the activated tumor endothelium. The non-invasive *in vivo* visualization of this integrin using multimodality contrast agents conjugated with αvβ3-specific cyclic-RGD-peptides would allow one to monitor angiogenesis and to follow the effects of angiostatic therapies.

Aims: (1) To develop αvβ3-specific paramagnetic QDs which are detectable with both MRI and optical imaging techniques. (2) To visualize angiogenic blood vessels in tumor bearing mice with MRI and intravital microscopy (IVM) using this multimodal contrast agent.

Methods: High quality core shell CdSe/ZnS core/shell QDs were synthesized by injection of appropriate precursors into a hot coordinating solvent mixture, followed by the synthesis of the zinc sulfide shell in a coordinating surfactant mixture of HDA/TOPO/Stearic-acid using zincstearate and elemental sulphur in TOP as the precursors. A micellular and paramagnetic coating, comprised of PEG-DSPE, Mal-PEG-DSPE and Gd-DTPA-BSA was applied to the QDs. Multiple cyclic- RGD-peptides were conjugated to the lipid coated quantum dots by sulfhydryl-maleimide coupling. The QDs were first tested *in vitro* on proliferating HUVEC [3]. 13 9-week-old male C57bl6 mice were inoculated with approximately 106 B16 colon carcinoma cells subcutaneously on the right flank. Between day 14 and 19, when tumors had grown to a size of 500-1000 mm3, mice were used for IVM and MRI (6.3 T scanner) measurements.

Results: *In vitro*, both MRI and fluorescence microscopy revealed a strong association of the RGD-pQDs with αvβ3 expressing HUVEC. IVM on tumor bearing mice revealed association of RGD-pQDs with activated tumor endothelium of tumor blood vessels. In Fig. 1A the activated endothelial cells and thus the contours of the blood vessel are indicated with yellow arrows. Association of RGD-pQDS with vessels was found as far as 0.5-1.0 cm from the tumor boundary. No association of RGD-pQDs with endothelial cells was found in the ears of mice. *T*1-weighted MRI measured before (Fig. 1B) and 20 min. after (Figs. 1C and D) the injection of RGD-pQDS showed the accumulation of the contrast agent in the tumor. The arrows in Fig. 1C indicate a bright region appearing at the periphery of the tumor. In Fig. 1D pixels in the tumor with signal enhancement of at least five times the noise level are color coded according to: 0 30% signal enhancement.

Conclusions: We have shown the unique possibilities of this QD-based contrast agent for parallel optical and MR imaging studies. In addition, the complementarity of *in vivo* MRI and IVM allowed us to study the kinetics of the contrast agent targeting, the specificity of the labeling of activated endothelium and the identification of angiogenic sites at the gross morphological level. Next to the RGD peptidic targeting ligand used in this study, the contrast

agent can be conjugated with other targeting ligands to allow the investigation of other disease processes, such as apoptosis, inflammation, or atherosclerosis.

References:

[1] Michalet *et al.*, Science. 2005 Jan 28;307(5709):538-44.; [2] Griffioen and Molema, Pharmacol Rev. 2000 Jun;52(2):237-68.; [3] Mulder *et al.*, Nano Letters 16(1), 1-6 (2006)

Assessing early effects of angiogenesis inhibitors using MR molecular imaging

Mulder WJM [1], Strijkers GJ [1*], van der Schaft DWJ [2], Hautvast PAI [2], Storm G [3], Mayo KH [4], Griffioen AW [2], Nicolay K [1]

*1Biomedical NMR, Department of Biomedical Engineering, Eindhoven University of Technology, the Netherlands; 2Angiogenesis Laboratory, Department of Pathology/Internal Medicine, Maastricht University & Hospital, the Netherlands; 3Department of Pharmaceutics, Utrecht Institute for Pharmaceutical Sciences (UIPS), the Netherlands; 4Department of Biochemistry, Molecular Biology and Biophysics, University of Minnesota, Minneapolis, USA; *presenting author*

Background: Angiogenesis, the formation of new blood vessels, is an important process important in sustaining tumor growth. Inhibition of angiogenesis could therefore be of considerable therapeutic use. Non-invasive imaging methods to establish the efficacy of anti-angiogenesis therapies are therefore becoming increasingly important.

Aim: To use αvß3 targeted bimodal cyclic-RGD-liposomes to quantify angiogenesis in a mouse, tumor model with MRI and to evaluate the therapeutic efficacy of the two angiogenesis inhibitors anginex [1] and endostatin [2].

Methods: 30 6-wk old C57BL/6 mice were inoculated with $1\times10_5$ B16F10 melanoma cells subcutaneously on the right flank. Mice were treated either 3 or 14 days with anginex or endostatin using subcutaneously placed osmotic minipumps. Mice that were not treated served as a control group. The tumor volume was assessed with a caliper on a daily basis. Paramagnetic and fluorescent cyclic RGD-liposomes were prepared as described previously [3]. T_1 weighted images (B=6.3T, TR=800ms,TE=10ms) of the tumor bearing mice were acquired before and after intravenously injection of the contrast agent. The area of tumor with significantly enhanced signal intensity served as an *in vivo* indicator for the amount of angiogenic activity, as described in previously [3]. After the MRI measurements the tumors were dissected and frozen. Slices were stained for nuclei and endothelial cells with DAPI and CD31. Microvessel density (MVD), which is as an *ex vivo* surrogate marker for angiogenic activity, was determined by counting vessels in 5 random tumor areas.

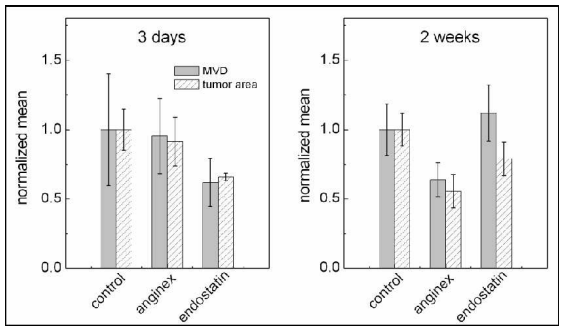

Figure 1: *Normalized mean MVD and tumor area with enhanced MRI signal for control as well as anginex and endostatin treated mice.*

Results: The 3 days treatment resulted in a significant inhibition of the tumor growth for both endostatin and anginex. The 14 days treatment resulted in no inhibition of tumor growth by endostatin as compared to the control group. In contrast, the tumor growth of anginex treated mice was significantly inhibited by 60%. For the 3 days treatment T_1-weighted MR images after contrast agent injection displayed significantly less enhanced area for treatment with endostatin. For the 14 days treatment the anginex treated animals displayed about 50% less enhanced tumor area as compared to untreated animals. This *in vivo* MRI data was compared to the *ex vivo* determined MVD, as shown in Fig. 1 above. Overall the trend found by *in vivo* molecular MRI of tumor angiogenesis reflected closely the treatment effects as deduced from *ex vivo* MVD quantification for both the 3 days and the 14 days treatment group.

Conclusions: A methodology is presented which allows the rapid evaluation of the efficacy of angiostatic therapy by quantifying angiogenesis with molecular MRI *in vivo*. The MRI findings show a very good correlation with the MVD determined *ex vivo*. Since the MVD is a useful prognostic tool for a wide range of tumor types molecular MRI by targeting the αvß3-integrin may be used to *in vivo* stage the disease, to facilitate treatment planning, and to predict survival chances.

References:

[1] Griffioen and Molema, Pharmacol Rev. 2000 Jun;52(2):237-68.
[2] Dubertret *et al.,* Science. 2002 Nov 29;298(5599):1759-62.
[3] Mulder *et al.,* FASEB J. 19(14), 2008-10 (2005). Epub 2005 Oct 4.

C^{11}-Methionine Positron Emission Tomography as a diagnostic marker for Malignant Progression in Recurrent Gliomas

Ullrich R[1], Kracht L. W.[1], Kesper K[1], Jacobs A. H.[1,2]

[1] Max-Planck-Institute of Neurological Research, [2] Department of Neurology, University of Cologne

Background: C^{11} Methionine uptake correlates with microvessel density and reflects the expression of the LAT1 amino acid transporter which is highly expressed in malignant tumours. C^{11} Methionine Positron Emission Tomography (PET) has been well established as a marker for active tumour progression in brain tumours.

Aims: In this study we investigate the intra-individual tumour progression of gliomas using C^{11} Methionine Positron Emission Tomography (PET).

Methods: Twenty-three Patients with histologically proven glioma were investigated repeatedly with C^{11}-methionine PET. In total 42 C^{11}-methionine PET scans were done. After all PET scans histological diagnosis was confirmed by open surgery or stereotatic biopsy within three months.

Results: During the study thirteen patients had histologically proven progression of tumor grade (in two cases in two steps from grade II to grade III and later to grade IV). Ten patients demonstrated no change in tumour grade. In all patients the ratio between C^{11}-methionine uptake in the tumour and in the contralateral cortex was determined.
In patients with malignant progression the mean increase of methionine uptake was 53.5% (± 60.9%) and in patients without change in tumour grade there was no change in methionine uptake (5,8%± 10.5%). The difference of the change in methionine uptake between the group with malignant progression and the group without malignant progression was significant (t-test, p=0.004).

Conclusion: We concluded that C^{11}-methionine PET is a useful tool to detect malignant progression in recurrent gliomas even in the progression from grade III to grade IV in intra-individual follow-up.

Molecular Imaging-Guided Vector Mediated Gene Therapy of Experimental Gliomas.

Waerzeggers Y, Rueger MA, Himmelreich U, Li H-F, Winkeler A, Klein M, Jacobs AH
Laboratory for Gene Therapy and Molecular Imaging, MPI for Neurological Research with Klaus-Joachim-Zülch-Laboratories of the Max Planck Society and the Faculty of Medicine of the University of Cologne, Germany

Background: We recently demonstrated in our laboratory that *in vivo* transduction of experimental subcutaneous gliomas with HSV-1 amplicon vectors encoding for the synergistic working prodrug-activating enzymes E. coli cytosine deaminase (*cd*) and HSV-1 thymidine kinase (*tk*) causes distinct levels of gene expression correlating to the therapeutic effect and that molecular imaging technologies can be used for (i) imaging-guided targeted vector application, (ii) determination of the tissue-dose of vector-mediated gene expression, and (iii) correlation to the induced therapeutic effect [1].

Aim: The aim of the present study is to use the molecular imaging technologies positron emission tomography (PET) and magnetic resonance imaging (MRI) for imaging guided vector application and assessment of the therapeutic effect in experimental intracranial gliomas.

Methods: Human Gli36dEGFR glioma cells were grown as intracranial tumours in the right striatum of nude mice (n=4), and were transduced *in vivo* with HSV-1 amplicons carrying *cd*, enhanced HSV-1-*tk* (*tk39*[2]) and *gfp* (green fluorescent protein) (HSV-*cd*IRES*tk39gfp*; 1-1,5 x10^6 t.u.). Mice bearing tumours grown from stably transduced *cd*IRES*tk39gfp*-expressing Gli36dEGFR cells served as positive controls (n=3). Prodrug administration was performed daily with 5-fluorocytosine (500mg/kg bw) and ganciclovir (25mg/kg bw). MR and PET-imaging was performed for (i) localization of tumours (MRI); (ii) identification of viable target tissue ([^{18}F]FLT-PET); (iii) assessment of tissue-dose of vector-mediated gene expression ([^{18}F]FHBG-PET); and (iv) induced therapeutic response (MRI and [^{18}F]FLT-PET). Therapeutic efficiency was quantified by differences in (i) tumour volume; (ii) [^{18}F]FLT-accumulation and (iii) animal survival.

Results: All positive control tumours disappeared within 10 days of prodrug therapy, both on MR images and on PET images ([^{18}F]FHBG and [^{18}F]FLT-PET).
Only in one *in vivo* transduced tumour there was a partial response to treatment with 40% reduction in [^{18}F]FLT-accumulation, early after the start of prodrug therapy. At the later stage of therapy tumour progression reoccurred. In all other cases prodrug therapy did not influence tumour growth. In the *in vivo* transduced group, animal survival was not affected by therapy.

Conclusions: Imaging vector-mediated gene expression by use of the HSV-1-*tk* system and microPET is possible in small animal models (mice) of intracranial growing gliomas. In the case of ideal transgene distribution (positive control tumours) the “tissue-dose” of HSV-1-TK as measured by FHBG-PET correlates with good response to prodrug therapy. *In vivo* transduction of HSV-*cd*IRES*tk39gfp* leads to a lower “tissue-dose” of vector-mediated gene expression, which can be directly assessed by microPET, with limited therapeutic efficiency. This imaging paradigm shall help in the establishment of safe and efficient therapeutic vectors and administration protocols for gene therapy of gliomas.

References:
[1] Jacobs AH, Rueger MA et al. (2006) submitted.
[2] Black ME et al. (1996) PNAS 93:3525-3529.

Microenvironmental influence on growth, metabolism and microcirculation of experimental prostate cancers differing in malignancy.

Christian M. Zechmann[1], Eva C. Woenne[2], Gunnar Brix[3], Nicole Radzwill[4], Martin Ilg[4], Peter Bachert[2], Peter Peschke[1], Stefan Kirsch[2], Hans-Ulrich Kauczor[1], Stefan Delorme[1], Wolfhard Semmler[2], Fabian Kiessling[2]

[1]*DKFZ, Department of Radiology Heidelberg, Germany*
[2]*DKFZ, Department of Medical Physics in Radiology Heidelberg, Germany*
[3]*DKFZ, Clinical Cooperation Unit Radiotherapy, Germany*
[3]*Federal Office for Radiation Protection, Neuherberg, Germany*
[4]*Bruker Biospin, Rheinstetten, Germany*

Prostate cancer (PCA) is the most frequent tumor of men. However, mortality is only 5% and mechanisms leading to an infiltrative and metastasizing phenotype are poorly understood.
In this study the influence of orthotopic and subcutaneous implantation site on growth, microcirculation, and metabolism of Hormone–sensitive (H), hormone–insensitive (HI) and anaplastic (AT1) Dunning–PCA was investigated using dynamic contrast enhanced MR imaging (DCE-MRI), ^{1}H MR spectroscopy (^{1}H MRS) and histological evaluation.
Orthotopic H–tumors grew significantly slower and developed a more differentiated phenotype as subcutaneous ones. In contrast, HI–tumors grew faster orthotopically and developed lymph node metastases only in this location. Growth of orthotopic and subcutaneous AT1–tumors was not significantly different. Histological analysis indicated that differences in tumor growth were attributed to a balance of apoptosis and proliferation. DCE-MRI indicated lower relative blood volume and perfusion in orthotopic H–, HI–, and AT1–tumors compared to subcutaneous ones. However, vessel permeability of subcutaneous and orthotopic tumors was higher in the implantation site with enhanced tumor growth and accompanied by a higher vessel maturity. ^{1}H MRS of all tumors yielded high choline–creatine signal intensity ratios indicating an increased cell membrane turnover. Signal intensity of unsaturated lipids increased from low to high malignant phenotypes.
In conclusion, implantation site influences growth, spread, microcirculation and phenotype of H– and HI–tumors, while it is less important for anaplastic AT1–tumors. In this context, DCE-MRI and 1H MRS show potential as discriminators of tumor dedifferentiation.

Contact: Christian M. Zechmann
Im Neuenheimer Feld 280
69120 Heidelberg
phone: +49 6221 422525
fax: +49 6221 422531
e-mail: c.zechmann@dkfz.de

PET/SPECT/CT Multimodal Imaging in a Transgenic Mouse Model of Breast Cancer

Raphael Boisgard, Jean Louis Albérini, Benoît Jego, Karine Siquier, Benoît Thézé, Stéphanie Guillermet, Bertrand Tavitian.
CEA, Département de Recherche Médicale, Service hospitalier Frédéric Joliot, Orsay, F-91400 France ; Inserm, U803, Orsay, F-91400, France.

Background : In the therapy monitoring of breast cancer, conventional imaging methods include ultrasound, mammography, CT and MRI, which are essentially based on tumor size modifications. Commonly used criteria are the response evaluation criteria in solid tumors (RECIST)., However these modifications represent a late consequence of the biological response and fail to differentiate scar or necrotic tissue from residual viable tumoral tissue. On the other hand, histology is essential for an accurate diagnosis and staging in breast cancer and provides reliable prognostic data helpful for the treatment strategy, but it requires invasive sampling which cannot be easily repeated and spatially restricted information. Therefore, a current objective is to develop tools able to predict early response to treatment. Positron Emission Tomography (PET) and Single Photon Emission Computerized Tomography (SPECT) are imaging modalities able to provide extremely sensitive quantitative molecular data and are widely used in humans and animals.

Objectives : (i) to assess the value of PET, SPECT and CT for early tumor detection in a mouse transgenic model of mammary tumours ; (ii) to compare with the histological staging and (iii) to assess the value of imaging for the monitoring of chemotherapy efficiency.

Results : Mammary epithelial cells of female transgenic mice expressing the polyoma middle T oncoprotein (PyMT), under the control of the mouse mammary tumour virus long terminal repeat (MMTV LTR) (1), undergo four distinct stages of tumour progression, from premalignant to malignant stages.. Stages are identifiable in the mammary tissue and can lead to the development of distant metastases (2). This model presents many similarities with breast cancer progression encountered in women (3).
Longitudinal studies by dynamic whole body acquisitions by multimodal imaging including PET, SPECT and Computed Tomography (CT) allow following the tumoral evolution in PyMT mice in comparison with the histopathological analysis. At 4 weeks of age, mammary hyperplasia was identified by histopathology, but no abnormalities were found by palpation or detected by PET with 2-deoxy-2-[^{18}F]fluoro-D-glucose. Such as in some human mammary cancers, the sodium iodide symporter (NIS) in tumoral mammary epithelial cells is expressed in this mouse model. In order to investigate the expression of NIS in the PyMT mice mammary tumours, [^{99m}Tc]TcO_4 imaging was performed with a dedicated SPECT / CT system camera (BIOSPACE GammaImager/CT). Local uptake of [^{99m}Tc]TcO_4 was detected as early as 4 weeks of age. Tumor detection with the different imaging modalities is summarized in the following table:

Weeks	4-6	8-9	9-12	more
Histological Stage	Hyperplasia	Hyperplasia adenoma	Early carcinoma	Late carcinoma
Positive contrast on Imaging	SPECT TcO_4	SPECT TcO_4 +PET FDG	SPECT TcO_4 +PET FDG +CT	SPECT TcO_4 +PET FDG +CT

The efficacy of chemotherapy was evaluated in the PyMT mouse model using a conventional regimen (Doxorubicine, 100 mg/kg) administered weekly from 9 to 12 weeks of age. Imaging clearly showed an inhibition of tumoral development at 11 and 12 weeks of age.

Conclusion : In the PyMT mouse model, SPECT with [^{99m}Tc]TcO_4 appears to detect mammary tumors more precociously than PET with 2-deoxy-2-[^{18}F]fluoro-D-glucose. Imaging methods can monitor the efficacy of chemotherapy. If confirmed in larger series, imaging in the PyMT mouse could prove useful for the evaluation of new drugs' efficacy in preclinical phases.

References

1. Guy CT, Cardiff RD, Muller WJ. Induction of mammary tumors by expression of polyomavirus middle T oncogene: a transgenic mouse model for metastatic disease. In: Mol Cell Biol; 1992. p. 954-61.
2. Lin EY, Jones JG, Li P, Zhu L, Whitney KD, Muller WJ, et al. Progression to malignancy in the polyoma middle T oncoprotein mouse breast cancer model provides a reliable model for human diseases. In: Am J Pathol; 2003. p. 2113-26.
3. Qiu TH, Chandramouli GV, Hunter KW, Alkharouf NW, Green JE, Liu ET. Global expression profiling identifies signatures of tumor virulence in MMTV-PyMT-transgenic mice: correlation to human disease. In: Cancer Res; 2004. p. 5973-81.

Selection of nucleic acids-based ligands on whole living cells : new radiotracers for *in vivo* imaging.

Pestourie C.[1], Cerchia L.[2], Gombert K.[1], Boulay J.[3], Aissouni Y.[3], de Franciscis V.[2], Libri D.[3], Tavitian B.[1], Duconge F[1].

[1] *Laboratoire d'Imagerie de l'Expression des Gènes CEA/DSV/DRM/SHFJ- INSERM U803; 4 place du Général Leclerc; 91401 ORSAY, France.*

[2] *Instituto per l'Endocrinologia e l'Oncologia Sperimentale del CNR 'G. Salvatore '; via Pansini 5; 80131 NAPOLI; Italy.*

[3] *Centre de Génétique Moléculaire CNRS; avenue de la Terrasse; 91198 Gif-sur-Yvette, France.*

The development of robust fluorine 18 labelling methods associated to Positron Emission Tomography (PET) open the way of oligonucleotides *in vivo* use as molecular imaging tools allowing their real time tissular quantitation in different organs hours after their injection.
Here we validated a general strategy to isolate nucleic acids-based antibodies (aptamers) to directly target transmembrane receptors in their native cell membrane inserted configuration. Our goal is to design these aptamers as specific radiotracer probes for *in vivo* imaging of cancer.
To this purpose we addressed to the transmembrane Ret receptor tyrosine kinase as a very suitable model system. Germline mutations in the RET gene are responsible for constitutive activation of the receptor and for inheritance of multiple endocrine neoplasia (MEN) type 2A and 2B syndromes and of familial medullary thyroid carcinoma. The C634Y mutation in the extracellular domain (95% of MEN 2A) results in constitutive dimerization whereas the M918T mutation in the intracellular domain (100% of MEN 2B) activates constitutively the receptor without dimerization. Therefore, using the extracellular domain of Ret as target would have the double advantage: first, to overcome any problem related to the delivery of ligands through the cell membrane, and second, to enrich for aptamers able to preferentially target the conformational variants caused by the activating mutations located within the extracellular domain.
We raised RNAse resistant 2'-F pyrimidine aptamers against PC12/MEN2A and counter selected with PC12 cells. One of the characterized aptamers, binds specifically to PC12/MEN2A cells with an approximate Kd of 50nM and can antagonize Ret action as measured by: a) inhibition of phosphorylation of RetC634Y and downstream targets; b) inhibition of GDNF-dependent Retwt signaling; c) reversion of the morphological phenotype of GDNF-stimulated cells; d) reversion of the transformed morphology of NIH3T3 cells expressing the RetC634Y receptor. Our results constitute a proof-of-principle that ex-vivo selection can be effective for the generation of oligonucleotide ligands that are potentially suitable for *in vivo* imaging studies.

Supported by EMIL (European Molecular Imaging Laboratories) EU contract LSH-2004-503569.

Pharmacokinetics and distribution of modified Small Interfering RNA studied with PET

T. Viel, B. Jego, K. Siquier, F. Hinnen, B. Kuhnast, R. Boisgard, F. Dollé, B. Tavitian
Laboratoire d'Imagerie de l'expression des gènes, CEA-SHFJ, INSERM U803

Background: Small interfering RNA (siRNA) is one of the most powerful tools to inhibit a gene at the post transcriptional level in cultured cell. *In vivo*, this approach is more difficult to achieve because of the limited distribution and stability of RNA. In order to study the pharmacokinetics and biodistribution of drugs, Positron Emission Tomography (PET) imaging is an exceptionally sensitive technique and is increasingly becoming an integral part of the drug development process.

Aim: To evaluate the pharmacokinetics of non-modified and 2'sugar-modified siRNA by imaging their *in vivo* biodistribution and analyzing their plasmatic metabolism. This study aimed at evaluating if chemical modifications are able to improve the pharmaceutical properties of siRNA *in vivo* as they do *in vitro*.

Methods: The ability of different modified siRNA to inhibit the synthesis of the target enzyme luciferase in cells expressing this protein were tested at the RNA level by quantitative RT-PCR and at the protein level by measuring bioluminescence of the treated cells. After labelling the antisense strand with a [^{18}F]-fluoropyrimidine-based bromoacetamide reagent, the two strands of siRNA were hybridized and the preservation of the RNAi effect was controlled. Biodistribution of radiolabelled siRNA was followed in nude mice, C57Bl6 mice and in Wistar rats by PET imaging. Plasmatic metabolism was studied in Wistar rats by RP-HPLC analysis.

Results: siRNA with 2'Fluoro-modified pyrimidines on the two strands have the same activity as the non-modified siRNA. 2'OMethyl-modifications every second nucleotide are compatible with interference only if the sense strand and not the antisense strand is modified. All the radiolabelled siRNA were obtained in more than 92.5% purity (controlled by HPLC and electrophoresis gel analysis) and showed the same interference efficiency as the non-conjugated oligonucleotides. The main route of siRNA elimination are the renal system (value for the kidney at 8.0 min post-injection [p.i.] 4.7 ± 0.2% Injected Dose/g for 2'Fluoro-siRNA; 3.4 ± 0.75% ID/g for 2'OMethyl-siRNA and 3.8 ± 0.77% ID/g for non-modified siRNA) but siRNA are also eliminated by the hepato-enteric route (value for the liver at 8.0 min p.i. 1.3 ± 0.3% ID/g for 2'Fluoro-siRNA; 1.5 ± 0.2% ID/g for 2'OMethyl-siRNA and 1.5 ± 0.1% ID/g for non-modified siRNA). The kinetics of radioactivity is quite similar for non-modified siRNA and 2'OMethyl-modified siRNA. 2'Fluoro-siRNA behaves quite differently from the two other siRNA. In the elimination organs, the radioactivity peak is reached later (10 min for 2'Fluoro-siRNA versus 6 min for the non-modified siRNA in the kidney; 14.5 min versus 8.5 min in the liver). This oligonucleotide is eliminated more slowly from the liver (value at 30 min p.i. 1.1 ± 0.2% ID/g for 2'Fluoro-siRNA; 0.83 ± 0.14% ID/g for non-modified siRNA), heart (value at 10 min p.i. 0.67 ± 0.12% ID/g for 2'Fluoro-siRNA; 0.38 ± 0.03% ID/g for non-modified siRNA) and muscles (value at 50 min post-injection [p.i.] 0.13 ± 0.02% ID/g for 2'Fluoro-siRNA; 0.09 ± 0.03% ID/g for non-modified siRNA). Its initial peak in the muscles is also higher than the peaks of the two other siRNA (value at 3.5 min p.i. 0.21 ± 0.04% ID/g for 2'Fluoro-siRNA; 0.16 ± 0.03% ID/g for non-modified siRNA). The biodistribution of 2'Fluoro-modified single-strand oligonucleotide shows that organ absorption of single-strand is weaker than that of the double-strand oligonucleotide. The 2'Fluoro-modified single-strand oligonucleotide shows also a renal retention which is not observed with the double-strand (value at 50 min p.i. 1.2 ± 0.3% ID/g for double-strand 2'Fluoro-siRNA; 2.3 ± 0.4% ID/g for non-modified siRNA).

Conclusions: The double-strand nature of siRNA improves their bioavailability and their potential as therapeutic agent. These observations are particularly true for 2'Fluoro-modified siRNA on the two strands, which has a half-life in plasma increased by three compared with non modified siRNA, accumulates more in all the organs and is eliminated more slowly. These properties combined with the very good efficiency of gene inhibition indicate that siRNA distribution *in vivo* may be compatible with their promising activity as therapeutic agents.

References: Elbashir et al; Nature 411:494-498 (2001)
Tavitian et al; Nat Med 4: 467-471 (1998)
Kuhnast et al; Bioconjugate Chem. 15 : 617-627 (2004)

Supported by EMIL (European Molecular Imaging Laboratories) EU contract LSH-2004-503569

Fluorescent imaging of vascular shutdown in-vivo

Valentini G[1], D'Andrea C[1], Ferrari R[1], Pifferi A[1], Cubeddu R[1], Martinelli M[2], Natoli C[2], Ubezio P[2], Giavazzi R[2]
[1]CNR-INFM and IFN-CNR, Politecnico di Milano, Dipartimento di Fisica; [2]Mario Negri Institute for Pharmacological Research, via Eritrea 62, 20157 Milano, Italy

Background: Vascular Damaging Agents (VDAs) are anticancer drugs that cause the rapid and selective shutdown of the tumor vasculature. Indocyanine Green (ICG) is a well known contrast agent used to label blood vessels for fluorescence imaging.

Aim: This study was intended to visualize and quantify the changes induced in blood flow in mice, as a consequence of treatment with VDAs. The final goal of the research is to establish an optical protocol based on fluorescence imaging to follow day by day the effect of VDA *in-vivo* without sacrificing the animals.

Methods: Two experiments were performed. For the first experiment, the human breast carcinoma MDA-MB-435 was transplanted subcutaneously into the flanks of nude mice. Animals of one group were injected with the VDA ZD6126, which is a tubulin targeting agent by AstraZeneca, three hours before ICG fluorescence measurement. The animal of the control group were injected with the drug vehicle only, before undergoing the same measurements. The second experiment was designed to check the reliability of our ICG fluorescence protocol to assess the homodynamic in murine tumor models. The tumor was the human ovarian carcinoma 1A9-VS1, stably transfected with the vascular growth factor VEGF(121) that increase the vascular volume. Control animals were bearing the 1A9-VAS3 carcinoma, which is similar to 1A9-VS1 except that it was transfected with the antisense VEGF(121). Hence no enhancement in the vasculature was expected. The fluorescence measurements were performed using a home built molecular imaging setup made of a high sensitivity CCD camera and laser excitation devices. The contrast agent (ICG) was injected in the caudal vein immediately before the fluorescence measurement. For each mouse about 50 fluorescence images were acquired with a time interval of 3s between each other.

Results: Mice that received the vascular damaging drug 3 hours before the fluorescence measurement showed a dim ICG fluorescence in the tumor, compared to healthy tissues (ratio = 0.86), and a delay in the transit of the ICG bolus. These results indicate that a significant vascular shutdown took place after VDA treatment. For control mice the contrast was reversed and the perfusion in tumor was higher than that in healthy tissues (ratio = 1.1). In mice bearing the tumor overexpressing the VEGF factor, the fluorescence ratio between tumor and healthy tissues was 1.5, as a consequence of the vasculature enhancement. Control mice showed the same fluorescence behavior in tumor and healthy tissue (ratio = 1.1). Finally, an almost complete clearance of the contrast agent was verified 24 hrs after injecting the ICG bolus.

Conclusions: Fluorescence imaging with ICG has been used to monitor *in-vivo* the effect of a vascular damaging agent. The fluorescence depletion in the tumor of mice treated with VDA demonstrates that this method can be used to verify the effect of such agents in a longitudinal experiment (day by day measurement on the same animal). The reliability of the method that use the ICG fluorescence to assess the perfusion in mice has been successfully checked using a tumor model characterized by an enhanced vasculature due the VEGF factor.

References:

1. G. Micheletti et al; *Cancer Res.* 63:1534-7 (2003)

2. L. Manenti et al; Mol Cancer Ther. 4:715-25 (2005)

CARDIOVASCULAR MEDICINE

MR imaging of atherosclerosis in rabbit aortas with MS-325

Lobbes M.B.I.[1], Heeneman S.[2], Miserus R.J.J.H.M.[1], Leiner T.[1], Kessels A.F.[3], Wiethoff A.[4], Daemen M.J.A.P.[2], Van Engelshoven J.M.A.[1], Kooi M.E.[1]

Cardiovascular Research Institute Maastricht, departments of Radiology[1] and Pathology[2], Maastricht, the Netherlands. Clinical Epidemiology and MTA[3], University of Maastricht, Maastricht, the Netherlands. EPIX Medical Inc.[4], Cambridge, USA.

Background: Contrast-enhanced magnetic resonance imaging improves atherosclerotic plaque visualization. An initial study suggested that MS-325 specifically leaks into atherosclerosis-prone sites.

Aim: To compare contrast-enhanced MRI of atherosclerotic lesions with MS-325 (Vasovist®, Schering AG, Germany) and Gd-DTPA (Magnevist®, Schering AG, Germany).

Methods: In 8 out of 14 male New Zealand White (NZW) rabbits, atherosclerotic plaque development was induced by surgical balloon denudation. Starting from two weeks prior to balloon denudation, these rabbits were fed a cholesterol-enriched diet (1.0%) for ten weeks. The remaining 6 rabbits were sham-operated and received regular rabbit chow (controls). The diseased rabbits and controls were then subdivided into groups of 3-4 rabbits each: an MS-325 and a Gd-DTPA group. Subsequently, pre- and post-contrast MR imaging was performed with a whole-body 1.5 Tesla MRI system using a synergy cardiac coil and a dose of 50 µmol/kg MS-325 or 500 µmol/kg Gd-DTPA. Post-contrast imaging was performed at 5 times the elimination half-life of the contrast agents. A 3D, double inversion recovery (black blood) turbo spin echo sequence was used with the following scan parameters: 9 transversal slices (thickness 3 mm), TR 570 ms, TE 14 ms, echo train length 5, field-of-view 90x90 mm, matrix 304x304, resulting in an in-plane resolution of 0.3x0.3 mm. Signal intensities (SI) corrected for scaling were determined. Pre-contrast SI of adjacent muscle tissue served as reference. Enhancement was defined as the ratio between pre- and post-contrast signal intensities. Clustered analysis was used to test enhancement and differences between groups.

Results: Mean signal enhancement for the MS-325 group was 1.8±0.6 for the atherosclerotic rabbits and 1.2±0.3 for controls (p=0.02). No significant signal enhancement differences between atherosclerotic and control rabbits were seen in the Gd-DTPA group (2.6±0.7 and 2.3±0.6, respectively (Figure 1). However, additional animals need to be included to verify these preliminary results.

Conclusions: Post-MS-325 signal enhancement of atherosclerotic vessel wall is significantly larger than that of normal vessel wall. In contrast, Gd-DTPA enhanced MRI does not seem to be able to distinguish between atherosclerotic and normal arterial vessel walls of NZW rabbits.

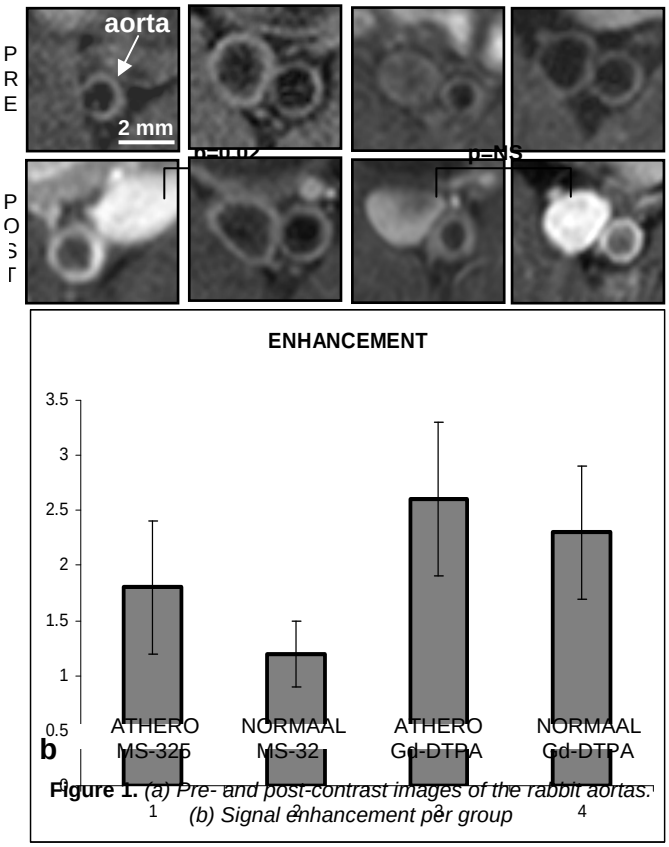

Figure 1. *(a) Pre- and post-contrast images of the rabbit aortas. (b) Signal enhancement per group*

Liposome-enhanced MRI of neointimal lesions in the ApoE-KO mouse

Mulder WJM 1, Douma K 2, Koning GA 3, van Zandvoort M 2, Lutgens E 4, Daemen MJ 4, Nicolay K 1, Strijkers GJ 1*

*1Biomedical NMR, Department of Biomedical Engineering, Eindhoven University of Technology, the Netherlands; 2Department of Biophysics, CARIM, University of Maastricht, the Netherlands; 3Department of Radiation, Radioisotopes and Reactors, Section of Radiation and Isotopes for Health, Faculty of Applied Sciences, Delft University of Technology, the Netherlands; 4Department of Pathology, CARIM, University of Maastricht, the Netherlands; *presenting author*

Background: Conventional high resolution MRI is capable of detecting atherosclerotic plaques, both in human atherosclerosis and in animal models of atherosclerosis [1]. However, MRI is not very effective in visualizing early atherosclerotic lesions with low lipid content, since the proton density, *T*1, and *T*2 of these lesions are similar to those of surrounding tissue. Contrast-enhanced
MRI in combination with an appropriate contrast agent might be able to detect such lesions.

Aim: To assess the potential of long-circulating paramagnetic liposomes in ApoE-KO mice to visualize the neointimal thickening in lesions induced in one of the carotid arteries with MRI.

Methods: Paramagnetic liposomes were prepared as described previously [2]. ApoE-KO mice were put on a high cholesterol diet and a collar was surgically positioned around the right carotid artery. Nine to 12 days after cuff placement mice were used for the experiments. Two mice were assessed histologically with hematoxylin-eosin-staining and 6 mice were scanned on a 6.3 T MRI scanner. *T*1-weighted imaging (TR=800ms, TE=12ms, black-blood spin-echo) was performed before and at 3 time points (15 min., 45 min. and 24 hrs.) after injection with contrast agent. Three mice were injected with the paramagnetic liposomes and 3 mice with Gd-DTPA as a control.

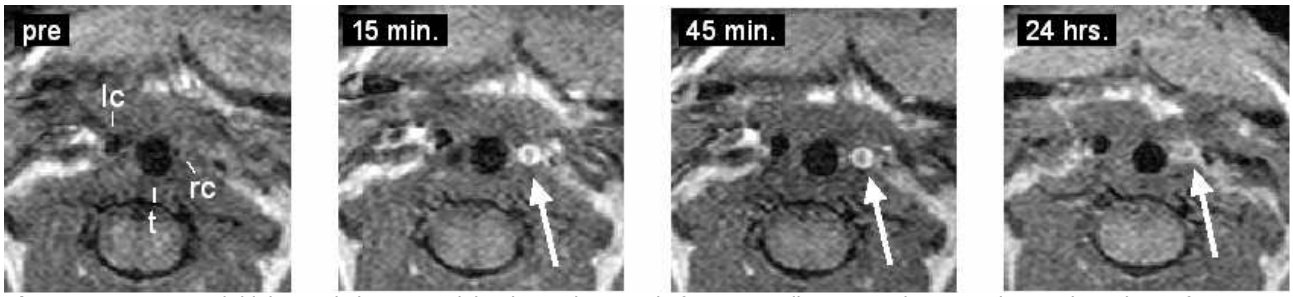

Figure 1: *Transversal high resolution T1-weighted MR images before as well as 15 min., 45 min., and 24 hrs. after administration of the paramagnetic liposomes (lc=left carotid, t=trachea, rc=right carotid).*

Results: The collar around the right carotid led to severe intimal thickening proximal to the cuff, while a normal morphology of the untreated carotid was observed. *T*1-weighted images from the mice that were intravenously injected with Gd-DTPA revealed no significant signal change in the lesion at any time point. Upon injection of paramagnetic liposomes, a large signal enhancement was observed, as shown in Fig. 1 indicated with the arrows. The wall of the right carotid artery became clearly highlighted, because of the accumulation of the contrast agent. As early as 15 min. after contrast agent injection signal enhancement was observed at the site of the lesion proximal to the collar. This signal enhancement remained present 45 min. after the injection and was still observed after 24 hrs. The signal intensity of the vessel wall of the left carotid artery did not change after injecting the liposomal contrast agent. Average signal enhancements of 93 ± 10 %,
111 ± 10 %, and 96±9 % were observed at the lesion site at 15 min., 45 min., and 24 hrs., respectively. Although the exact mechanism of accumulation has to be established we infer

that the collar placement caused a localized blood flow disturbance by narrowing of the arterial lumen and hence an increased permeability of the endothelial layer, which resulted in passive accumulation of the liposomes.

Conclusions: We have shown the possibility of imaging the collar induced neointimal thickening in the carotid artery of ApoE KO mice with high resolution MRI. Most importantly, we were able to detect intimal thickening in this mouse model using *T*1-weighted MRI after intravenously injecting paramagnetic liposomes. Furthermore, these results demonstrate efficient targeting of liposomes to atherosclerotic lesions.

References:

[1] Choudhury *et al.*, Arterioscler Thromb Vasc Biol. 22 (2002).
[2] Mulder *et al.*, Bioconjugate Chemistry 15, 799 (2004).

High resolution X-ray microtomography as a tool for the detection and quantification of vascular calcifications in live rats with chronic renal failure

Postnov A[1] ,Persy V[2],Neven E[2],Dams G[2],De Broe M[2], D'Haese P[2], De Clerck N[1] ,
[1]*Laboratory of Microtomography and* [2]*Department of Pathophysiology , University of Antwerp, Antwerp, Belgium*

Background: High resolution X-ray microtomography (micro-CT), is a suitable imaging device to visualize bone and calcified tissue. A major advantage of *in vivo* micro-CT is its non- invasive nature [1],[2]. Vascular calcification is a prominent feature of cardiovascular disease in patients with end-stage renal failure.

Aim: In the present report, we examined the application of *in vivo* micro-CT as a tool to detect and to follow-up vascular calcifications in living rats with chronic renal failure (CFR).

Methods: CRF was induced by feeding rats a diet containing 0.75% adenine (0.92% P and 1.0% Ca) for 4 weeks, which has been shown to induce a stable, moderate to severe renal function impairment[3].
For scaning a desktop *in vivo* X-ray micro-CT system was used (Skyscan 1076, Aartselaar, Belgium) without gating for cardiac or respiratory motion. With this system, both the X-ray source (focal spot size 5 µm, energy range 20-100 keV) and the detector (CCD camera 2.3kx4k) rotate around the animal (field of view was 68mm). For *in vivo* acquisition a Ti filter was used. Living rats were scanned repetitively at different time intervals, to detect and to follow-up calcifications in the aorta. In addition to *in vivo* scanning, the whole aorta was extracted and embedded in paraffin after sacrifice of the rats. These paraffin blocks were scanned again with Al filter. Both in the *in vivo* and the *in vitro* condition, voxel size was 35x35x35 µm.

Results: We could show that *in vivo* micro-CT was a sensitive method to detect vascular calcifications. Imaging by micro-CT allowed non-invasive discrimination between rats that developed calcifications and animals that did not. The presence of these calcifications was validated by histology and by the determination of the bulk calcium content in the tissue. Moreover, imaging by *in vivo* micro-CT proved to be reproducible as shown by repetitive scans. For quantification, the volume and area of the calcified tissue could be calculated after *in vitro* scanning of the paraffin blocks. A good correlation was found between all observations.

Conclusions: *In vivo* micro-CT scanning proved to be a sensitive method to detect vascular calcifications in rats with chronic renal failure. This non-invasive imaging technique allows to follow-up and to quantify the development, and potential reversal during treatment, of vascular calcifications in living animals.

References:

[1] Postnov, A. et al.; *Physiol. Meas,* 24, 165-178, (2003).
[2].Waarsing, J.H. et al; *Bone* 34, 163-169, (2004).
[3] Okada H et al., *Clin Exp Immunol* 3:82-88, (1999)

Towards imaging of vulnerable atherosclerotic plaques using bimodal quantum dots in optical and MR imaging

Prinzen L[1], Miserus RJJHM[3], Dirksen A[2], Hackeng TM[2], Backes WH[3], Kooi ME[3], Slaaf DW[1], Reutelingsperger CPM[2], van Zandvoort MAMJ[1]
[1]Department of Biophysics and [2]Biochemistry, University of Maastricht; [3]Department of Radiology, University Hospital Maastricht (AZM)

Background: Since conventional imaging techniques are unable to discriminate between stable and vulnerable plaques, a bimodal probe was designed based on Annexin A5 (AnxA5). AnxA5 binds to phosphatidylserine (PS), cell surface expressed after onset of apoptosis and after platelet activation. AnxA5 specifically labels vulnerable plaques because of their apoptotic contents and thrombus formation subsequent to plaque rupture[1]. The bimodal probe allows Magnetic Resonance Imaging (MRI) as well as fluorescence imaging at the subcellular level.

Aim: Development of a PS targeted bimodal (optical and MR) probe to detect vulnerable plaques *in vivo.*

Methods: Quantum dots (QDs) are brightly fluorescent, non-bleachable probes that have broad excitation and narrow emission spectra[2]. Streptavidin-coated QDs were used as a scaffold to conjugate biotinylated (bio)molecules. Biotinylated AnxA5, coupled to QDs in a 1:1 stoichiometry, was used to label apoptotic cells and activated platelets. The remaining binding sites (around 30) were occupied by biotinylated lysine-wedges; each containing eight Gadolinium-DTPA molecules (MR contrast agents). This probe was tested in vitro on apoptotic Jurkat cells and whole-blood clots by both Two Photon Laser Scanning Microscopy (TPLSM) and MRI. The TPLSM was excited at 800 nm and pulsed at 100 fs[3]. MRI was performed with a 1.5T whole body system using an inversion recovery TSE sequence with TI/TE/TR 546/13/1580 ms and an in-plane resolution of 0.21x0.21 mm^2.

Results: Relaxivity (R_1) of the probe in solution was calculated to be nearly 5000 $ms^{-1}M^{-1}$ per QD. TPLSM demonstrated specific AnxA5-binding of the probe to apoptotic Jurkat cells. MR images of cells showed a 34-fold increase in signal intensity compared to unlabeled cells, confirming bimodality of the probe. TPLSM also showed AnxA5-specific binding of the probe to activated platelets in whole-blood clots. When the probe was added after clot-formation, a 0.1 mm thick rim exhibited AnxA5-labeled platelets, as confirmed by fluorescence microscopy on frozen sections. When added before clot-formation, also AnxA5-labeled platelets were visible on the outside of the clot when imaged with TPLSM. With MRI, however, neither of the two clots showed increased signal intensity. Most likely, probe addition after clot-formation resulted in insufficient labeled platelets. When the probe was added before clot-formation, platelets probably did bind sufficient AnxA5-QD, but due to the anti-coagulant effect of AnxA5 these platelets were rinsed from the clot after incubation when washed in buffer. This was concluded because a significantly lower MR signal intensity was observed when adding a higher amount of probe.

Conclusions: The bimodal probe enables imaging of apoptotic cell samples in fluorescence microscopy and MRI. This new probe is therefore promising as a verification method at the subcellular level (TPLSM) for *in vivo* experiments (MRI). The effectiveness of the probe on whole-blood clots is being further investigated.

References:

[1] B. L. Kietselaer, et al.; *N Engl J Med* 350: 1472-3 (2004)
[2] A. Watson, et al.; *Biotechniques* 34: 296-300, 302-3 (2003)
[3] M. van Zandvoort, et al.; *J Vasc Res* 41: 54-63 (2004)

^{99m}TC-ANNEXIN-V FUNCTIONAL IMAGING OF LUMINAL THROMBUS ACTIVITY IN ABDOMINAL AORTIC ANEURYSMS

Laure Sarda-Mantel[1,2], Michèle Coutard[3], Olivier Raguin[1,2], Jean-Marc Vrigneaud[1,2], Florence Hervatin[2,4], Geneviève Martet[2], François Rouzet[1,2], Pascal Merlet[1,2], Dominique Le Guludec[1,2] and Jean-Baptiste Michel[3].

[1] Médecine Nucléaire Hôpital Bichat, Paris, France; [2] INSERM U773 CRB3, UFR Bichat, Paris, France; [3] INSERM U698, Hôpital Bichat, Paris, France; [4] CEA-DRM, Orsay, France;

Background: The mural thrombus of abdominal aortic aneurysms (AAA) is considered to play an important role in the pathogenesis of aneurysm progression, by contributing to smooth muscle cells disappearance via several interdependent biological processes including platelet activation-induced fibrin formation [1,2]. ^{99m}Tc-annexin-V (ANX) is a scintigraphic tracer that binds to phosphatidylserine exposed on activated platelets and apoptotic cells [3,4].

Aim: To evaluate the potential of ANX imaging to assess mural thrombus biological activity in an experimental AAA model. The clinical applicability was further tested on human samples of excised AAAs.

Methods: Experimental AAA was created by infusing elastase into infra-renal abdominal aorta in 17 anaesthetized rats [5]. Abdominal ANX scintigraphic images were recorded 2 weeks later, using a small animal SPECT/CT system (Biospace Mesures, Paris, France). Quantitative autoradiography and histological studies of infra-renal aorta were finally obtained.

Results: Four rats did not develop AAAs and showed negative ANX scintigraphy, with negative autoradiography in 3 of 4 cases. Among the 13 rats which developed AAA, 11 displayed intense ANX uptake in AAA on scintigraphy (Target/Non Target ratio: 5.7+/-0.9 on tomoscintigraphy) and autoradiography (302+/-99 counts/mm^2 versus 16+/-7 in normal thoracic aorta, $p<10^{-7}$; R=26+/-14), 2 showed negative scintigraphy and autoradiography. ANX uptake on scintigraphy correlated with ANX activity on autoradiograms (R=0.68, p<0.02), and was located in the thrombus area where activated platelets expressing P-selectin and PMNs accumulated. Increased specific ANX binding was also observed in the biologically active luminal thrombus layer of 7 excised human AAA harvested during surgery.

Conclusions: ANX imaging may assess non-invasive in vivo evaluation of mural thrombus renewal, an important determinant of vascular remodeling in patients with AAA.

References

[1]Kazi M, Zhu C, Roy J, Paulsson-Berne G, Hamsten A, Swedenborg J, Hedin U, Eriksson P. Difference in matrix-degrading protease expression and activity between thrombus-free and thrombus-covered wall of abdominal aortic aneurysm. *Arterioscler Thromb Vasc Biol.* 2005;25:1341-1346.

[2]Touat Z, Ollivier V, Dai J, Huisse MG, Bezeaud A, Sebbag U, Palombi T, Rossignol P, Meilhac O, Guillin MC, Michel JB. Renewal of mural thrombus releases plasma markers and is involved in aortic abdominal aneurysm evolution. *Am J Pathol.* 2006;168:1022-1030.

[3]Stratton JR, Dewhurst TA, Kasina S, Reno JM, Cerqueira MD, Baskin DG, Tait JF. Selective uptake of radiolabeled annexin V on acute porcine left atrial thrombi. *Circulation.* 1995;92:3113-3121.

[4]Blankenberg FG, Katsikis PD, Tait JF, Davis RE, Naumovski L, Ohtsuki K, Kopiwoda S, Abrams MJ, Strauss HW. Imaging of apoptosis (programmed cell death) with 99mTc annexin V. *J Nucl Med.* 1999;40:184-191.

[5]Anidjar S, Salzmann JL, Gentric D, Lagneau P, Camilleri JP, Michel JB. Elastase-induced experimental aneurysms in rats. *Circulation.* 1990;82:973-981.

Long term perfusion imaging indicates poor functionality of vegf-induced vasculature in vivo

Ennio Tasciotti1, Serena Zacchigna1,4, Claudia Kusmic2, Nikola Arsic1, Oreste Sorace2, Cecilia Marini2, Paolo Marzullo2, Silvia Pardini2, Debora Petroni2, Lucia Pattarini1, Silvia Moimas1, Mauro Giacca1, GianMario Sambuceti2,3

1Molecular Medicine Laboratory, International Centre for Genetic Engineering and Biotechnology (ICGEB), Trieste, Italy;

2Istituto di Fisiologia Clinica (IFC), CNR, Pisa, Italy;

3Institute of Nuclear Medicine, Department of Internal Medicine, University of Genoa, Italy

4Department of Normal Human Morphology, University of Trieste, Italy

Background: Although the angiogenic effect of VEGF is widely recognized, a central question is whether the vessels formed upon its overexpression effectively increase functional tissue perfusion in vivo or other factors are required for proper vessel maturation.

Aim: To explore this issue, we exploit adeno-associated virus (AAV)-mediated gene delivery to obtain the prolonged expression of VEGF and angiopoietin-1 (Ang1) in the rat skeletal muscle.

Methods: Over a period of 6 months after transduction, muscle blood flow (MBF) was measured using PET and N13-ammonia, and vascular permeability and total blood volume using SPECT after Tc99m-DTPA injection. All measurements were performed in both resting conditions and after electrically-induced muscle exercise.

Results: Despite the potent angiogenic effect of VEGF, documented by vessel counting and intravascular volume assessment, the expression of this factor alone did not account for any improvement in resting MBF, while it even decreased perfusion in response to exercise. This deleterious effect was related to the formation of abnormal and leaky vascular lacunae, which accounted for the occurrence of artero-venous shunts that excluded the downstream microcirculation, as also detected by the injection of Tc99m-macroaggregates followed by SPECT. These effects were significantly counteracted by the co-injection of VEGF and Ang1, which determined a marked increase of resting MBF and, most notably, induced a highly significant improvement after exercise that persisted over time.

Conclusions: Taken together, these results raise important concerns about the effectiveness of VEGF as a sole factor to induce angiogenesis and prompt the use of factor combinations to achieve competent blood vessel formation in vivo.

CHEMISTRY

Gd(III) chelates of DOTA-type glycoconjugates: studies of internalization on a Hep-G2 cell line, gamma scintigraphy and magnetic resonance imaging on a rat model

Torres S[a], Martins JA[a], André JP[a], Prata MI [b], Santos AC [b], Neves M [c], Rodrigues TB [d,e], López-Larrubia P[e], Garcia-Martin ML[e], Cerdán S[e], Geraldes CFGC[d]

[a] Dep. Química, Universidade do Minho, Braga, Portugal;[b] IBB, Fac. Medicina, Universidade de Coimbra, Portugal; [c] ITN, Lisbon, Portugal; [d] Dep.Bioquímica, Centro de RMN e Centro de Neurociências e Biologia Celular, Universidade de Coimbra, Portugal; [e]LIERM, Instituto de Investigaciones Biomédicas "Alberto Sols", Madrid, Spain.

Background: The development of new and more efficient contrast agents (CA) is an area of intense research, such as extracelular agents, those targeted to the macrophage-monocytic phagocytic system (MMPS), hepatobiliary and intravascular or blood-pool agents.[1] We have developed Ln(III)–thioglycoconjugates of different sugars as potential liver MRI contrast agents.[2] These small Gd(III) complexes were designed for targeting the asialoglycoprotein receptor (ASGP-R) which recognizes β-galactosyl residues on desialylated glycoproteins and is expressed on hepatocyte cells.

Aim: To study the effect of valency, topology and sugar type on the internalization on a HepG2 cell line, which expresses ASGP receptors, and in biodistribution of several small ^{153}Sm (III)-labelled thioglycoconjugate complexes in Wistar rats using gamma scintigraphy. To assess some of the Gd(III)-thioglycoconjugate complexes as CA in a MRI study in mice.

Results: The radioligand [^{153}SmDOTAGal$_2$] is taken up by the Hep-G2 cells, which is reduced to 50% after 120 min in the presence of an excess of asialofetuin or galactose. Biodistribution, gamma scintigraphic images and time-activity curves at various regions of interest of Wistar rats injected with ^{153}Sm(III)-DOTA-X (X = Gal, Gal$_2$, Gal$_4$, Lac$_2$ and Glc$_2$) show strong liver uptake for all cases except Glc$_2$, which lasts more than 24 h for Gal$_4$. This uptake is strongly blocked (90%) by co-injection of an excess of asialofetuin. Pharmacokinetics of the MRI CAs was analyzed by the time course of signal intensity of several ROIs (liver, kidney medulla, kidney cortex and muscle), during T_1 weighted spin echo MRI experiments in mice with GdDOTALac$_2$ and GdDOTAGal$_2$, and compared with GdDTPA (Magnevist). The liver-to-kidney cortex contrast ratio caused by the glycoconjugates is comparable but not better than that induced by GdDTPA.

Conclusions:
Despite the specific uptake via the ASGP-R and good scintigraphic imaging performance of the galactose-bearing multivalent ^{153}SmDOTA compounds, the animal MRI assessment of the corresponding Gd^{3+} chelates shows liver-to-kidney contrast effects similar to GdDTPA. This probably results from the high hydrophilicity of the complexes, which are quickly washed out from the liver, limiting their use as contrast agents for lectin-mediated molecular imaging.

References:
[1] Mahfouz AE, Hamm B, Taupitz M, *Eur Radiol.* 7: 507-513 (1997)
[2] a)Baía P, André JP, Geraldes CFGC, Martins JA, Merbach AE, Tóth É, *Eur J Inorg Chem.* 2110-2119 (2005). b) André JP, Geraldes CFGC, Martins JA, Merbach AE, Prata MIM, Santos AC, de Lima JJP, Tóth É, *Chem Eur J.*10: 5804-5816 (2004)

Gd-loaded LDL for MRI visualization of tumor cells

S. Lanzardo[2], S. Geninatti-Crich[2], G.B Giovenzana, S. Belfiore[2], C. Lovazzano[2], R. Pagliarin, S. Aime[2]
[2]*Department of Chimica I.F.M., University of Torino, via P. Giuria 7, 10125 Torino, Italy.*

Background: Low Density Lipoproteins (LDLs) are naturally occurring nanostructures that in mammalian system specifically transport cholesterol to cells expressing the LDL receptor. LDL receptors are overexpressed in tumor cells. Therefore LDLs may be considered a good candidate for MRI visualization of tumor cells once loaded with Gd complexes.

Aim: To use Gd-labeled LDL for visualize tumor cells.

Methods: The uptake of the Gd-labeled LDL were tested in vitro on HepG2 (human hepatoblastoma cancer cell line) and B16 (melanoma) tumor cells line and then administered to mice inoculated with B16 cells line subcutaneously into right flanks. Magnetic Resonance Imaging (MRI) was performed before, 5 and 24 hr post-contrast injection. The MRI analysis were then compared with the slices obtained from the same tumors, excised, fixed, embedded and prepared to histochemical analysis.

Results: The binding to LDL of two Gd-based Imaging Probes bearing a lipophilic substituent has been investigated in detail. Then the system showing the highest efficiency has been tested for the uptake in the tumor cells HepG2 and B16 via the LDL receptor route.

The cellular labelling experiments proved that, after 24 hours of incubation in the presence of 30 ug/ml of LDL and 18uM of the Gd (III) containing probes, the amounts of internalised Gd is sufficient to generate hyper intense signals in the corresponding MR images. Work is in progress to assess the potential of the proposed procedure on tumor bearing animal models.

Conclusions: Gd-loaded LDLs have potental utility as a targeted MRI contrast agent for in vivo tumor detection.

MRI visualization of Cells Labeled with Gd-containing compounds

Terreno E[1], Geninatti Crich S[1], Biancone L[2], Cabella C[3], Cantaluppi V[2], Esposito G[1], Camussi G[2], Aime S[1]
[1] *Department of Chemistry IFM and Molecular Imaging Center, University of Torino, Italy.*
[2] *Department of Internal Medicine, CeRMS, Ospedale Molinette, University of Torino, Italy.*
[3] *Bracco Imaging, BioIndustry Park, Colleretto Giacosa (TO), Italy*

Background: MRI visualization of cells labeled with Gd-based imaging probes appears a promising route for pursuing novel applications in the field of cellular and molecular imaging. In fact, it has been shown that the problems associated with the intrinsic low sensitivity of MRI can be overcome by the intracellular accumulation of a high number of paramagnetic Gd(III) chelates.

Aim: i) To test the possibility to visualize *in vivo* Gd(III) labeled cells by MRI, and ii) to compare the cell internalisation efficiency and the relaxometric properties of Gd(III)-labeled cells between pinocytosis and electroporation routes.

Method: Transplanted pancreatic mouse and human islets have been labeled with Gd-HPDPO3A by exploiting pinocytosis route. Cells were incubated at 37℃ for 16 hours in the presence of the Gd(III) complex (0-50 mM) in the incubation medium.[1] The labeled cells were visualised by MRI at 7 T, before and after intrahepatic and kidney subcapsular grafting on mice.

Results and Conclusions: It has been demonstrated that the exploitation of the pinocytosis route, entraps the Gd(III)-chelate into endosomic vesicles, where its relaxometric efficiency is markedly quenched by the slow exchange of water protons between endosome and cytosol compartments.[2] Although this drawback clearly represents a limitation, the Gd(III)-labeled transplanted pancreatic mouse and human islets can be visualized by MRI either *in vitro*, after dispersion in agar, or *in vivo*, after kidney subcapsular and intrahepatic grafting (see the

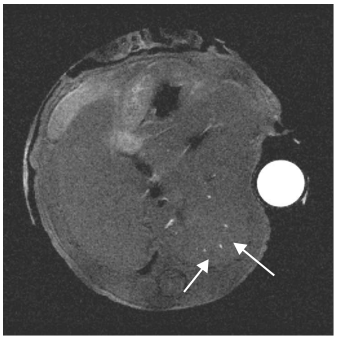

figure below) on mice.

A significantly higher relaxometric efficiency was observed when the Gd(III) complex has been internalised by the electroporation route. In fact, this pathway allows the imaging probe to be entrappeed in the cytosolic compartment, thus reducing to only one the number of membranes to be crossed by water molecules. The efficiency and safety of the different labeling method has been compared on both stem cells (endothelial progenitor cells) and tumor cells (HTC).

References:
[1] Geninatti Crich SG et al.; *Magn Reson Med.* 51: 938-44 (2004)
[2]Terreno E et al.; Magn Reson Med. 55: 491-497 (2006)

Rhenium and Technetium Tracers That Target Integrins *In Vivo*: Some Combinatorial Approaches

Le Gal J, Aufort M, Chaignon N, Thai R, Lelait MA, Ménez A, Dugave C*
CEA/Saclay, Département of Protein Engineering and Study (DIEP), Building 152, 91191 Gif sur-Yvette, FRANCE

Background: Imaging of integrins enables an early detection of cancer recurrence and metastasis however, limited biodisponibility and low specificity of tracers limits its use for *in vivo* diagnosis.

Aim: To use combinatorial chemistry and in vivo screening for the selection of efficient tracers (labelled with ^{99m}Tc, a □ emitter) and therapeutic radiopharmaceuticals (labelled with $^{186/188}$Re, a □$^{-}$ emitter).

Methods: Integrins form a family of □□ heterodimeric receptors that play an essential part in cell-cell and cell-matrix adhesion. Overexpression of several integrins are related to tumor neoangiogenesis which facilitates tumor progression and metastasis. Consequently, integrins (in particular integrins □V□3) are specific markers of many human cancers [1,2]. Various molecules which mimic the canonical RGD sequence specifically bound by several integrins may be employed for diagnostic and therapeutic purposes. Presently, *in vivo* studies have been carried out using cyclic pentapeptides derived from c(RGDfV) and bearing an exogenous label (^{18}F, ^{64}Cu, ^{99m}Tc…). On the one hand, we synthesized a series of linear analogs of the RGD 3-mer which may be cyclized through $Re^{V}O^{3+}$ and $Tc^{V}O^{3+}$ coordination. On the other hand, we prepared collections of independent motifs which are anticipated to mimic the RGD sequence, by metal core complexation, using the combinatorial assembly method previously validated with cyclophilin modular ligands [3].

Results: A series a modified tripeptides R^{1}-(D/L)Arg–Gly/□Ala–(D/L)Asp/Glu–R^{2} were synthesized on a methoxytrityl resin using classical combinatorial techniques. Peptides bearing a NS_2 motif at the N-terminus and various thioalkyl and thioaryl moieties were obtained with good yields and purities. Intramolecular coordination of $Re^{V}O^{3+}$ and $^{99g}Tc^{V}O^{3+}$ gave the corresponding cyclic complexes. Evaluation of their chemical and biological stabilities is underway.
The synthesis of modules mimicking either arginine (module A) or aspartate (module B) and bearing NS_2/S motifs capable of coordinating $Re^{V}O^{3+}$ and $Tc^{V}O^{3+}$ cores (•) was done by solution organic chemistry. Combinatorial assembly of the modules through metal complexation enables the constitution of a 80-members library (A•B) which display satisfactory stabilities in mice sera.

Conclusions: Cyclization of modified tripeptides and assembly of modular dipeptides through $Tc/Re^{V}O^{3+}$ coordination lead respectively to the synthesis of 64 and 80 member libraries. Theses compounds will be tested *in vivo* on Balb-C nu/nu mice bearing a U-87 MG human glioblastoma astrocytoma which overexpresses integrins □$_V$□$_3$.

References:
[1] Guo W, Giancotti FG, *Nature Mol. Cell Biol.* 5:816-826 (2004)
[2] Rust WL, Carper SW, Poppler GE, J. Biomed. Biotechnol. 2:124-130 (2002)
[3] Clavaud C, Heckenroth M, Stricane C, Lelait MA, Ménez A, Dugave C*, *submitted*

Combinatorial Assembly of Rhenium and Technetium Coordinates: an *In Vitro* Evaluation using Cyclophilin hCyp-18

Clavaud C, Heckenroth M, Stricane C, Lelait MA, Ménez A, Dugave C*
CEA/Saclay, Département of Protein Engineering and Study (DIEP), Building 152, 91191 Gif-sur-Yvette, FRANCE

Background: Accelerated clearance and decreased affinity and specificity of tracers derived from classical bioactive molecules are major drawback for the development of novel radiopharmaceutics usable for imaging and therapeutic purposes.

Aim: To develop a new combinatorial methodology for the synthesis of large collections of molecules usable for in vivo screening of radiopharmaceuticals.

Methods: Combinatorial assembly of sub-libraries of independent but complementary modules A (n modules) and B (m modules) through rhenium or technetium (•) coordination leads to the formation of libraries of n X m stable metal complexes A•B. In order to validate the strategy *in vitro*, we screened 2 independent libraries of metallopeptides containing the $Re^{V}O^{3+}$ core. These rhenium complexes were anticipated to mimic the peptide sequence Ala/Gly-Pro-Xaa-*p*NA that specifically interact with cyclophilin hCyp-18, an important peptidyl-prolyl isomerase implicated in several diseases including AIDS, cancer and neurologic disorders [1]. In preliminary attempts, cyclic and acyclic rhenium-peptide coordinates were used to evaluate the effect of the rhenium core on the binding to hCyp-18. All pure modular compounds were screened as ligands of hCyp-18.

Results: Use of cyclic and acyclic peptides containing the canonical sequence Ala-Pro-Xaa-*p*NA bearing the $Re^{V}O^{3+}$ core and fluorescence quenching experiments [2] showed that introduction of the oxorhenium core did not perturb the interaction of the peptide with the protein [2]. The reconstitution of potential cyclophilin ligands was then carried out by combinatorial assembly. Modules A and B mimicking respectively the N- and C-terminal parts of peptide Ala/Gly-Pro-Phe-*p*NA were synthesized by solution peptide synthesis and polymer supported synthesis using Kaiser or sulfamylbutyryl resins. Two libraries of rhenium complexes were prepared from 7 X 16 and 11 X 16 compounds to give respectively 112 and 176 compounds. Two compounds, selected by in vitro screening, displayed affinities increased by 13 and 18 folds relative to the reference peptide. The preparation of a small library of Re and ^{99m}Tc complexes was done to give either a collection of individual compounds or a mixture of identified complexes [3].

Conclusions: Two libraries of rhenium complexes were prepared by combinatorial assembly of independent modules. Several of these complexes bind hCyp-18 with a significant better affinity than the corresponding substrate peptide. Use of easily accessible rhenium/technetium cores enables the application of the method to the preparation of ^{99m}Tc-containing tracers usable for in vivo studies as well as the corresponding $^{186/188}$Re complexes whose have been proposed as radiotherapeutics.

References:
[1] Dugave C, Demange L, *Chem. Rev.* 103:2475-2532 (2003)
[2] Clavaud C, Heckenroth M, Stricane C, Lelait MA, Ménez A, Dugave C*, Bioconjugate Chem. *Accepted*
[3] Clavaud C, Heckenroth M, Stricane C, Lelait MA, Ménez A, Dugave C*, *submitted*

A Novel Method for the Direct Labeling of Proteins with ^{99m}Tc on endogenous sites.

Loïc Le Clainche*, Ludivine Courson, Philippe Cuniasse
Département d'Ingénierie et d'Etude des Protéines, CEA Saclay, 91191 Gif sur Yvette, France.

Aim: To incorporate a technetium core into a protein without any modification of the protein chemical structure to obtain stable technetium-protein complexes.

Methods: The proteins were labeled with 99m-Tc using gluconate as a co-ligand. The complexes were characterized using ITLC, radio-HPLC and ESI-MS spectroscopy. The stability of the obtained complexes was tested against both 1mM of histidine and cysteine. The stability of the compounds was also tested in mouse serum, and the results analyzed by electrophoresis.

Results: We developed a general method for the direct radio-labelling of proteins with $^{99m}TcO^{3+}$. This approach is based on the presence, at the surface of proteins, of endogenous sites formed by chemical functions able to coordinate the technetium core. We evaluated this approach by synthesizing complexes with different proteins of interest in diagnostic imaging. For these complexes, we obtained specific activities in the range 1-30 MBq/µg. These protein-$^{99m}TcO^{3+}$ complexes were shown to be stable in the presence of competitors like histidine and cysteine. In addition, we showed that the protein-$^{99m}TcO^{3+}$ complexes synthesized were stable for 6 to 12 hours in mouse serum.

Conclusions: Our method provides stable technetium-protein complexes. The technetium atom is coordinated on endogenous binding sites which do not include disulfide bonds. These results demonstrated the considerable potential of our approach for the use of proteins in the field of molecular imaging.

Contrast Agents for High field Mri applications

Eva Toth,[1] João Bruno Livramento,[2] Paulo Loureiro De Sousa,[2] Angélique Sour,[2] André Merbach,[2] Lothar Helm,[2] William Même[3], Bich-Thuy Doan[1], Jean-Claude Beloeil[1]
[1]*Centre de Biophysique Moléculaire, Orléans, France*
[2]*Ecole Polytechnique Fédérale de Lausanne, Switzerland*
[3] *U.P.R.E.S. E.A. 2633, Université d'Orléans, Orléans, France*

eva.jakabtoth@cnrs-orleans.fr

The development of a high relaxivity Gd(III)-based MRI contrast agents involves the fine-tuning of several determining parameters such as the water exchange rate and the rotation of the thermodynamically stable Gd(III) complex. Given the greater spatial resolution and sensitivity associated with higher frequencies, the current tendency in MRI is to increase the magnetic field. In the clinics today, most MRI machines work at 1.5 – 3 Tesla. However, for experimental animal studies, much higher fields are commonly applied (up to 9.4 Tesla or even higher). Macromolecular contrast agents often have a high proton relaxivity peak centred between 20-60 MHz, however, above this frequency the longitudinal relaxivity strongly decreases with increasing field and, at high fields, macromolecular agents are hardly superior to small molecular weight chelates. At very high fields intermediate size molecules, such as those presented here, are favourable over very large ones.
We have synthesized a bipyridine-based poly(amino carboxylate) ligand (L) which has been used to obtain a dinuclear complex Gd_2L and a metallostar $Fe(Gd^2L)_3$ [1]. A novel contrast agent, B12A, composed of 3 gadolinium chelates around a phenyl ring has been also obtained. The physico-chemical characterization of these compounds showed a limited flexibility, a very high relaxivity, particularly at high magnetic field and an exceptional density of relaxivity. We will present ^{17}O NMR and NMRD studies on these complexes. In addition to the in vitro characterization, we have performed in vivo feasibility studies at high magnetic field, which confirmed the remarkable relaxivities.

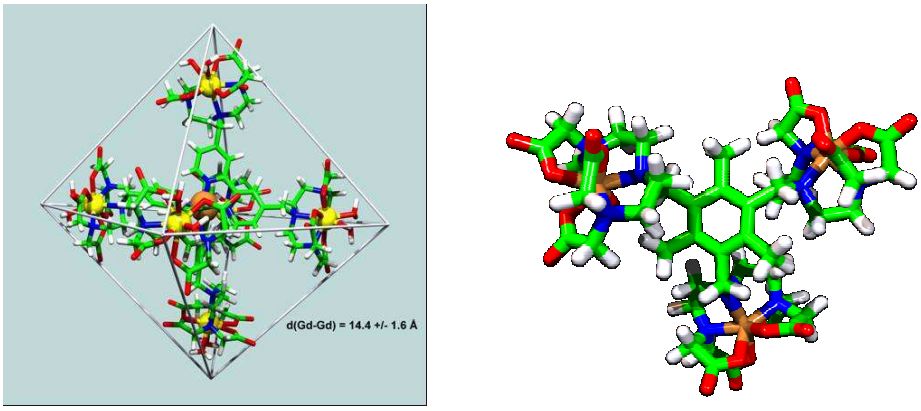

Figure 1. Structure of the metallostar and of B12A ($\{[Gd(DTTA)(H_2O)_2]3B12A\}^{3-}$)

[1] J.B. Livramento, A. Sour, A. Borel, A.E. Merbach, E. Toth, *Chem. Eur. J.*, 2006, 12, 989.

Detection of the VEGF receptor 2 in monolayers of cultured endothelial cells with magnetic resonance imaging at 3T

Heneweer C[1*], Kossel E[1*], Schlorf T[2*], Both M[1], Glüer C-C[1], Heller M[1], Mentlein R[2]
[1]Clinic for Diagnostic Radiology, University of Kiel; [2]Anatomical Institute, University of Kiel
[*]These authors contributed equally to the study.

Background: Primary systemic vasculitides are difficult to diagnose with conventional methods. Therefore, the development of molecular imaging based diagnoses for this disease pattern is of major interest. A possible target for the contrast agent is the vascular endothelial growth factor (VEGF), whose involvement in primary vasculitides has been reported[1][2].

Aim: The aim of this project is the development of superparamagnetic particles that are specific for inflammatory changes in endothelial cells (EC) and that can be detected non-invasively with magnetic resonance imaging (MRI) techniques.

Methods: Human umbilical vein EC (HUVEC) were cultivated as monolayers on transwell membrane filters. Initially, different superparamagnetic particles were tested in order to find the ideal particle for specific labelling. For this purpose, different concentrations of clinically approved as well as experimental iron oxide based contrast agents synthesized according own protocols were added to the cell culture medium. The unspecific uptake rate of the particles in the cells and the detection limit of the 3T MR scanner were investigated. Subsequently, an iron oxide based contrast agent against VEGF receptor 2 (anti-VEGFR-2) was developed. Specifically labelled HUVECs were then investigated with a 3T MR scanner.

Results: Monolayers of HUVEC with an iron concentration of lower than 50 ng/cell could be detected with MRI at 3T. The lowest unspecific contrast agent uptake rate was found for N20 and N70 particles (Micromod, Rostock). As a consequence, N20 particles were bound to anti-VEGF receptor 2 antibody and used for specific coupling to VEGF receptor 2 on HUVEC. MRI could distinguish the labelled cells from unlabelled cells and from cells that were immersed in N20-doped cell culture medium for unspecific uptake.

Conclusion: In conclusion, we present a specific superparamagnetic contrast agent against VEGF receptor 2 that can be detected by MRI after binding to HUVEC.

Acknowledgement: This work was supported by the State of Schleswig-Holstein under the research grant "Molecular Imaging North - Schleswig-Holstein (MOIN-SH) und Molecular Imaging Center (MIC)".

References:
[1] Li CG et al; *Br J Rheumatol.* 37:1303-6 (1998)
[2] Rueda B et al; *J Rheumatol.* 32 :1737-41 (2005)

In vivo evaluation of [^{123}I]FIAU, [^{123}I]IVFRU and [^{123}I]IVFAU in mice for potential non-invasive of HSV-1 thymidine kinase gene expression in gliomas

H-F. Li, A. Winkler, S. Moharram*, E.E. Knaus*, W.-D. Heiss, L.I. Wiebe*, A.H. Jacobs.
*Laboratory for Gene Therapy and Molecular Imaging, Max-Planck-Institute for Neurological Research, Center for Molecular Medicine and Department of Neurology, University of Cologne, Germany, *Faculty of Pharmacy and Pharmaceutical Sciences, University of Alberta, Canada*

Background: *I-FIAU is most commonly used for non-invasive assessment of herpes simplex virus type 1 thymidine kinase (HSV-1-tk) gene expression. However, it does not permeate the intact blood brain barrier (BBB) because of its moderately lipophilicity (-0.14 [1]).

Aim of this work is to compare biodistribution and brain uptake of two more lipophilic uracil nucleosides (s. structures)[1,2] with FIAU through radioiodinated compounds in order to test the permeablility to BBB in mice for potential measurement HSV-1-*tk* gene expression in gliomas.

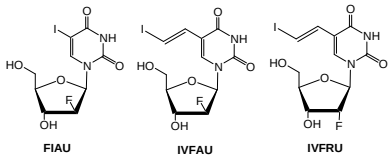

Methods and Results: All three tracers were labeled according to a described procedure [3]. The radiochemical yields ranged from 65 to 85%. The n.c.a. products were isolated using RP-HPLC. The partition coefficients (logP) of [^{123}I]IVFRU and [^{123}I]IVFAU were 1.21 and 1.64, respectively. Biodistribution studies were carried out using nude mice (n=3) at 2, 15, 60 and 120 min post injection. The brain uptake (%ID /g) and brain / blood ratios (see table), indicate that the more lipophilic IVFAU produces the higher brain / blood ratios, despite having the lower uptake (%ID /g).

Time p.i.	Brain uptake (%ID /g)			Brain/blood ratio (×10)		
	[^{123}I]FIAU	[^{123}I]IVFRU	[^{123}I]IVFAU	[^{123}I]FIAU	[^{123}I]IVFRU	[^{123}I]IVFAU
2 min	0.17	0.51	0.19	0.03	0.24	0.40
15 min	0.25	0.52	0.17	0.02	0.40	0.65
60 min	0.28	0.32	0.16	0.05	0.29	0.68
120 min	0.25	0.25	0.17	0.07	0.29	0.66

Conclusion: The biodistribution data show that brain uptake and retention of these nucleosides is not directly related to their lipophilicity. Since all three nucleosides are effectively transported by the equilibrative, NBMPR-sensitive nucleoside transporter [1], the low uptake in brain suggests that nucleoside-specific transport is also not modulating uptake into brain. The higher and constant brain/blood ratio of IVFAU may reflect greater stability against hydrolysis of the N-glycosidic bond or deiodination. These effects could be attributable to the steric effects of the C-2'-F substituent. In vivo PET evaluations of [^{124}I]IVFRU and [^{124}I]IVFAU in tumor-bearing mice are warranted in order to determine effects of the pathologically compromised integrity of the BBB.

Reference:

[1] K.W. Morin, W. Duan, L. Xu, A. Zhou, S. Moharram, E.E. Knaus, A.J.B. McEwan, L.I. Wiebe. Nucl Med Biol (in press).
[2]. J.R. Mercer, L.H. Xu, E.E. Knaus, L.I. Wiebe. , Am Chem Soc 32(1989) 1289-1294.
[3] G. Vaidyanathan, M. Zalutsky, Nucl Med Biol 25(1998) 487-496.

Synthesis of new oxygen tension probes (pO2) for 1H magnetic resonance spectroscopy imaging

Pacheco, Jesus[1]; Lopez-Larrubia, Pilar[1]; Soriano, Elena[1]; Perez-Mayoral, Elena[2]; Cerdán, Sebastián[1]; Ballesteros, Paloma[2]

[1] Laboratorio de Resonancia Magnética, Instituto de Investigaciones Biomédicas, Arturo Duperier 4, E-28029 Madrid, Spain.[2]Laboratorio de Síntesis Orgánica e Imagen Molecular por Resonancia Magnética, Instituto Universitario de Investigación, UNED, Facultad de Ciencias, UNED, Paseo Senda del Rey 9, E-28040 Madrid, Spain

Background: Hypoxia has been known for a long time to be an important physiological parameter in tumour development. Both human and animal tumours have been reported to contain regions of low oxygen tension.(1) A wide variety of methods have been developed to measure tumour oxygenation(2) and, in recent years, several nitroimidazoles derivatives (e.g., SR-4554, EF5) have been used for this aim.(3) These nitroimidazoles undergo a one-electron reduction catalysed by cellular reductases, resulting in reactive intermediates which form adducts with cellular components(4) under anaerobic conditions. Presence of molecular oxygen hinders this process.(5)

Aim: The development of new molecular probes, based on nitroimidazolyl derivatives, for non-invasive studies of physiological events using ^{1}H Magnetic Resonance spectroscopic Imaging (MRSI).

Results: Our probes **4** and **5** were obtained following the synthetic pathway shown in scheme 1. In order to investigate if these molecules can be used as oxygen tension probes, we have carried out different experiments: measurement of redox potential by cyclic voltammetry; enzymatic reduction experiences with Xanthina/XOD system and *in vitro* behaviour studies of these probes in C6 glioma cell cultures.

Conclusions: We communicate in this work the first synthesis of a new family of nitroimidazoles derivatives as pO_2 indicators for ^{1}H MRSI. The redox potential of compounds **4** and **5** are described, making them good candidates for measurement of hypoxia in tumours employing this approach. We have also observed that these compounds are reduced by biological reductases *in vitro*.

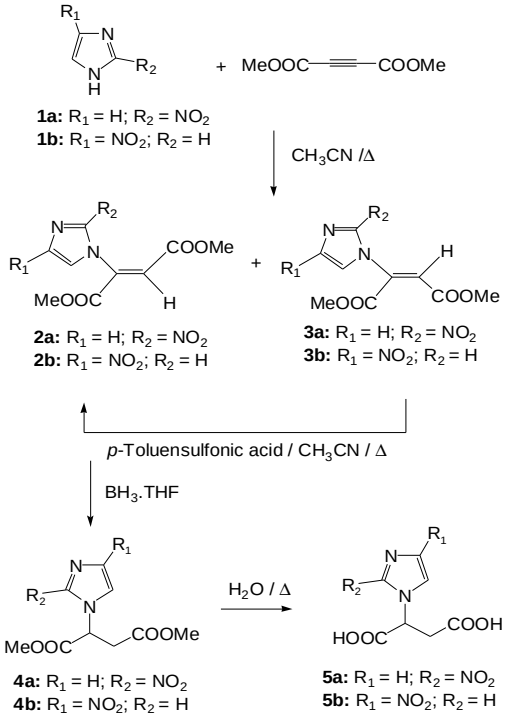

Scheme 1 : Synthethic Pathway

References:

[1] Thomlinson, R. H. and Gray, L. H.; *British Journal of Cancer*; **1955**; *9*; 539.

[2] Menon, C. and Fraker, D. L.; *Cancer Letters*; **2005**; *221*; 225.

[3] Workman, P. and Stratford, I. J.; *Cancer and Metastasis Reviews*; **1993**; *12*; 73.

[4] Walton, M. I. and Workman, P.; *Biochemical Pharmacology*; **1987**; *36*; 887.

[5] Viode, C., Bettache, N., Cenas, N., Krauth-Siegel, R., Chauviere, G., Bakalara, N., and Perie, J.; *Biochemical Pharmacology*; **1999**; *57*; 549.

(4-fluorobenzylamine)platinum - nucleic acid complexes: A facile approach to imaging of RNA-protein interactions?

Radek Liboska, and Ivan Rosenberg
Institute of Organic Chemistry and Biochemistry, Academy of Sciences, Prague, Czech Republic;

E-mail: liboska@uochb.cas.cz

Background: Platinum(II) complexes are known for their exceptional binding affinity towards guanine bases in the nucleic acid chains [1-3]. The patented Universal Linkage System (ULS) method which was developed at KREATECH Diagnostics is based on the use of a platinum-dye complex that forms a stable adduct with the N-7 position of guanine.

Aim: To find the fast, reliable, and efficient synthetic route to the 4-fluorobenzylamine platinum(II) complex, and to check its binding properties with guanine-rich oligonucleotide strands.

Methods: ES+ TOF MS (Q-Tof micro; Waters), and MALDI TOF (Reflex IV; Bruker Daltonics) were used for measurements of ligands, oligonucleotides, and oligonucleotide-platinum(II) complexes. The composition of ligands were also confirmed by NMR experiments carried out on Varian UNITY-500 spectrometer (^{1}H at 500 MHz; ^{13}C at 125.7 MHz frequency). The purity of oligonucleotide and ligand, as well as the course of complexation, and progress of the hydrolysis of the ligand were measured on HPLC system (Alliance 2695; Waters). Standard chemical methods, based mostly on precipitation and filtration [4,5], were used for the preparation of the ligands.

Results: The original concept has been proved, and a novel fluorine-containing platinum ligand for oligonucleotide labeling has been developed. Fast synthetic route for the preparation of the ligand was elaborated. Several modifications of the platinum(II) complex ligand were prepared and tested, but the simple bis(4-fluorobenzylamine) platinum(II) has been found to be the most promising one.

Conclusions: The hopeful results indicate the capability of 4-fluorobenzylamine platinum(II) complexes (the ^{18}F modification) to serve as a good alternative to the existing methods of oligonucleotide labeling [6]. Such labeled oligonucleotides could be used as the probes for molecular imaging (PET).

References:

[1] Roberts; J.J., Thomson; A.J. *The mechanism of action of antitumor platinum compounds.* Prog. Nucleic Acid Res. Mol. Biol. 1979, 22, 71-133.
[2] Pinto; A.L., Lippard; S.J. *Binding of the antitumor drug cis-diamminedichloroplatinum(II) (cisplatin) to DNA.* Biochim. Biophys. Acta 1985, 780, 168-180.
[3] Ellis; L.T., Er; H.M., Hambley; T.W. *The Influence of the Axial Ligands of a Series of Platinum(IV) Anti-Cancer Complexes on their Reduction to Platinum(II) and Reaction with DNA.* Aust. J. Chem. 1995, 48, 793-806.
[4] Dhara; C.S. *A Rapid Method for the Synthesis of [Pt(NH$_3$)$_2$Cl$_2$].* Indian J. Chem. 1970, 8, 193-194.
[5] Kidani; Y., Inagaki; K., Iigo; M., Hoshi; A., Kuretani; K. *Antitumor Activity of 1,2-Diaminocyclohexane Platinum Complexes Against Sarcoma-180 Ascites Form.* J. Med. Chem. 1978, 21, 1315-1318.
[6] Kuhnast; B., Dolle; F., Tavitian; B. *Fluorine-18 Labeling of Peptide Nucleic Acids.* J. Labelled Cpd. Radiopharm. 2002, 45, 1-11.

Structure-function analysis of b-TGS-GdDTPA, a bioactive contrast material for molecular imaging of tissue Transglutaminase (tTG)

[1]Galit Mazooz, [2]Tali Scherf, [3]Debbie Baute, [3]Daniella Goldfarb [4]Mark W. Dewhirst and [1]Michal Neeman

[1]Department of Biological Regulation, [2]Department of Chemical Research Support, and [3]Department of Chemical Physics, The Weizmann Institute of Science, Rehovot, 76100 Israel, and [4]Department of Radiology Oncology, Duke University Medical Center, Durham, NC 27710 USA

Background: Transglutaminases (tTG) form a family of enzymes that have evolved for covalent cross-linking of proteins in stabilization of atherosclerotic plaques, and generation of clots, providing mechanical strength during tissue remodeling, and in association with angiogenesis at the invading front of tumors.

Aim: Chemical characterization of a peptide based contrast material (b-TGS-GdDTPA) developed as a substrate for tTG specific MRI mapping of tTG activity (1).

Methods: DTPA-dianhydride was conjugated to the b-TGS peptide via one of the two lysine residues on the carboxy end of the peptide. The conjugation occurs through the lysine side chain amine Nε, which after conjugation becomes an amide proton. 2D ^{1}H-NMR spectroscopy (mainly TOCSY and NOESY), combined with mass-spectrometry (MS/MS). Sequential assignment of the peptide signals was based on ^{1}H-^{1}H NOE connectivities between spin systems of neighboring residues. Electron nuclear double resonance (ENDOR) spectroscopy was used for the direct determination of the water coordination number (q; 2). Mims ENDOR pulse sequence was used based on stimulated echo sequence with three non selective m.w $\pi/2$ pulses.

Results: b-TGS-GdDTPA showed high relaxivity of 14.3 $mM^{-1}s^{-1}$ compared to 4.2 $mM^{-1}s^{-1}$ of GdDTPA. We hypothesized that the binding site of GdDTPA could explain the high relaxivity. Mass spectrometry (MS/Ms) revealed that the DTPA was conjugated only to the first lysine in the peptide sequence. High resolution NMR spectroscopy showed that the b-TGS peptide does not adopt a well-defined conformation, assuming a random coil structure, as expected for small peptides. 2D NMR (TOCSY and NOESY mostly) showed that there was no evidence of random mix of DTPA conjugated to both of the lysines, since we could not detected 2 sets of spin systems, which would be mostly notified in the lysine peaks. Preliminary ENDOR experiments were performed, and the hydration number (q) was determined to be zero from comparison of the ENDOR signal amplitude to that obtain for the reference compound $[Gd^{3+}(H_2O)_8]$.

Conclusions: 2D NMR methods combined with mass-spectrometry revealed that the DTPA was conjugated only to the first lysine in the peptide sequence. Using ENDOR the hydration number of the peptide was determined to be zero. Namely, there was no direct interaction of the water protons with the metal ion in the complex of the contrast material. We hypothesize that relaxivity may be enhanced though exchange of NH protons on both lysine side chains and could arise from outer sphere water molecules and exchangeable protons of the peptide.

References

1. Mazooz, G., Mehlman, T., Lai, T. S., Greenberg, C. S., Dewhirst, M. W., and Neeman, M. Cancer Res, *65:* 1369-1375, 2005.

2. Stephan G. Zech, Wei-Chun Sun, Vincent J., Caravan P., Astashkin, A.V., and Raitsimring A. M., Probing the water coordination of protein targeted MRI contrast agents by pulsed ENDOR spectroscopy, Chem. Phys. Chem., 2005

Acknowledgement: This work was supported by Varian Biosynergy.

Metabolic Stable Phosphonate 2',5'-Oligoadenylates: A Tool For Rnase L Imaging?

Ondřej Páv, Eva Protivínská, Jan Snášel, Jiří Jiráček, and Ivan Rosenberg
IOCB, AS Prague, Czech Republic; E-mail: pav@uochb.cas.cz

Background: RNase L is a latent endoribonuclease that is a part of antiviral defence mechanism of cells induced by interferon. It is converted from a latent to an active form upon binding to short 2´-5´ oligoadenylates (2-5A), causing degradation of single-stranded RNA.[1] It has been reported that this phenomenon provides chance for the use against certain viruses or tumor proliferation.[2]

Aim: To define the role of stereochemical factors influencing the binding process of 2´,5´-oligoadenylates to RNase L and its activation, especially those associated with the internucleotide linkage.

Methods: A series of 2´-phosphonate-modified trimers and tetramers were synthesized from appropriate monomeric units and evaluated for their ability to bind to and to activate murine RNase L. The binding affinities of natural 2-5A and its phosphonate-modified analogues to RNase L were examined in radiobinding assay. This assay is based on the ability of modified oligoadenylates to compete with [^{32}P]-labeled pA_4pCp probe for specific binding to RNase L and was performed with a 126,000 *g* supernatant prepared from murine spleen homogenate. The activation of murine RNase L was determined by monitoring of the ability of the enzyme to cleave the specific radiolabeled substrate 5´-[^{32}P]-r($C_{11}U_2C_7$). For the cleavage assay, streptavidin-coated magnetic beads modified by biotinylated pA_4 were used as an affinity matrix for selective immobilization and purification of RNase L from the murine spleen homogenate.[3] The stability of 2-5A and its phosphonate-modified analogues against nucleases of murine spleen supernatant was examined under the conditions of the binding assay.

Results: Tetramers pAAXA modified by *ribo, arabino* or *xylo* 2´-phosphonate unit X in the third position were capable of binding to RNase L in nanomolar concentrations. Replacement of the first residue (pXAAA), or of both the first and the third one (pXAXA), was also tolerated by the enzyme. In contrast, in all cases the replacement of the second residue (pAXAA) resulted in significant decrease of binding ability. Additionally, no more than two phosphonate modifications in tetramer were allowed to retain the binding affinity to the enzyme. Although all three tetramers pAAXA were found to be potent enzyme binders, only tetramers modified by *ribo* and *xylo* 2´-phosphonate unit X activated the RNase L-catalyzed cleavage of RNA substrate. Surprisingly, tetramer pAAXA modified by *arabino* 2´-phosphonate unit X did not activate the enzyme and can be considered a potent antagonist. The phosphonate analogues of pA_4 exhibited, in comparison with their natural counterpart, superior resistance toward nucleases present in murine spleen homogenate.

Conclusions: Tetramers pAAXA modified by *ribo* and *xylo* 2´-phosphonate units were found to be potent binders and activators of RNase L. In addition, these compounds were considerably stable against nuclease cleavage. The obtained data indicate that prepared high-affinity phosphonate oligoadenylates could be used as a tool for targeting and imaging RNase L during a viral infection or tumour proliferation.

References:

[1] Player, M.R.; Torrence, P.F. *Pharmacol. Ther.* **1998**, *78*, 55-113.
[2] Leaman, D.W.; Cramer, H. *Methods Enzymol.* **1999**, *18*, 252-65.
[3] Páv, O.; Protivínská, E.; Pressová, M.; Collinsová, M.; Jiráček, J.; Snášel, J.; Masojídková, M.; Buděšínský, M.; Rosenberg, I. *J. Med. Chem.* **2006**, in press.

Preliminary characterizations of gadolinium oxide nanoparticles

Elisenda Rodriguez, Sophie Laurent, Luce Vander Elst, Robert N Muller
Departament of General, Organic and Biomedical Chemistry. NMR and Molecular Imaging Laboratory. University of Mons-Hainaut. Mons. Belgium.

Background: There is a growing interest in the synthesis and characterization of nanosized magnetic materials. This relatively new class of materials has found use in a large variety of applications ranging from magnetic data storage devices to magnetic resonance contrast agents (1,2).
Gadolinum oxide (Gd_2O_3) nanoparticles are considered to be used for magnetic resonance imaging (3). Stability at physiological pH and the absence of free Gd^{3+} ions should be therefore a matter of concern.

Aim: A complete relaxometric characterization of commercial and laboratory-made Gd_2O_3 nanoparticles is presented.

Results and Conclusions: Results show a paramagnetic behavior and a questionable stability in biological solutions.

References:
(1) Pankhurst Q. A., Connolly J., Jones S. K., Dobson J. Applications of magnetic nanoparticles in biomedicine. *J. Phy. D: Applied Physics*. 2003, *36*, 167-181.
(2) Burtea,C., Laurent,S., Roch,A., Vander ELst,L., Muller,R.N. C-MALISA (cellular magnetic-linked immunosorbent assay), a new application of cellular ELISA for MRI. *J. Inorg. Biochem.* 2005, *99*(5), 1135-1144.
(3) Louis C., Bazzi R., Marquette C. A., Bridot J-L., Roux S., Ledoux G., Mercier B., Blum L., Perriat P., Tillment O. Nanosized Hybrid Particles with Double Luminiscence for Biological Labelling. *Chem. Mater*. 2005, *17*, 1673-1682.

Labelling of tumour cells by ironoxide nanoparticles

T. Schlorf[1], C. Henneweer[2], E. Kossel[3], D. Emme[4], C.-C. Glüer[3], R. Mentlein[1*]
[1]Department of Anatomy, Universität Kiel, [2]Radiology, [3]Medical Physics, [4]Molecular Oncology, Universitätsklinikum Schleswig-Holstein, Kiel, Germany
** Phone +49431 8802460 Fax +49431 8801557 e-mail rment@anat.uni-kiel.de*

Tracking of cells in vivo can be achieved by in vitro labelling with supra-paramagnetic particles followed by injection and in vivo labelling by MRT. For this approach, particles are best suited that are rapidly internalized at high rates, non-toxic and yield a stable labelling even after many cell divisions.
We compared different types of particles (Resovist, M-Dextran coated iron oxide, non-coated Fe_3O_4, dextran-coated N70 and N20 maghemit) for internalization kinetics, toxicity and stable labelling using human U118 glioma cells, PancTu human pancreatic tumour cells and human umbilical vein endothelial cells (HUVEC, non-malignant comparison) as models. Furthermore, labelled cells were visualized by MRT in vitro and in vivo.

Methods

Resovist was obtained from Schering (Berlin), M-Dextran and the non-coated Fe_3O_4 were delivered from Dr. Norbert Buske (Berlin), N70 and 20 were from Micromod (Rostock). Cell-toxicity was detected by the release of the lactate dehydrogenase (LDH); iron uptake was quantified by use of the iron test-Kit (Fe-AN, Spectroquant, Merck) and visualized by Berliner Blue staining.

Results

In all cell types investigated, Resovist, M-Dextran and non-coated Fe_3O_4 were absorbed fundamental stronger than N70 or N20 (Figure 1). With decreasing concentrations, uptake of iron oxide nanoparticles into the cells likewise receded.

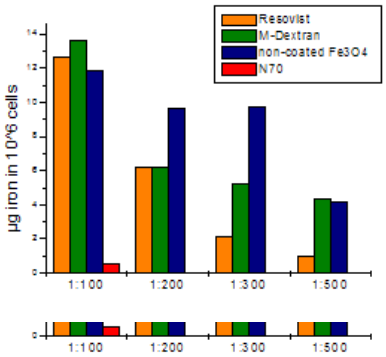

Figure 1: Absorption of ironoxide nanoparticles in U118 glioma cells at different concentrations (24 h exposure).

For definition of the ideal internalization, time kinetics was investigated. A strong assimilation was observed from 24 h through to 36 h exposure (Figure 2). Afterwards uptake decreased.

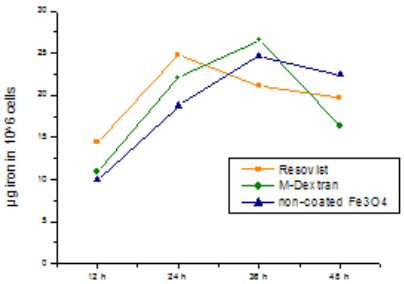

Figure 2: Time kinetics of iron oxide nanoparticle uptake over a period of 48 hours; U118 glioma cells

Since the application of iron oxide nanoparticles could damage the cells, we determined their cell-toxicity in vitro by measuring the release of the cytosolic enzyme lactate dehydrogenase (LDH, Figure 3).

Figure 3: The ironoxide nanoparticles effected only a slightly release of LDH. (U118 glioma cells, 24 h exposure)

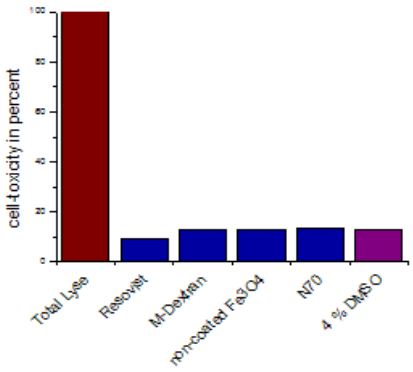

To clarify whether the nanoparticles wer adsorbed at the cell surface or internalized, we visualized them by Berliner Blue staining and electron microscopy (Figures 4 and 5).

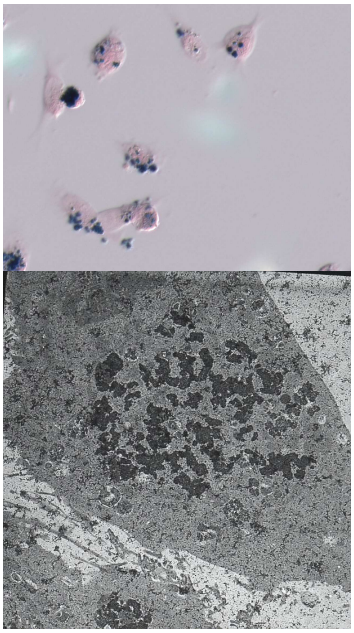

Figure 4: Berliner Blue staining of Resovist in U118 glioma cells show primarily labelling within the cells, but partly also at / near the cell surface.

Figure 5: Electron microscopic visualisation of M-Dextran in U118 glioma cells reveals a clustered localisation deep within the cells.

Stabilität der markierung
MRT-Daten

Conclusions

Resovist and similar iron oxide nanoparticles can be used for efficient in vitro labelling of tumours cells for in vivo models or cell tracking. The labelling is most efficient after 24 h, and yields stable intracellular aggregates. All particles have low toxicity.

In contrast, meagre assimilation of N20 and N70 particles make them ideal tools for specific labelling of molecular targets. The high non-specific uptake of Resovist and similar particles render them inappropriate for such application.

NEUROSCIENCE

Paired voxel-wise statistical mapping of in vivo Diffusion Tensor Imaging (DTI) data to assess the seasonal neuronal plasticity in the brain of a songbird

De Groof G[1], Verhoye M[1,2] , Leemans A[2], Sijbers J[2], Van der Linden A[1]
[1]Bio-Imaging Lab, University of Antwerp, Belgium; [2]Vision Lab, University of Antwerp, Belgium

Background: The neural substrate for song behaviour in songbirds, the song control system, is the best documented brain circuit to study neuroplasticity. Not only the volume of the key song control nuclei HVC, RA and X change in size, but also the density of the connections between them changes as a function of seasonal and hormonal influences.

Aim: In the current study *repeated in vivo Diffusion Tensor Magnetic Resonance Imaging (DT-MRI or DTI)* and the resulting parameters (FA=Fractional Anisotroptry, MD=Mean Diffusion, λ_r=Radial diffusivity, $\lambda_\parallel$=Axial diffusivity) were used to quantify seasonal changes in the connections between different SCN and other nuclei in starling brains.

Methods: Nine male starlings (Sturnus vulgaris) were measured repeatedly in spring and in summer. DTI was performed on a 7T-system (MRRS) using multislice Diffusion Weighted-Spin Echo and diffusion sensitizing gradients along 7 directions. Sagittal slices with image resolution of 100*100*400µm³ were obtained covering one hemisphere of the brain. Images were accurately coregistered using non-linear warping allowing voxel-wise paired statistical mapping of tensor invariant differences between the spring and summer groups (Fig 1).

Results: FA (0.20±0.03 vs 0.14±0.02, p-value:<0.001) and $\lambda_\parallel$ (600±31 vs 652±43 µm²/s, p-value:0.0097) values in the HVC-to-RA-Tract were significantly increased in spring and reflect the neuronal sprouting from RA-projecting HVC-neurons well known from literature [1]. The laminae harbouring other song control nuclei connections such as LMAN-RA (0.25±0.03 vs 0.21±0.01, p-value: 0.01) and HVC-X (0.21±0.02 vs 0.20±0.02, p-value: 0.02) also showed a significant seasonal difference in FA-values while no seasonal changes were discerned in the lamina which do not harbour song control nuclei connections. Another connection seemingly not related to the song control system, namely the Tractus Quintofrontalis also showed a significant decrease in FA (0.22±0.05 vs 0.15±0.04, p-value: 0.007) (Fig 1).

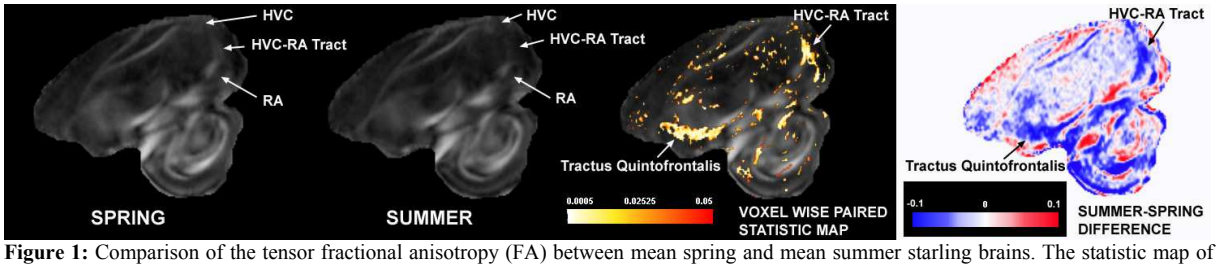

Figure 1: Comparison of the tensor fractional anisotropy (FA) between mean spring and mean summer starling brains. The statistic map of the Wilcoxon Signed Rank test for the (summer-spring) difference in the FA is also shown. The colorscale is red-yellow and has been constrained to the range 0.05 > P > 0.0005. The last image shows the (summer-spring) difference. The difference colorscale is dimensionless.

Conclusions: The different DTI-parameters FA, Radial (λ_r) and Axial ($\lambda_\parallel$) diffusivity clearly allowed discriminating seasonal changes in the amount of axonal projections in the songbird brain. The songbird brain offers the exclusive opportunity to validate new (MRI) imaging tools for their capacity to study different features accompanying neuronal plasticity and neurogenesis.

References: [1] Rasika S, Nottebohm F, Alvarez-Buylla A. Testosterone increases the recruitment and/or survival of new high vocal center neurons in adult female canaries. Proc. Natl. Acad. Sci. USA, 1994, 91; 7854-7858

Acknowledgement: This study was supported by a GOA fund from the University of Antwerp

Development of Molecular Probes for *in Vivo* Optical Imaging of Neuronal Degeneration

Jolivel V[1,2], Romieu A[3], Renard PY[3], Leprince J[1], Noack P[2], Massonneau M[2], Parrein P[2], Vaudry H[1], Gonzalez BJ[1], Vaudry D[1]
[1]INSERM U413, Lab. Neuroendocrinol. Cell. & Mol., IFRMP23, Univ. Rouen, France; [2]Société QUIDD, Mont-Saint-Aignan, France; [3]CNRS UMR6014, IRCOF, IFRMP23, Univ. Rouen, France

Background: Stroke induces a cascade of events that leads to a lesion. Cells die by necrosis in the centre of the lesion, while they will be eliminated by an apoptotic process involving caspase activation in the peripheral zone, called the penumbra[1].

Aim: *In vitro* first-step validation of smart probes developed to detect apoptotic cell death by *in vivo* optical imaging.

Methods: The probes currently under development are designed to target caspase activity using fluorescence resonance energy transfer (FRET)[2] and are characterized on cultured cerebellar granule cells. Hydrogen peroxyde is used to induce apoptosis by activation of caspases[3]. We present the results obtained with two of these probes AR68 and AR78 which are labeled with the same fluorochromes: cyanine 3 (Cy3) and cyanine 5 (Cy5) but present different lipophilic natures.

Results: Both of these probes do not interfere with neuronal survival. As expected, AR78 penetrates into the cells with a better efficiency due to its higher lipophilic nature. However, AR68 presents at native state 100% of FRET efficiency while AR78 exhibits only 66% efficiency. Cellular lysates are able to induce the cleavage of both probes as demonstrated by an increase of the Cy3 emission and a decrease of Cy5 one. Moreover, induction of apoptosis in cultured cells by hydrogen peroxide increases the cleavage rate of the probe AR68 when compared to control cells.

Conclusions: These data indicate that the synthesized optical probes can represent a valuable new tool to measure apoptotic cell death. A few optimizations of these probes open the perspective of *in vivo* application, the next step of development. In particular, with a quencher as FRET acceptor, the probe becomes an accurate marker (no signal in absence of apoptosis) of this molecular event.

References:
[1] Davoli MA et al.; *Neuroscience*. 115:125-136 (2002)
[2] Karvinen J et al.; *Anal Biochem*. 325:317-325 (2004)
[3] Vaudry D et al.; *Eur J of Neuroscience*. 15:1451-1460 (2002)

Supported by INSERM, QUIDD and the Conseil Régional de Haute-Normandie.

In situ labeling of stem cells in the adult mouse brain with superparamagnetic particles

Vreys R[1]; Geraerts M[2]; Svensson L[3], Debyser Z[2], Baekelandt V[2], Timmermans J-P[3], Van der Linden A[1]

[1]Bio-Imaging Lab, University of Antwerp; [2]Laboratory for Molecular Virology, Neurobiology and Gene Therapy, University of Leuven; [3]Laboratory of cell biology and histology, University of Antwerp, Belgium

Background: MRI has become a powerful tool for in vivo non-invasive monitoring of the migration of magnetic labeled stem cell. A protocol for in situ labeling endogenous neuronal stem cells (NSC) has first been described by Shapiro et.al[1]: subventricular NSC were labeled in the rat brain by injection of micron-sized superparamagnetic iron oxide particles (MPIO's) in the lateral cerebral ventricle and their recruitment along the rostral migration stream (RMS) up to the olfactory bulb was visualized with MRI.

Aim: The goal of this study was to test the in situ labeling protocol in healthy adult mice aiming at future applications in different mouse models for neurodegenerative diseases. To that end we wanted to test the efficacy of a lower MPIO's concentration to reduce the blooming effect at the injection site in these smaller brains.

Methods: Adult healthy mice were stereotactic injected in the lateral ventricle (group 1: n=4, 10µl, Fe-concentration 3mgFe/ml; group 2: n=4, 1.5µl, Fe-concentration: 0.67mgFe/ml) with 1.63 micron MPIO's (a green fluorescent chemical is impregnated into the shell; Bangs Laboratories, Inc). Following in vivo 2D GE MRI at 3, 5 and 8 weeks post injection, one mouse of each group was perfused and decapitated for high (66µm isotropic) resolution ex vivo 3D FLASH MRI at 7 Tesla. After imaging, brains were sectioned and stained for Dcx (migrating NSC) and NeuN (mature neurons) using immunohistochemistry (IHC). Electron microscopy on the two remaining animals to determine particle uptake by the precursor cells is currently being done.

Results: Ex vivo MRI of the mouse forebrain and olfactory bulb 3 weeks (A), 5 weeks (B) and 8 weeks (C) after a 10µl injection is shown in figure 1. The amount of dark contrast spots reaching the olfactory bulb increases over time. The dark spots (arrows) extend rostral from the lateral ventricle to enter the olfactory bulb where they eventually spread out (star). The 1.5µl injection did not result in any relocation of dark contrast. Confocal microscopy revealed the same migration pathway for the endogenous NSC, known as the RMS. Figure 2 shows a confocal microscopic image from the core of the olfactory bulb, where the NSC (red) differentiate into adult neurons (blue), and illustrates a differentiating NSC that contains green fluorescent MPIO's (arrow). Electron microscopy will give a decisive answer about whether the particles are taken up or not.

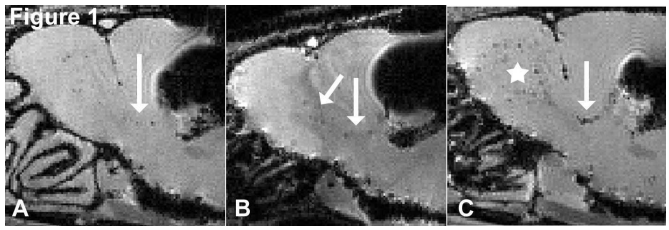

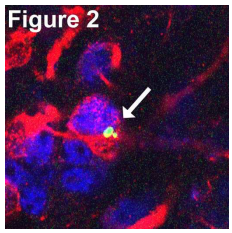

Conclusion: These results suggest the possibility of labeling in vivo endogenous stem cells located in the mouse brain by direct injection of a contrast agent at high concentration into their environment. Migration of endogenous stem cells towards brain lesions in mouse models or new discoveries of endogenous stem cells deficiencies in different neuronal diseases may become apparent with this labeling method by in vivo MRI.

References: [1] Shapiro E et al; *ProcISMRM.* #166 (2004)
This study was funded by: the EC - FP6-project DiMI, LSHB-CT-2005-512146; a Ph.D. grand and the SBO-project AniMone of the IWT-Vlaanderen

MicroPET evaluation of new tracers for neuroinflammation imaging

F. Chauveau*, H. Boutin*, C. Thominiaux[§], P. Hantraye[§†], F. Dollé[§], V. Brulon[§], Y. Fontyn[§], S. Jan[§], R. Trebossen[§], and B. Tavitian*

* *CEA, Département de Recherche Médicale, Service hospitalier Frédéric Joliot, Orsay, F-91400 France ; Inserm, U803, Orsay, F-91400, France.*

[§] *CEA, Département de Recherche Médicale, Service hospitalier Frédéric Joliot, Orsay, F-91400 France*

[†] *URA CNRS-CEA 2210, Service Hospitalier Frédéric Joliot, Orsay, France*

Background: Chronic or acute neuroinflammation has been identified in several degenerative disorders (e.g. Alzheimer and Parkinson diseases) and in stroke. Peripheral benzodiazepine receptor (PBR) is mainly expressed by activated microglia in the brain, and is therefore a marker of neuroinflammation.

Aim: To evaluate by positron emission tomography (PET) two new PBR radioligands, namely [^{11}C]DPA-713 and [^{11}C]CIINME, and to compare them to the reference radiotracer, [^{11}C]PK11,195, which use is hampered by a high non specific signal giving rise to a difficult quantification of its pharmacological parameters.

Methods: The three compounds were tested in two animal models, unilaterally striatum-lesioned rats, and transgenic mice which progressively develop β-amyloid plaques by over-expressing presenilin-1 (PS1) and β-amyloid precursor protein (APP).

Results: Imaging of the lesioned rats shows a higher contrast between the lesioned area and the symmetrical area in the intact contralateral hemisphere with DPA-713 and CIINME, compared to PK11,195 (ratio ipsi/contro 20 min post-injection : DPA-713, 2.7 ± 0.6, n = 4 ; CIINME, 2.2 ± 0.3, n = 4 ; PK11,195, 1.7 ± 0.1, n = 5). DPA-713 is totally displaced by an excess (1 mg/kg) of PK11,195. This displacement is only partial with CIINME, and occurs with slower pharmacokinetics compared to DPA-713. Imaging of the transgenic mice with DPA-713 or CIINME enables earlier detection of β-amyloid-associated inflammation in APP/PS1 mice compared to PK11,195 imaging (longitudinal study at 12 and 22 months). Immunohistochemistry correlates with PET imaging by showing strong activation of microglia in and around the lesion in rats, and around the cortical β-amyloid plaques in mice.

Conclusions: This preliminary study in rodent models of neuroinflammation demonstrates that those two new tracers give rise to a better signal/noise ratio than PK11,195. They thus have the potential to improve the efficiency of neuroinflammation study and follow-up in humans.

TECHNOLOGY

High Resolution X-ray microtomography analysis for Evaluation of the Surgical Positioning of Cochlear Implant Electrodes

Postnov A[1], Peeters S[1], De Clerck N[1], Vanpoucke F[3], Offeciers FE[2], Van Dyck D[1] & Zarowski A[1,2] ,
[1]Department of Physics, Department of Biomedical Sciences University of Antwerp, [2] University ORL Department, Medical Institute St. Augustinus, [3] Advanced Bionics Corporation, European Research Lab, Antwerp, Belgium

Background: In biomedical research, X-ray microtomography (micro-CT) has not only been applied for studying bones and calcified tissues [1] but also for imaging soft tissues [2]. The major advantage of micro-CT is that the analysis is fully non-invasive. A potential new application of micro-CT is visualization of the inner ear tissues and the evaluation of the surgical aspects of newly developed cochlear implant electrodes. A cochlear implant is an electronic device replacing the human hearing organ by a direct electrical stimulation of the auditory nerve.

Aim: In the present report, we applied micro-CT for the *in vitro* visualization of the inner ear tissues as well as for evaluation of the electrode damage and/or surgical insertion trauma during implantation of the cochlear implant electrodes.

Methods: A desktop micro-CT scanner (Skyscan-1076, Aartselaar, Belgium) was used with a voxel size of 9μm; implementation of a Ti filter was combined with extra long scanning times. Cylindrical blocks of human temporal bones containing the inner ears were used. After the patient's death, classical surgical drilling as for cochlear implantation was performed with preservation of the most important surgical landmarks. The main advantage of micro-CT is the practically artefact-free preparation of the samples and the possibility of evaluation of interesting parameters along the whole insertion depth of the electrode.

Results: Good visualization of the intracochlear soft tissues was achieved. These high resolution scans reached nearly histological quality. Basic elements of the cochlea could be visualized and used for evaluation of the electrode position while the sample remained intact. 3D orientation of the electrode towards the membrane and the cochlear walls, which is of key importance in evaluating the quality of implantation, was obtained from the virtual slices.

Conclusions: Micro-CT can provide visualization of the inner ear structures in human temporal bones. Thus evaluation of the surgical positioning of the cochlear implant electrodes relative to the intracochlear soft tissues is possible. This technique can greatly aid in design and development of new cochlear implant electrodes and is applicable for temporal bone studies.

References:

[1] Waarsing, J.H et al., Bone *34 , 163-169, (2004)*.

[2] De Clerck, N.M. et al., *Neoplasia* 6, 374-379, (2004).

Fluorescence lifetime imaging of unstained resected human tissue: Towards an endogenous fluorescence technique for *in vivo* molecular imaging

McGinty J[1]., Galletly N. P[2]., Talbot C[3]., Hegyi L[2]., Munro I[1]., Elson, D.S[3]., Dunsby C[1]., Neil M.A.A[1]., Cohen P[4]., Lever M. J[3]., Stamp G. W. H[2]. and French P.M.W[1].
[1]Photonics Group, Department of Physics; [2]Histopathology Department, Hammersmith Campus; [3]Institute of Biomedical Engineering; [4]Department of Histopathology, Charing Cross Hospital, Imperial College London.

Background: It is generally accepted that early detection and characterisation of disease leads to the increased success of treatment and disease management. For example the majority of gastrointestinal (GI) malignancies are diagnosed at an advanced stage. Consequently there is major interest in the development of new diagnostic imaging techniques to improve the visualization of neoplastic changes in the mucosa of the GI tract.
Fluorescence lifetime imaging (FLIM) [e.g. 1] is a novel wide-field imaging technique which measures the characteristic decay time of the fluorescence and can be applied to naturally occurring fluorophores in tissue such as NADH, collagen and elastin. Imaging fluorescence lifetimes can potentially improve the specificity of fluorescence-based wide-field imaging techniques and enhance their ability to characterise and discriminate between diseased and healthy tissue.

Aim: To examine the efficacy of fluorescence lifetime imaging as a non-invasive diagnostic tool utilising laser induced auto-fluorescence.

Methods: Fresh unfixed macroscopic tissue samples from the colon and skin were obtained immediately following resection for malignancy. Tissue auto-fluorescence was induced by exciting the samples *en face* with a pulsed UV (355nm) Nd:YVO_4 laser. Wide-field fluorescence lifetime images were acquired for areas macroscopically diagnosed as containing normal and cancerous mucosa.
Fluorescence lifetime images of sections of human carotid endarterectomy were aquired after excitation at 400 nm during low magnifiaction microscopy. In both cases tissue samples were subsequently stained and underwent standard histological examination.

Results: Marked changes in the lifetime characteristics of malignant colonic tissue compared to normal epithelium. Clear lifetime contrast was observed between basal cell carcinoma, squamous cell carcinoma and healthy skin samples. For the majority of malignant lesions, wide-field FLIM images provided clear contrast between the areas of normal and malignant tissue.
Lifetime imaging of the plaques provided detailed information about their composition, including the fibrous cap (fc), the lipid core and calcified areas. The fc exhibited longer lifetimes (due to high elastin and collagen composition) than lipid-rich or calcified areas. Increased vunerability due to fc thinning could also be observed.

Conclusions: FLIM generates wide-field images demonstrating inherent contrast between malignant and non-malignant GI tract and skin tissue. It can also characterise the composition of human atherosclerotic plaques and identify features of vulnerability, suggesting its use as a clinically relevant tool.

References:
[1]Elson D.S., Requejo-Isidro J. *et al. Photochem. Photobiol. Sci.* **3**, 795-801 (2004).

3D Imaging of fluorescence patterns in Drosophila melanogaster with OPT

Meyer H [1], Metaxakis A [2], Darrell A [3], Atrops S [1], Savakis B [2] and Ripoll J [1]
[1] *Inst. of Electronic Structure & Laser,* [2] *Inst. of Molecular Biology & Biotechnology,* [3] *Inst. of Computer Science, – Foundation for research & Technology Hellas*

Background: *Drosophila melanogaster* (fruit fly) is a fundamental model organism for understanding many molecular and cellular mechanisms in biology [1,2]. 3D imaging of fluorescent markers for gene expression in-vivo in this organism in all stadiums of its life cycle would represent a powerful tool in modern genetics.

Aim: Our aim is to use optical projection tomography *(OPT)* [3-6] in fluorescence mode to quantitatively reconstruct fluorophore concentration in opaque organs such as the adult head in the drosophila. To that end, a modified radon transform that takes into account the isotropic emission of the fluorophores has bee developed [7].

Methods: GFP expression patterns of transgenic *D. melanogaster* in various life cycle stadiums were imaged and reconstructed using a custom made CCD based microscope setup. The excitation was generated with a halogen lamp using specific excitation filters, and the specimen rotated using a capilary tube and index-matching liquids as in [4]. In order to account for the point source propagation of the fluorescence intensity, a novel modification of the radon transform was employed [7]. The accuracty of the approach was verified with phantom measurements.

Results: The reconstruction of the phantom experiments yields good comparison with the novel theoretical approach [7]. This approach is also used to image several organs in drosphila at several stages, reaching good results, which we compare with those obtained using the standard radon transform [3-6].

Conclusions: In order to obtain quantitative fluorescence images, we have found that a modification to the standard radon transform which takes into account the isotropic emission of the fluorophores is needed. The accuracy of this approach has been shown both with phantom and measurements in drosophila melanogaster.

References:

[1] C.J. O'Kane, "Modeling human diseases in Drosophila and Caenorhabditis," Seminars in Cell & Developmental Biology, vol. 14, pp. 3-10, 2003
[2] P.R. Hiesinger and H.J. Bellen, "Flying in the face of total disruption", Nature Genetics, vol. 36, pp. 211-212, 2004
[3] J. Sharpe, et al., "Optical Projection Tomography as a Tool for 3D Microscopy and Gene Expression Studies", Science, vol. 296, pp. 541-545, 2002.
[4] M. Fauver, E. J. Seibel et al, 'Three-dimensional imaging of single isolated cell nuclei using optical projection tomography', Opt. Exp. **13**, 4210 (2005)
[5] S. Kikuchi, S. Kazuo, and N. Ohyama, "Three-dimensional microscopic computed tomography based on generalized Radon transform for optical imaging systems," Opt. Commun. 123, 725-733 (1996)
[6] S. Kikuchi, K. Sonobe, L. S. Sidharta, and N. Ohyama, "Three-dimensional computed tomography for optical microscopes," Opt. Commun. 107: 432-444 (1994)
[7] A. Darrell, et al., "Accounting for Point Source Propagation Properties in 3D Fluorescence OPT", (submitted to EMBC Conference 2006, IEEE, New York)

Performance evaluation of the new electronics YAP-(S)PET small animal PET/SPECT scanner and its applications in neuroscience

Bartoli A.1, Belcari N.1, Del Guerra A.1, Moresco R.M.2, Lecchi M.3, Belloli S.2, Stark D.4, Piel M.4, Roesch F.4, Erba A. P.5, Mariani G.5, Corsini G. U.6, Sgado' P.6
1Department of Physics "E. Fermi", University of Pisa, Pisa; 2Scientific Institute H S Raffaele, University of Milano-Bicocca, Milan;3University of Milan, Milan;4Institut of Nuclear Chemistry,University of Mainz, Mainz;5Nuclear Medicine Department, University of Pisa, Pisa;6 Department of Neuroscience, University of Pisa, Pisa

Background: At the Department of Physics of the University of Pisa, a new and fully engineered version of the YAP-(S)PET small animal scanner has been recently installed. This scanner is the only one that combines the PET and SPECT techniques and offers the unique possibility of developing new and interesting protocols for the investigation of many biological phenomena.[1]
The scanner is made up of four heads: each one is composed of a 4 × 4 cm2 YAlO3:Ce (or YAP:Ce) matrix of 20 × 20 elements, 2 × 2 × 25 mm3 each, coupled to a PS-PMT (Hamamatsu
R2486). The four modules are positioned on a rotating gantry. The switching to the SPECT modality is easily made by mounting a high resolution parallel hole (0.6 mm Ø, 0.15 mm septum) lead collimator in front of each crystal. The scanner has a Field of View (FOV) of 4 cm × 4 cm Æ.

Aim: The scanner was tested for preliminary assessment of its imaging capability for studies related to neuropharmacology and psychiatry. In a first evaluation, dopamine D2/D3 receptor studies were performed both in PET and SPECT modalities using rats and mice.
In order to improve the scanner capabilities, a completely new and faster readout electronics has been installed. The new electronics offers a reduced system dead time leading to a maximum acquisition rate ten times higher than the previous one. The new circuitry also includes a proprietary pile-up rejection technique.
In this work we present some animals studies performed both in PET and SPECT modalities and the performance evaluation in terms of absolute sensitivity, spatial resolution and count rate capability of the new version of the scanner.

Methods: The scanner performance were evaluated both in PET and SPECT modalities.
In PET mode the spatial resolution was evaluated using a 22Na point source (1 mm Ø) positioned
at the center of the FOV (CFOV) and moved radially with 0 mm, 3 mm, 8 mm and 13 mm offset.
For each position, the radial, transaxial and axial FWHM and FWTM have been measured. The exact methodology for measuring the scatter fraction and count rate performance (NEC) in small animal PET scanners is still an open question. The PET performance assessments described here are based on the preliminary standards proposed by the small animal PET NEMA task force.
The scatter fraction and NEC curve were evaluated using a mouse-like phantom filled with a known quantity of activity of a 18F solution. The PET system sensitivity was measured with a linear source placed inside a metal tube. The measure was repeated five times with increasing wall thickness.
The effectiveness of the new pile-up rejection technique has been evaluated by comparing the uniformity of the reconstructed images of an uniform phantom, at various count rates, with and without the pile-up rejection capability.
In SPECT mode a glass capillary filled with 99mTc solution was used for the evaluation of both spatial resolution in the transaxial plane and sensitivity.

Images of a Derenzo-like phantom and of the NEMA PET image quality phantom are presented for both PET and SPECT modalities.
The animal studies were related to neuropharmacology and psychiatry and were performed in different institutes. The PET studies were performed at the University of Mainz (18F-Fallypride) and at the S. Raffaele Hospital in Milan (11C-Raclopride), while the SPECT studies (123I-FP-CIT) were performed within the framework of the Center of Eccellence AmbiSEN of the University of Pisa, in collaboration with the Nuclear Medicine Department. The high-affinity ligand for the postsynaptic D2-like dopamine receptor, ^{18}F-Fallypride, was used to perform dynamic PET studies on normal rats. The ^{11}C-Raclopride was used to follow the evolution of the rat model of Huntington's disease performed with a QA induced monolateral lesion. To confirm and extend previous analyses on the EnHT mice as a new model for Parkinson's disease, in the SPECT studies with ^{123}I-FP-CIT we evaluated the binding of DatSCAN as indicator of integrity of dopaminergic system in asintomatic EnHT mice.

Results: In PET mode the spatial resolution is about 4.4 µl and 8.5 µl at CFOV using EM and FBP reconstruction, respectively, and a 50-450 keV energy window. The sensitivity at CFOV is about 2 % with an energy window of 50-850 keV. The absolute sensitivity, averaged over the whole axial FOV, is 1.1%. The measured scatter fraction is about 22% with a 50-850 keV energy window. The NEC curve has a maximum value of about 50 kcps at 33 MBq, while using the pile-up rejection technique the NEC maximum decreases to 30 kcps at 22 MBq.
In SPECT modality, the spatial resolution is nearly costant over the whole FOV and is about 3 mm.
The sensitivity is 30 cps/MBq using an energy window of 140-250 keV for ^{99m}Tc.
The PET animal studies showed that the sensitivity and the spatial resolution of the YAP-(S)PET scanner are sufficient to image the uptake of dopaminergic targeting vectors even injecting low activities (less than 7 MBq for ^{11}C-Raclopride studies). [2], [3]
The SPECT studies performed on mice with ^{123}I-FP-CIT exposed some more difficulties due to the reduced sensitivity of the SPECT technique and the dimension of the mouse striatum.

Conclusions: The animal studies showed the YAP-(S)PET capabilities in performing good quality PET and SPECT dopamine receptors studies and that the scanner could be adequately applied to pre-clinical studies.
The new electronics YAP-(S)PET scanner has been fully characterized following the most recent NEMA standards.

References:
[1] Del Guerra A et al., "Simultaneous PET/SPECT imaging with the small animal YAP-(S)PET scanner", presented at the 2002 annual conference of the Academy of Molecular Imaging, October 23-27, 2002, San Diego, CA, (USA) (abstract)
[2] Moresco R M et al., "Evaluation of the YAP-(S)PET scanner for pre-clinical studies with ^{11}Cligands in small animals", presented to the 4th annual Meeting of the SMI, September 2005
[3] Bartoli A et al. , "Preliminary assessment of the imaging capability of the YAP-(S)PET small animal scanner in neuroscience", to be published in NIMA 2006

Multi-modality: Combining Fibered Confocal Fluorescence Microscopy and Whole Body Imaging System for Complete Exploration.

Charlotte Cavé [1], Frédéric Ducongé [2], PhD, Raphaël Boisgard [2], PhD, Bertrand Tavitian [2], PhD,, Emilie Roncali [3,] Serge Maîtrejean [3,] Jérôme Lopez [1], PhD, Benjamin Abrat [1]
1. Mauna Kea Technologies, Paris, France
2. CEA SHFJ, Inserm, ERM 109 Orsay France
3. Biospace Mesures, Paris, France

Introduction

The development of the Cellvizio 660, using a red 660 nm laser, makes it possible to obtain microscopic *in vivo* images with the large range of red fluorescent dyes that are widely used in the field of molecular imaging.

Aims and Methods

The Cellvizio™, based on Fibered Confocal Fluorescence Microscopy, enables *in vivo* and *in situ* microscopy down to a resolution of 2.5 µm. Until now, the Cellvizio™ was only available with a blue 488 nm laser compatible with the range of fluorophores and transgenic animals that have an emission bandwidth of 500 to 650 nm. The introduction of the Cellvizio 660 now offers the possibility to cover a large number of fluorophores like Cy5.5 or animal models that emit fluorescent signal between 650 and 750 nm. Such wavelengths are being widely used in whole body optical imaging techniques and hence the Cellvizio 660 allows the use of the same models to obtain microscopic *in vivo* real-time images in combination with whole body imaging systems.
The Cellvizio was used to image xenograft tumors in mice in combination with a fluorescence whole body imaging system (Photon Imager, Biospace, Paris, France). The animal were imaged after administration of various fluorophores

Results

The Cellvizio 660 is a stand-alone imaging system including a Laser Scanning Unit, a range of fibered objectives made of tens of thousands of optical fibers (the “ProFlex”) and the ImageCell image processing and analysis software. High definition images with 2.5 µm lateral resolution, 15 to 20 µm axial resolution, and a field of-view up to 600 µm x 500 µm can be obtained at a rate of 12 frames per second on living anesthetized animals. These images can be obtained at depths up to 100 µm. The fibered microprobes have diameters ranging from 300 µm to 1.8 mm and thus offer unique access capabilities.
.In the results we present here, the fluorescence whole body imaging system was first used to detect the area of interest. The Cellvizio was then used to acquire the cellular resolution, leading to the visualization of angiogenesis and tumor cells.

Conclusion

The Cellvizio has been applied to scientific research across the world in the areas of peripheral nerve studies, deep brain imaging, microcirculation, angiogenesis, immunology, oncology and ophthalmology. Now working at 660nm, the Cellvizio is the perfect tool to complete data provided by whole body imaging systems.

List-mode image reconstruction for the ClearPETTM Neuro

Musmann P, Schramm N, Pietrzyk U*, Weber S
*Central Institute for Electronics, *Institute for Medicine, Forschungszentrum Juelich*

Background: ClearPET™ is a new family of small-animal PET scanners which are currently un-der development within the Crystal Clear Collaboration (CERN) [1,2]. All scanners are based on the same detector block design using individual LSO and LuYAP crystals in phoswich □onfigure-tion, coupled to multi-anode photomultiplier tubes. ClearPET™ Neuro is designed for applica-tions in neuroscience. Data acquisition acquires single events that are stored with a time mark in a dedicated list mode format. Coincidences are associated off line by software.
Conventionally, PET data are sorted into sinograms. This leads to a loss in spatial and temporal resolution due to the histogramming of the events. An alternative data representation is the so-called list-mode format [3], which allows to store more attributes of each individual event, like involved detectors, energy, time, gantry state or even the depth of interaction. The format has the advantage, that it keeps the data in their highest possible temporal and spatial resolution.

Aim: Reconstruction directly from list-mode data makes it possible to take the additional infor-mation into account. This information can be used to calculate a more accurate system model and therefore could improve the image quality in some aspects, like resolution and contrast.
We have developed a list-mode-based reconstruction for the ClearPET Neuro™ and describe an algorithm to approximate the coincidence response function via ray-tracing using the three di-mensional detector geometry and Siddon's method [4]. The algorithm is implemented in a list-mode reconstruction framework similar to [5] and applied to listmode data from the ClearPET™ Neuro.

Methods: We use the ray-tracing technique to compute an enhanced system model. The algo-rithm approximates the three-dimensional coincidence response function (CRF) for two arbitrary oriented cubic detector elements. The physical and geometrical properties of the involved detec-tor modules are evaluated at event time, tracing the ray paths of gamma quanta from one detec-tor to the other through the field of view.

Results: The algorithm has been assessed using list-mode data form the ClearPET Neuro™, and is compared to a standard ordered-subset ML-EM reconstruction method for projections. Both resolution and contrast can be improved with the list-mode reconstruction.

Conclusions: We have developed a ray-tracing technique, which calculates the fully three-dimensional coincident response function for two arbitrary oriented cubic detector modules. Further this technique can be easily expanded to other detector geometries, because the ray tracing approach is feasible for arbitrary shaped detectors. When this technique is applied to list-mode reconstruction for ClearPET Neuro™, we have demonstrated that we can achieve better image quality in some aspects, like contrast and resolution, as compared to the reconstruction from projections. So this is a promising reconstruction technique for preferably retaining the pre-cision of the data.

References :
[1] E. Auffray et al ; *Nucl. Instr. Meth. A* 527 :171-174 (2004)
[2] K. Ziemons et al ; *Nucl. Instr. Meth. A* 537 :307-311 (2005)
[3] H.H. Barrett et al ; *J. Opt. Soc. Am. A* 14:2914-2823 (1997) „List-mode likelihood"
[4] R.L. Siddon; *Phys. Med. Biol.* 43:252-255 (1985) „Fast calculation of the exact radiological path for a three-dimensional CT array"
[5] A.J. Reader et al; *Phys. Med. Biol.* 43:835-846 (1998) "Fast accurate iterative reconstruction for low-statistics positron volume imaging"

Preliminary results obtained with the CT/SPECT components of AMISSA

Brasse D, Bekaert V, Leroux K, Humbert B and Guyonnet J-L
Institut Pluridisciplinaire Hubert-Curien, UMR 7178, ULP Strasbourg 1, CNRS-IN2P3

Background: The interest of small animal imaging has been primarily due to the recent advances in genetics with the need to perform longitudinal studies on mice or rats. Recent work has shown that functional imaging of small animals such as SPECT and PET systems can provide high spatial resolution with a high sensitivity where the addition of an X-ray CT system provides the lack of anatomical structures.

Aim: In our institute, we are developing a multimodality imaging system for small animal (AMISSA) combining X-ray, SPECT and PET devices. In this paper, we discuss the performances of the combined CT/SPECT components already available.

Materials: The micro-CT system is based on a commercially available X-ray detector and a micro-focus X-ray source. The sensor contains a CsI scintillator plate combined to a two dimensional 2400 x 2400 pixel CMOS photodiodes array. The size of a pixel is 50 µm. The acquisition rate is 2 projections per second up to 9 projections per second using 4 x 4 binning. The maximum tube voltage is 90 kV with a maximum intensity of 250 µA. The entire system rotates continuously around the animal or using a step and shoot approach.
The micro-SPECT system consists of four individual cameras arranged around the animal with one pinhole aperture and 5 detector modules per camera. Each module is based on a scintillator array of 2.3 x 2.3 x 28 mm^3 YAP:Ce optically isolated pixels coupled to a 8 x 8 multi anode PMT. The axial field of view (FOV) is 10 mm and the transverse FOV is adapted to the animal.

Results: We previously introduced an inline acquisition and reconstruction architecture to obtain in real time the 3D reconstructed volume of the animal using the micro-CT system [1]. With the proposed architecture, we demonstrated that it is already possible to obtain a real-time reconstructed image of a whole body mouse in 358s. This value corresponds to the time required to acquire 768 projections of 2048 x 2048 pixels and to backproject them inside a volume of 140 Mega voxels with 100 µm spatial resolution. Using a 4 x 4 binning and a reduced number of projections, the entire mouse can be acquired and reconstructed in less than a minute. The intrinsic spatial resolution of the SPECT system is measured to be 2.3 mm in both directions leading to a 1.3 mm spatial resolution in the center of the FOV using a 0.5 mm diameter pinhole aperture. The detection efficiency is 140 cps/MBq for a point source centered in the FOV. The system energy resolution is 30 % at 140 keV.

Conclusions : We propose a high performance modular combined CT/SPECT system dedicated to small animal imaging fulfilling the requirements of in-vivo imaging.

References :
[1] Brasse D et al, Towards an Inline Reconstruction Architecture for micro-CT Systems, Phys. Med. Biol. 50 (2005) 5799-5811.

Successful labelling of cells with Gadolinium for visualization by MRI

Bernsen MR_1, van Tiel ST_1, van der Graaf LMG_1, Mulder WJM.$_3$, Nicolay K.$_3$, Wielopolski PA_1, Krestin GP_1, Koning GA_2

$_1$Department of Radiology, Erasmus MC – the University Medical Center Rotterdam, Rotterdam, the Netherlands; $_2$Department of Radiation, Radioisotopes and Reactors (R3) Faculty of Applied Sciences, Delft University of Technology, the Netherlands; $_3$Department of Biomedical Engineering, Eindhoven University of Technology.

Background: Labeling of cells with paramagnetic particles for visualization by MRI has received a lot of attention recently [1]. Generally, iron oxide particles are being used for paramagnetic labeling of cells, resulting in a hypo intense (T2) contrast in MR imaging. However, for some applications hyper intense contrast (T1) of the cells would be preferable [2].

Aim: To develop a method for successful labeling of cells with Gadolinium (Gd): a T1 contrast agent.

Methods: Two different Gd formulations were used for incorporation into cationic lipid-based nanoparticles (lipid carriers). Gd-DTPA (Magnevist®) was used for incorporation of Gd into the water phase of the lipid carrier and Gd-DTPA-bis(stearylamide) was used for incorporation of Gd into the lipid phase of the lipid carrier. For control purposes also lipid carriers without Gd were prepared. To allow for visualization of the lipid carriers and labeled cells by fluorescence microscopy, a lipidic fluorescent label was also incorporated in all types of lipid carriers. Cells were incubated with different doses of the various lipid carriers for various incubation times. Incorporation efficiency of the lipid carriers and Gd was determined by Fluorescence microscopy, ICP-OES and MRI. In addition, the effect of the lipid carriers with and without Gd on cell viability was tested.

Results: Efficacy and toxicity of lipid carrier incorporation was dependent on labeling dose and incubation time used. An optimal labeling efficiency, without significant toxicity was obtained by incubating cells for 4 hours with 1 µmol of lipid carrier. This resulted in incorporation of 10-90 µg of Gd per 10^6 cells depending on the type of contrast agent used. These amounts of Gd incorporation were sufficient for visualization by MRI under in vitro conditions as well as in vivo conditions.

Conclusions: Efficient non-toxic labeling of cells with Gd resulting in a hyper intense (T1) contrast with MRI is feasible through the use of cationic lipid carriers.

References:

[1] Zhang Z et al; *Magma* 18:175-185 (2005*)*
[2] Kusterman E et al.; *NMR Biomed.* 18:362-370 (2005)

Automated Classification and Visualization of Breast Tumour Classes based on High-Resolution 1H Nuclear Magnetic Resonance Spectroscopy

Althaus M1, Noelte M2, Leibfritz D3, Bonk U4, Peitgen HO1
1 MeVis – Center for Medical Diagnostic Systems and Visualization, Bremen; 2 ZeTeM – Zentrum für Technomathematik, University of Bremen; 3 AG Instrumentelle Analytik, University of Bremen; 4 Zentralkrankenhaus Bremen-Nord, Bremen

Background: In recent years pattern recognition techniques have gained increasing attention in the interpretation of nuclear magnetic resonance (NMR) spectroscopy datasets [1]. Furthermore, in vitro NMR spectroscopic examinations of tissue extracts (e.g. of breast carcinomas) play an important role for a detailed understanding of the underlying metabolic changes in pathological conditions. Analysis of these datasets using pattern recognition and visualization techniques will be a major prerequisite for the dissemination of the NMR spectroscopy technique from the basic research arena into the clinical setting.

Aim: To differentiate breast tumour classes based on high-resolution 1H-NMR spectroscopy in combination with an appropriate feature extraction and visualization method based on k-nearest neighbour classifiers and self-organizing maps and to select and to characterize the metabolites relevant to the differentiation of breast tumour classes.

Methods: Specimens of human breast tissue have been obtained from 49 patients after surgery.
Tumour samples have been characterized histologically and have been registered with patient data. If available, healthy control tissue outside the tumour margin has been added to the database which consisted of 42 breast tumour samples of various tumour grades and 29 samples of healthy tissue. The metabolic profile has been investigated using a dual extraction technique and high-resolution 1H-NMR spectroscopy. Spectra of lipophilic and the hydrophilic compounds have been assigned to three groups according to different malignancy grades of the respective tissue samples. The group characteristics were analyzed using the k-nearestneighbor method and self-organizing-map [2] visualizations.

Results: According to the tumour grade an increase of the phosphocholine, phosphoethanolamine and UDP-hexose concentrations has been detected. In the malignant samples higher concentrations of taurine were detected. In benign tissue samples myo-inositol and glucose content were elevated compared to malignant tissue. Several lipid metabolites showed a characteristic elevation with high malignancy (WHO grade 3) possibly reflecting increasing turnover in membrane lipid metabolism according to proliferation and malignant transformation [3].

Conclusions: Advanced data analysis techniques allowed the automatic and robust identification of relevant biochemical information for characterizing distinct malignancy groups in breast cancer and provided a simple, yet efficient visualization of the underlying metabolic differences. The applied methods turned out to be a good means to explore the complex nature of high-resolution NMR datasets obtained from tissue extracts. We expect this method to be of even greater importance for the analysis of Magic-Angle-Spinning (MAS) NMR datasets [4].

References:
[1] Tate AR et al; *NMR Biomed* 11:147 (1998)
[2] Kohonen T; *Self-Organizing Maps*. Springer: Berlin (1995)
[3] Beckonert O et al; *NMR Biomed.* 16:1-11 (2003)
[4] Sitter B et al; *NMR Biomed.* 19:30-40 (2006)

TOPIC: TECHNOLOGY	POSTER 74

3D in-vivo imaging of gene expression in mice

Garofalakis A.[1], Zacharakis G.[1], Meyer H.[1], Economou E.N.[1], Mamalaki C.[2], Papamatheakis J.[2], Kioussis D.[3], Ntziachristos V.[4], Ripoll J[1].
[1]Institute of Electronic Structure and Laser, Foundation for Research and Technology-Hellas, Heraklion Greece; [2]Institute of Molecular Biology and Biotechnology, Foundation for Research and Technology-Hellas, Heraklion, Greece; [3]Division of Molecular Immunology, National Institute for Medical Research, The Ridgeway, Mill Hill; [4]Laboratory for Bio-Optics and Molecular Imaging, Center for Molecular Imaging Research, Massachusetts General Hospital, Harvard Medical School, Charlestown.

Background: In the field of molecular imaging, fluorochromes and fluorescent proteins (FPs) can be invaluable tools for probing molecular events and pathways inside living systems [1].

Aim: Generation and application of optical methods for non-invasive imaging of biomolecular function and gene expression in-vivo in whole animals.

Methods:
We have setup a CCD-based Fluorescence Molecular Tomography (FMT) imager that enables large data acquisition and full 360 measurements by using non-contact measurements [2]. Increased data information is being currently implemented by including multi-spectral measurements of different fluorescent proteins in the visible [3]. Transgenic mice were used for the investigation of various features of the immune system, particularly for studies of lymphocyte differentiation and tolerance.

Results:
The system was tested in realistic experiments with mice and its performance and accuracy in detecting and quantifying fluorescence emission was contrasted against data from FACS (Fluorescence Activated Cell Sorter) analysis, i.e. data obtained ex-vivo by counting each fluorescent cell independently. We were able to image for the first time T cell function *in-vivo* in the thymus and the spleen in response to a reaction induced by a systematically injected antigen peptide and monitor it over time. The results were contrasted against data from FACS analysis reaching remarkable agreement.

Conclusions: We have developed a 3D non-contact fluorescence tomography imaging system suitable for in-vivo whole body imaging of gene expression. Tomographic methods can be used for the quantification of the fluorescence activity. FMT is capable of following biological function on the same specimen over time with remarkable correlation with ex-vivo FACS measurements.

References:
[1] Weissleder R. and U. Mahmood; *Radiology.* 219 :316-333 (2001)
[2] Ripoll J. et al, ; *Phys. Rev. Lett.*, 91:103901 (2003).
[3] Zacharakis et al.; *PNAS* 102: 18252–18257 (2005).

Semi-automatic segmentation of ROIs/VOIs from small animal images

Gudrun Wagenknecht, Markus Surudo, Markus Losacker, Regine Wolff, Hendrik Belitz, Joaquín Castellanos, Lin Chen
Central Institute for Electronics, Research Center Juelich, D-52425 Juelich, Germany

Background: Segmentation of anatomical structures and tumors is an important prerequisite for the interpretation and further quantitative analysis of multimodal small animal images. Measuring tumor progression and treatment response over time are both important issues in cancer research. Which structures are to be examined depends on the particular research being done.

Aim: To develop methods for segmenting regions-of-interest (ROIs) or volumes-of-interest (VOIs) from small animal images which are adaptable, extendible and applicable to multimodal image data from different experimental and clinical animal and patient trials.

Methods: Semi-automatic segmentation approaches were developed to provide flexible region extraction methods adaptable to different image modalities and research questions. They require minimal user interaction and yield more reliable and user-independent results than does drawing regions manually. On the other hand, user interaction makes them more adaptive than purely automatic methods. Methods based on dynamic programming (2D live wire) [1-3], 2D active contours[3] as well as 3D active surface models[4] were developed.
The live wire prototype is being extended and integrated into the MITK software environment (developed at DKFZ Heidelberg). A combination of the 2D live wire and 3D active surface approach is currently being developed and intergrated into MITK. MITK yields the GUI for user interaction, parameter adjustment and 2D as well as 3D data visualization. It is based on the Insight and the Visualization Toolkit (ITK, VTK).

Results: The 2D approaches were applied to six rats and mice MRI data sets of different resolution and image quality and evaluated regarding user interaction and segmentation consistency. In addition to the original images noise-reduced images were examined[3,5]. All in all, the user interaction needed is accaptable for the live wire and active contour-based approach. Noise reduction has a positive influence on the user interaction required and the consistency of the results in most cases.

Conclusions: The results show that semi-automatic segmentation is a good choice to deal with different kind of images, image quality and regions. Next, the combined 2D/3D method as well as images from other modalities (e.g., CT, fluorescent images) should be examined.

References:
[1] Mortensen EN et al.; Proc. 22nd annual conference on Computer graphics and interactive techniques. 191-198 (1995)
[2] Wischnewski L et.al.; BVM 2004. 55-59 (2004)
[3] Wagenknecht G et al.; Nuclear Instruments and Methods in Physics Research, Section A. (in press)
[4] Belitz H et al.; Proc. 2006 IEEE Int. Symposium on Biomedical Imaging: From Nano to Macro. 402-405 (2006)
[5] Castellanos J et al.; Proc. MICCAI 2005. 320-327 (2005)

In Vivo Imaging of Oxygen Distribution in the Ischemic Mouse Model

R. Favicchio[1], A. Garofalakis[2], G. Zacharakis[2], J. Papamatheakis[1], C. Mamalaki[1] and J. Ripoll[2]
[1] *Institute of Molecular Biology and Biotechnology, FORTH, Heraklion, Crete, Greece*
[2] *Institute of Electronic Structure and Laser, FORTH, Heraklion, Crete, Greece*

Background: In the near infrared region (NIR) absorption and scattering by biological tissues is reduced to its minimum. At these wavelengths the major component of blood, haemoglobin, shows two different characteristic absorption profiles depending on its oxygenation state[1]. Oxyhaemoglobin (HbO) and deoxyhaemoglobin (Hb) values are hence used to monitor relative blood volume and oxygen saturation levels[2].

Aims: Near-Infrared Spectroscopy (NIRS) is used to measure *in vivo* tissue oxygenation[3] levels and assess localised response to tissue damage in the surgically-induced hind limb ischemic mouse model.

Methods: Hind limb ischemia was surgically induced in C57bl mice by ligation of the left femoral artery. A purpose-modified optical tomography setup was used to acquire *in vivo* images at time intervals for up to 3 weeks. Hb and HbO absorption was measured in the near-infrared spectral region using a CCD camera in combination with a set of filters (780 and 830nm respectively) mounted in front of a light source to specifically select for either one of the two compounds. Extent of tissue damage following surgery and blood reperfusion of the ischemic area was monitored over time by comparing oxygen saturation values. The non-operated right limb was used as a negative control and used as a baseline value to assess damage and recovery.

Results: Absorption was measured at 780nm and 830nm and plotted as 2-dimensional surface-overlaid images of ischemic and non-ischemic mice limbs. The intensities recorded were used to quantify the relative oxy- and deoxyhaemoglobin levels using the Beer-Lambert equation. These values allowed in turn for: (1) total blood volume and oxygen saturation levels to be calculated and (2) localisation of the areas in which the ischemia-induced tissue damage was strongest.

Conclusions: Modification of the Fluorescence Molecular Tomography (FMT) setup to perform *in vivo* absorption spectroscopy allows the mapping and following of changes in oxygen saturation in the mouse at desired time intervals. The data, presented as 2D images, enables to select for a region of interest and individuate the ischemic regions. The relative quantification of the oxygen saturation values in these areas can be plotted against time and therefore can be used in the ischemic murine model as a method to follow tissue reperfusion.

References:
[1] Wray S. *et al.*; Biochim Biophys Acta. 933:184-92 (1988).
[2] Ntziachristos V. *et al*.;.Med Phys. 27:410-21 (2000).
[3] Srinivasan S. *et al*.; Proc Natl Acad Sci U S A. 100:12349-54 (2003.)

Targeted lipid-based bimodal contrast agents for the detection of apoptosis

Van Tilborg GAF 1, Mulder WJM 1, Deckers N 2, Chin PTK 3, Reutelingsperger CPM 2, Strijkers GJ 1, Nicolay K 1.
1Biomedical NMR, Department of Biomedical Engineering, Eindhoven University of Technology, 2Department of Biochemistry of the Cardiovascular Research Institute of Maastricht, University of Maastricht, 3Laboratory of Macromolecular and Organic Chemistry, Eindhoven University of Technology.

Background: Apoptosis plays an important role in the etiology, pathology and treatment of a variety of diseases, including myocardial infarction and cancer [1]. Detection of apoptosis *in vivo* would allow for disease staging and evaluation of disease treatment at an early stage. The protein annexin A5 is shown to bind with high affinity to the phospholipid phosphatidylserine, which is exposed on the outer leaflet of the apoptotic cell membrane. Therefore the use of annexin A5-functionalized multimodal contrast agents, that contain both fluorescent and MRI labels, allows parallel high-resolution MRI and optical imaging to study apoptosis *in vitro* and *in vivo*.

Aim: Preparation of annexin A5-functionalized lipid-based nanoparticles that differ in size, magnetic properties and fluorescent properties.

Methods: Three types of lipidic nanoparticles were prepared, which are based on micellular or liposomal aggregates. The core of the micellular contrast agents contains either oleic acid coated superparamagnetic iron oxide particles for MRI or TOPO/HDA capped quantum dots with a CdSe/ZnS core/shell for optical imaging [2]. Bimodality was obtained by additional incorporation of fluorescein lipids (1%) or paramagnetic Gd-DTPA-BSA lipids (50%) within the lipid monolayer, respectively.
Alternatively, liposomes with Gd-DTPA-BSA (25%) and fluorescein lipids (0.1%) incorporated in the lipid bilayer were developed [3]. All contrast agents were functionalized with annexin A5 to target apoptotic cells. Apoptotic Jurkat cells were incubated with the nanoparticles for 30 minutes to determine their specificity. Subsequently, cells were pelleted and T1- or T2-weighted images and fluorescence microscopy images were obtained for visualization of the contrast agents with both imaging modalities.

Results: The mean diameter of each nanoparticle was measured with dynamic light scattering. Relaxivities r1 and r2 were measured at 20 MHz or 60 MHz and room temperature (Table). T1- or T2-weighted images (D-F) of pelleted apoptotic cells (*right*) that were incubated with superparamagnetic micelles (D), paramagnetic liposomes (E) or paramagnetic micellular quantum dots (F) showed significant contrast enhancement compared with pelleted control cells that were not exposed to contrast agents (*left*). Fluorescence microscopy images of the apoptotic cell pellets demonstrated specific association of the nanoparticles to cells (A-C).

Conclusions: Three different annexin A5- functionalized lipidbased nanoparticles were prepared that differ in size, magnetic properties and fluorescent properties.
All contrast agents were shown to enable the detection of apoptotic Jurkat cells both with MRI and fluorescence microscopy *in vitro*. The targeted nanoparticles presented in this study may have applications for the *in vivo* detection of apoptosis with MRI. In addition the paramagnetic micellular quantum dots can also be used for the *in vivo* visualization of apoptosis with intravital microscopy.

References: [1] Haunstetter A., Izumo S., *Circ Res.*,15 ; 82(11):1111-29 (1998).
[2] Mulder W.J.M. *et al.*, *Nanoletters*, Jan;6(1):1-6 (2006).
[3] Mulder W.J.M. *et al*., *Bioconjug Chem.,* Jul-Aug;15(4):799-806 (2004).
Diameter (nm) r1 (mM-1s-1) r2 (mM-1s-1)
Superparamagnetic micelles ~10 13.3 159.9
Paramagnetic liposomes ~100 4.1 6.8
Paramagnetic micellular quantum dots ~10 12.4 18.0

Simultaneous Dual-Isotope PET Imaging

Gispert JD[1], Pareto D[1], Llop J[1], Gómez V[1], Rojas S[2], Martín A[2], Millan O[1], Planas AM[2].

[1]Institut d'Alta Tecnologia - Parc de Recerca Biomedica de Barcelona, Barcelona, SPAIN; [2]Institut d'Investigacions Biomèdiques August Pi i Sunyer, Barcelona, SPAIN.

Background: SPECT imaging allows performing dual-isotope studies based on the different energy spectra of the isotopes used. On the contrary, PET imaging does not allow this procedure since positron annihilation yields two 511 KeV gamma rays regardless of the original isotope/s used.

Aim: To statistically discriminate the activity concentration of two different positron emitter isotopes administered simultaneously as a function of their different decay periods.

Methods: To enable this approach dynamic acquisition of emission data must be performed with no decay correction. Then, the time-data in every pixel is fitted to a weighted sum of the expected decay functions for every isotope by a non-linear least squares method, so that these weights represent an estimation of the activity concentration of every isotope. Limitations to this technique include the assumption of a constant activity concentration and the decrease in the signal to noise ratio of the single-isotope images.

Results: In this work, we have implemented this methodology and evaluated the impact of different practical factors such as the number of temporal bins or the benefits of a smoothing strategy for improving the signal to noise ratio in the images. We have validated the accuracy and precision of this methodology with phantoms containing different concentrations of 18F-FDG and 13N-NH3, as well as performing several experiments with living rodents.

Conclusions: This approach could be extended to the clinical practice providing reductions in the scan time and therefore higher patient throughput, for example in myocardial viability studies.

Quantification and Imaging of Integrin Receptors

Jörg Hamm[1], Sabrina Benedetto[1], Roberta Pulito[1], Simonetta Geninatti Crich[2], Guido Tarone[1], Silvio Aime[2], Lorenzo Silengo[1]
[1]Department of Genetics, Biology and Biochemistry and CERMS, University of Turin, 10126 Turin, Italy; [2]Department of Chemistry IFN and Center for Molecular Imaging, University of Turin, 10125 Turin, Italy

Background: Targeted imaging of cell surface receptors requires the site specific accumulation of contrast agent. The characteristics of the contrast agent have to be compatible with the abundance of the target molecule and the sensitivity of the imaging modality employed.

Aim: Determination of the number of exposed target molecules per cell to provide a rational basis for design of suitable imaging platforms.

Method: The expression level of the integrin receptor subunits α_v and β_3, and for comparison of the EGFR, of several tumour cell lines (U251, U87, A549, A431), an human monocyte cell line (THP1) and human primary cells (HUVEC) was determined by flow cytometry analysis[1]. Cells were first incubated with mono-biotinylated antibodies against receptor subunits, washed and incubated subsequently with streptavidin-FITC. The antibody induced fluorescent shift was normalised to the shift of 2µm biotin-coated reference beads with of known number of exposed biotin molecules. Targeted imaging was performed by incubating adherent cells with iron-oxide beads coated with receptor-specific antibodies and analysis of cells by magnetic resonance imaging of cells suspended in agarose.

Results: The observed values of integrin receptor abundance are $3 \cdot 10^3$–$1.4 \cdot 10^4$/cell for α_v and $5.3 \cdot 10^2$–$1.1 \cdot 10^4$/cell for β_3. These values are lower than generally expected based. Despite the low number of exposed receptors we show that up to single cell MR visualisation is possible by using iron oxide beads complexed with antibodies as contrast agents.

Conclusions: Numerical quantification of receptor numbers per cell are rarely reported in the literature, this is even true for “popular” targets like integrins, which we can show to be far less abundant than generally anticipated. However, the presented results strongly emphasise the fact that the number of expressed receptor molecules to be targeted by contrast agent should be determined experimentally prior to the design of the desired imaging platform to avoid synthesis and experimentation of CAs inapplicable for the intended target receptor. Furthermore, we show that up to single cell MR visualisation is possible by using iron oxide beads complexed with antibodies as contrast agents.

References:
[1] Artemov D, Mori N, Okollie B, Bhujwalla ZM. Magn Reson Med 2003;49(3):403-408.

Cellular in vivo imaging of fluorescent protein-tagged transgenic mice : application to the hypothalamic-pituitary system

C. Lafont,/ M. Desarménien, T. El Yandouzi, F. Molino, G. Menessier, P.F. Mery, A. Lacampagne, D. Carmignac, I. Robinson, P. Mollard
Institut de Génomique Fonctionnelle, Montpellier, France

GH cells form a highly organized and plastic cell network that pervades the entire anterior pituitary. This prompts the question how the GH cells function together within the network to mount large GH pulses in response to physiological needs. To address this question directly requires an understanding of how GH cells respond */in vivo/* to secretagogue inputs, in order to generate coordinated pulses of hormone release into the pituitary circulation.
We have developed a strategy that allows simultaneous study of both GH cells and pituitary blood flow at single cell resolution in living mice. Using anaesthetized GH-eGFP transgenic mice, we have developed a surgical procedure that exposes the ventral pituitary surface to direct epifluorescence illumination and imaging, whilst monitoring breathing movements, heart rate and blood flow through pituitary vessels.

This approach allows real-time */in vivo/* imaging of large numbers of fluorescent somatotrophs with single cell resolution (up to a final 600x magnification) at the ventral pituitary surface, recorded as time-lapse movies, after correction for regular movements of respiration and cardiovascular beats. We can also monitor cytosolic calcium signals in populations of GH cells by bolus cell loading with fura-2, a UV-excitable calcium dye, and recording calcium transients induced by GH secretagogue administration. Finally, i.v. injections of Texas-Red-labelled 70 kD dextran allow us to visualize blood flow directly in individual pituitary blood vessels in close proximity with the distinct topological GH cell organizations (strands of GH cells vs larger GH cell clusters) that form the network architecture. Examples of all of these */in vivo/* imaging modalities will be illustrated, and the relationship of local GH release, activity, and blood flow discussed. This approach can directly reveal the organisational basis of the coordination of GH secretory events necessary to generate pulses that regulate body growth and metabolism across lifespan. Furthermore, it is directly applicable to other pituitary endocrine cell populations with other fluorescent transgene markers.

Far Red Imaging of Beta-galactosidase Activity for Stem Cell Detection in the Brain.

Kaijzel EL[1], Belenkov[2] AI, Que I[1], Pierre Couture P[2], and Löwik CWGM[1].
[1] *Leiden University Medical Center, Department of Endocrinology, the Netherlands*
[2]*Advanced Research Technologies, ART Inc. 2300 Alfred-Nobel, Saint-Laurent, Canada.*

Background: Genetic reporter systems based on the enzyme β-galactosidase have been widely used for *in vitro* and *in vivo* reporter applications because of the ease of their *in situ* tissue sample analysis. However, the destructive nature of this approach for gene expression and regulation monitoring severely limits the use of β-galactosidase for *in vivo* applications where repetitive monitoring of the same animal is desirable. As such, several groups have attempted to extend the applicability of this reporter protein to non-destructive and repetitive *in vivo* imaging.

Aim: The purpose of this study was to explore the possibilities for imaging of deeply lying β-gal/luciferase expressing cells using optical approaches.

Methods and Results: Beta-galactosidase and luciferase expressing C17.2 mouse neural progenitor cells (NPCs) were stereotaxically implanted into the parenchyma of the left hemisphere of the BalbC *nu/nu* mouse brain and imaged 10 days after implantation. Following both DDAOG and luciferin i.v. administration fluorescent and bioluminescent signals were detected respectively only from the left hemisphere of the mouse brain. Serial imaging revealed a rapid increase in the fluorescent signal intensity over the right hemisphere of the animal with the highest signal to peak at 10-15 min after substrate administration. Postmortem staining of the brain cross-sections with X-gal confirmed the presence of the *β-gal*-expressing C17.2 cells in the left hemisphere.

Conclusion: Our results indicate that β-galactosidase may be successfully employed for *in vivo* imaging of deeply-lying *β-gal*-expressing cells not only as a stand-alone fluorescence reporter system, but also multiplexed with bioluminescent reporters, especially when the assessment of more than one molecular event is desirable within a single experimental subject.

Bioluminescence imaging of local transgenic expression induced by heat in mice

Deckers R[1], Quesson B[1], Rome C[1], Couillaud F[1], Moonen CTW[1]
[1]*Laboratory for Molecular and Functional Imaging, ERT CNRS/Université Victor Segalen, Bordeaux, France*

Background

Gene therapy has a great potential for treating a broad array of human diseases, but requires tight control of both spatial and temporal expression of the therapeutic transgene. Heat-shock promoters (*Hsp*) have been proposed for gene therapy strategies because they are both heat-inducible and efficient. Combined with a non invasive physical approach, developed in our laboratory [1], which allows for a local temperature control, this strategy could be a good way of controlling both spatial and temporal expression of the therapeutic transgene [2].

Aim

This study shows the feasibility of spatial control of a transgenic expression induced by heat in mice. The spatial correlation between the area heated with a warm water bath and the region that produces light during bioluminescence imaging in transgenic mice is investigated. Further, the kinetics of *Hsp70* expression were monitored.

Methods

Heating experiments were performed with a warm water bath. The left leg of a transgenic mouse (NLF1) was exposed to a temperature of 43.5º C for 5 minutes. The transgenic mice express a gene consisting of a luciferase reporter gene under control of a mouse *Hsp70a1b* promoter. 3, 6, 9, 12 and 25 hours after heating the location of the light production due to luciferase activation was monitored with bioluminescence imaging. Prior to sedation with isoflurane, 100 µl of an aqueous solution of luciferin (29 mg/ml stock) was injected into the peritoneal cavity of the mouse. A bioluminescence image (2 minutes exposure time, 2×2 binning) was taken 10 minutes after the luciferin injection using the NightOWL LB 981 NC 100 CCD camera. Further, a grey-scale body-surface reference image was collected. A pseudocolor luminescent image from blue (least intense) to red (most intense), representing the spatial distribution of the detected photons emitted from active luciferase within the animal, was generated using WinLight software (Berthold Technologies). To monitor the kinetics of *Hsp70* expression the signal intensity was quantified as the sum of all detected photon counts within a region of interest prescribed over the mouse left leg using Winlight software (Berthold Technologies).

Results

Figure 1 shows the pseudocolor luminescent image taken 6 hours after heating the left leg of the mouse with the warm water bath. The color scale indicates the intensity of light emission in photon counts. The kinetics of *hsp70* expression in mice is shown in figure 2. The maximum intensity of light emission was found 6 hours after heating.

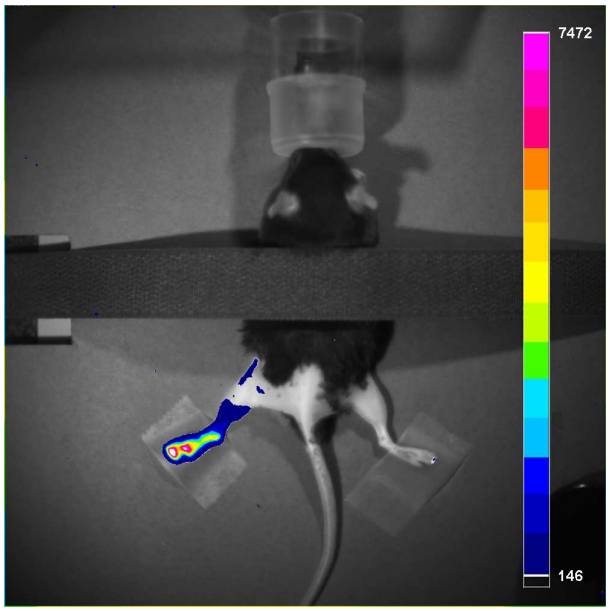

Figure 1: *Bioluminescent image taken 6 hours after heating. The color scale represents the number of photon counts.*

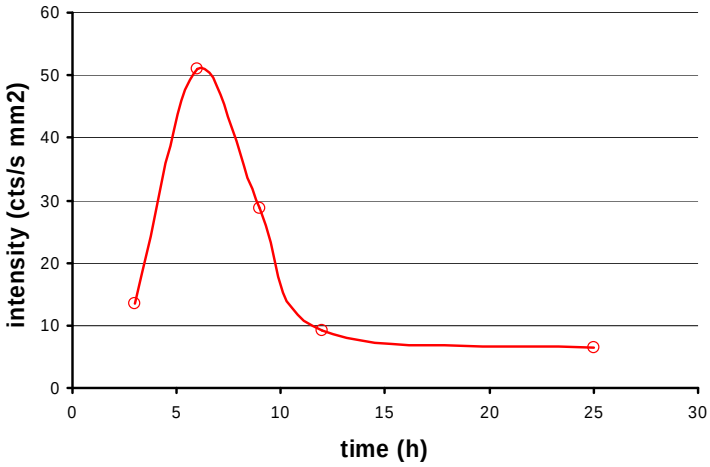

Figure 2: *kinetics of Hsp70 expression in mice. The light emission is measured at 3, 6, 9, 12 and 25 hours after heating.*

Conclusions

The high correlation between the region of heating with the water bath and the location of light emission in the mouse leg indicates that it is possible to spatially control transgenic expression. These results show that is feasible in future studies to heat transgenic mice with focused ultra sound (FUS) guided by MR and expect local expression of luciferase, verified with bioluminescence imaging.

Reference

[1] Salomir R et al; Magn Reson Med 2000; 43: 342-347
[2] Guilhon E et al ; J Gene Med 2003 ; 5 : 333-342

What is the meaning of susceptibility artefacts resulting from (transplanted) paramagnetically labelled cells?

Van Tiel ST, Wielopolski PA, Krestin GP, Bernsen MR
Department of Radiology, Erasmus MC – the University Medical Center Rotterdam, The Netherlands

Background: For a variety of disorders, cell therapy is seen as a valuable treatment method [1,2]. To study the effectiveness and safety of cell therapy, it is important that these cells can be tracked in the body, preferably without the need for invasive interventions. Several studies have indicated that this is possible with magnetic resonance imaging (MRI) and paramagnetically labelled cells. But, what do we really see on our MRI images? Are the artefacts seen in fact the labelled cells???

Aim: To determine what is seen on MRI scans of (transplanted) paramagnetically labelled cells by comparing them with histology.

Methods: (1) ROS-1 is an osteosarcoma cell line, which can be labelled with Endorem®, a FDA-approved contrast agent consisting of super paramagnetic iron-oxide (SPIO) particles [3]. To facilitate cellular uptake of Endorem, lipofectamine was used [4]. After labelling, cells were plated in a 4 well cell culture plate, and images were acquired with a 3.0T General Electric MRI scanner. In addition bright field photographs were taken of the same cell samples with a Zeiss photo-microscope. The two different images were compared.
(2) Immunologically competent rats (Wag/Rij) were injected subcutaneously with syngenic, SPIO labelled and unlabelled, ROS-1 cells and followed for up to 2 months with MRI. After 13 or 58 days, the tumour was removed. Tissue sections were stained with Haematoxylin-Eosin (HE) and Prussian blue (=iron staining). Histological images were compared with MR images.
(3) Immunologically competent rats (Brown Norway) were injected subcutaneously with syngenic BN175 sarcoma cells and allogenic ROS-1 cells. Both cell types were labelled with SPIO. The development of the tumours was followed with MRI. After 16 days, the tumour and skin at the injection site were resected. Tissue sections were stained with HE and Prussian blue. Histological images were compared with MR images.

Results:
(1) When comparing MR and light microscopy images, a good concordance between the location of cells and artefacts was generally found. However, large black artefacts were also observed, most likely resulting from air bubbles present in the medium. In addition, a number of smaller artefacts seen in the MR image corresponded to the location of iron particles, that were not contained within a cell.
(2) MRI scans showed large black artefacts at the sites where labelled tumour cells were injected. Prussian blue stained tissue sections showed a limited number (1:50) of iron-positive cells in the centre of the tumour. No susceptibility artefacts were seen at sites where non-labelled cells were injected.
(3) The SPIO labelled allogenic ROS-1 cells did not grow in Wag/Rij rats, as opposed to the rapid growth of BN175 cells. However, susceptibility artefacts at the injection site were still seen for a prolonged period of time. Histological analysis revealed the presence of iron at the injection site, despite the lack of ROS-1 cells at this site.

Conclusions:

Not all artefacts that can be seen with the MRI are (originally) iron labelled cells. In vitro, air bubbles and loose iron particles can result in susceptibility artefacts similar to those resulting from iron-labelled cells. In vivo, a large, continuous susceptibility artefact can be seen on MRI scans resulting from the dispersed presence of iron labelled cells. Genetically incompatible tumour cells do not survive in vivo; nevertheless, a susceptibility artefact persists at the site of injection for a prolonged period of time. These data emphasize the requirement that the experimental model is well characterized and initially verified by histology when performing cell imaging by MRI. Only then can reliable conclusions, about the meaning of susceptibility artefacts, be made.

References:

[1] Saeed M etal; MRI in guiding and assessing intra myocardial therapy. Eur Radiol. 2005 May;15(5):851-63.
[2] Wu, Yl etal; In situ labelling of immune cells with iron oxide particles: an approach to detect organ rejection by cellular MRI. Proc Natl Acad Sci U S A. 2006 Feb 7;103(6):1852-7. Epub 2006 Jan 27.
[3] Bulte JW, Kraitchman DL; Iron oxide MR contrast agents for molecular and cellular imaging. NMR Biomed. 2004 Nov;17(7):484-99. Review.
[4] van den Bos EJ etal; (2003) Improved efficacy of stem cell labelling for magnetic resonance imaging studies by the use of cationic liposomes. Cell Transplant 12:743–756

Registration of 3-D Multimodal Molecular Structures. Preliminary Study

Telenczuk B1,2, Ledesma-Carbayo MJ1, Velazquez-Muriel J3, Sorzano COS3,4, Carazo JM3, Santos A1
1Universidad Politecnica Madrid (Spain), 2Wroclaw Univ of Technology (Poland), 3Centro Nacional de Biotecnología-CSIC (Spain), 4Univ. San Pablo-CEU (Spain)

Background: Three-dimensional electron microscopy allows imaging macromolecular structures with a resolution in the order of 6 to 25 Å. The information provided can be complemented by imaging with higher resolution some of their domains using X-ray diffraction experiments or Nuclear Magnetic Resonance Imaging. However to combine these two data sets, the spatial location of the domain within the whole structure has to be determined.

Aim: This paper presents the possibility of using rigid registration methods to locate the high-resolution domain within the medium-resolution structure. As in principle there is no clue about the location, the full space of three translations and three rotations has to be explored.

Methods: The key points of the registration procedure are the similarity measure selected and the optimization approach. The registration algorithm is based on mutual information as similarity measure [1], as it provides a good procedure to detect nonlinear correlations between voxels' intensities from different modalities. A smoothing preprocessing step balances the resolutions of both data sets to be registered. Then a robust and powerful optimization is applied. The unconstrained location of the highresolution domain in the whole complex and the possible symmetries in the molecular structures suggest the use of a two-step optimization procedure: first there is a global optimization by means of a differential evolution [2] that tries to converge to a solution near the global optimum; then a Regular Step Gradient Descent method refines the solution found. The whole procedure has been implemented in C++ within ITK 2.1 [3].

Results: The proposed registration algorithm was evaluated on both simulated data (from PDB, Protein Data Bank) and experimental 3D Electron Microscopy reconstructions (from MSD, Macromolecular Structure Database). For each dataset, we generated 20 random initial transformations (angles ±180º, translations ±20 pixels).
Then we tested whether the registration procedure was able to recover the correct alignment. With the simulated datasets that happened in 65 % of the cases, while with the experimental reconstructions, the registration was successful in more than 76 % of the cases (95 % for several molecules).

Conclusions: The proposed rigid registration procedure seems to be a valid method to fit atomic models into 3D electron microscopy macromolecular structures. The results obtained with large translations and rotations, can be improved at the expense of longer computation times, but the present compromise seems adequate to incorporate the algorithm into molecular database searching.

References:
[1] P Viola, WM Wells, "Alignment by maximization of mutual information". *Int J Computer Vision,* 24(2): 137-154. Sep. 1997.
[2] R Storn, K Price. "Minimizing the real functions of the ICEC'96 contest by differential evolution". *IEEE Conference on Evolutionary Computation*, 1996.
[3] L Ibanez et al. *"The ITK Software Guide"*. Insight Software Consortium, 2003.

Geometric sensitivity of the ClearPETTM Neuro

Gundlich B, Weber S
Central Institute for Electronics, Forschungszentrum Juelich

Background: ClearPET(TM) Neuro is a small-animal PET scanner dedicated to brain studies on rats and primates. It belongs to the ClearPET family of small-animal PET scanners that are de-veloped within the Crystal Clear Collaboration (CERN) and use the same detector block design with LSO and LuYAP crystals in phoswich configuration, directly coupled with multi-anode pho-tomultiplier tubes [1,2]. ClearPET(TM) Neuro consists of 20 modules each with 4 detector blocks in line with 8x8x2 crystal matrices. Due to the extension of the photomultiplier tubes there are axial and transaxial gaps between the crystal blocks. To compensate for these gaps each se-cond module is axially shifted and the scanner rotates during data acquisition. Nevertheless, the design of ClearPET Neuro leads to a specific geometric sensitivity, characterized by strong in-homogeneous and - depending on the measurement setup - even incomplete sinogram data.

Aim: With respect to reconstruction techniques, homogeneous and complete data sets are a 'must' for analytical reconstruction methods like Filtered Backprojection and the use of Fourier Rebinning, whereas iterative methods take the geometrical sensitivity into account as correction factors during the reconstruction process. Therefore also for iterative reconstruction a homoge-neous as possible geometric sensitivity over the field of view is highly desirable. This contributi-on aims to study the impact of different scanner geometries (axial shift, scanner radius) and dif-ferent measurement setups (scanner rotation, various axial bed positions) on the geometric sen-sitivity.

Methods: A data set of coincident events is computed for certain settings that contains each possible crystal combination once. The lines of response are rebinned into normalizing sino-grams and backprojected into sensitivity images using STIR [3] (Software for Tomographic Image Reconstruction) tools. The sensitivity images are analyzed in terms of e.g. minima, maxi-ma and standard deviation.

Results: Both, normalizing sinograms and sensitivity images mirror the geometric sensitivity and therefore provide information which setting enables complete and homogeneous (as far as pos-sible) data sets. An optimal measurement set-up and scanner geometry in terms of homogene-ous geometric sensitivity is found by analyzing the sensitivity images.

Conclusions: The sensitivity image of a PET scanner depicts the respective geometric normali-zation factors. A well chosen scanner geometry and measurement setup can smooth the sensiti-vity image, and hence the distribution of geometric normalization factors, for scanners with an unconventional scanner geometry and can therefore prevent noise especially for low-statistics data sets.

References:

[1] E. Auffray et al; *Nucl. Instr. Meth. A* 527:171-174 (2004)
[2] K. Ziemons et al; *Nucl. Instr. Meth. A* 537:307-311 (2005)
[3] C. Labbé et al; Proceedings of "Bildverarbeitung fuer die Medizin 1999, Algorithmen-Systeme-Anwendungen", Informatik aktuell, Springer, Eds. H. Evers et al 268-272 (1999)

Selection of blood stable nucleotidic sequences by *in vivo* SELEX

Stephanie Guillermet, Raphael Boisgard, Benoit Jego, Karine Siquier-Pernet and Bertrand Tavitian.
CEA, Département de Recherche Médicale, Service hospitalier Frédéric Joliot, Orsay, F-91400 France ; Inserm, U803, Orsay, F-91400, France.

Background: SELEX (Systematic Evolution of Ligands by Exponential Enrichment) allows the screening of very large combinatorial libraries of oligonucleotides (RNA or DNA) by an iterative process of *in vitro* selection and amplification. The *in vivo* vulnerability of oligonucleotides is related to the nuclease enzymes present in most living tissues and represents the major pitfall for their *in vivo* use. Partial evidence suggests that *in vivo* stability of oligonucleotides is dependant on their sequence, but so far no correlation between sequence and stability has been evidenced.

Aim: In order to isolate DNA-oligonucleotidic sequences exhibiting increased stability *in vivo*, we used a combinatorial Darwinian method based on SELEX in a real biological environment, i.e. by performing selection directly in living animals.

Methods: A random library of single strand DNA was subjected to repeated cycles of SELEX, including IV injection in nude mice, recovery of the sequences resistant to degradation after 60 minutes and amplification by PCR. *In vivo* kinetics studies of selected sequences were realised in nude mice and the sequence with the best stability (seq.22) was further studied in two other mice strains (BALB/c and Swiss) and in rats. Electrophoretic Mobility Shift Assay (EMSA) and affinity chromatography studies were realised to check the possibility of a binding of the seq. 22 and a protein of the serum. To evaluate the resistance of the seq. 22 to nuclease degradation, *in vitro* kinetics were realised in presence of several commercially nucleases.

Results: After six cycles, four sequences were predominantly represented in the final pool, One of these (seq. 22) accounted for 30 % of the totality of the sequences. In nude mice, the AUC (0-1h) of seq. 22 in plasma was higher by a factor 10 than that of the random library (4 against 0.4 respectively). Increased *in vivo* stability of seq. 22 was also observed in BALB/c and Swiss mice (AUC (0-1h) ratio=3), but not in rats.
No binding of seq. 22 to circulating blood cells could be evidenced. Electrophoretic Mobility Shift Assay (EMSA) and affinity chromatography showed binding of seq. 22 to a serum protein. However, the naive random library bound similarly to the same protein, out ruling the possibility that binding to this protein could explain increased stability in mice. In contrast, kinetics of the i*n vitro* degradation by S1-nuclease, a single strand specific endonuclease, showed an improved resistance of seq. 22 to S1-nuclease.

Conclusion: This study provides preliminary results on the feasibility of an *in vivo* selection process. It suggests that the improved stability of sequence #22 is due to increased resistance to nucleases rather than to binding to circulating blood cells or serum proteins. Results confirm that the 3D structure of oligonucleotides, driven by their primary sequence, conditions in turn their interaction with other biomolecules such as nucleases.

Supported by EMIL (European Molecular Imaging Laboratories) EU contract LSH-2004-503569, and Fondation pour la Recherche Médicale

Visualisation of dendritic cells and their migration by MRI using USPIOs and responsive Gd-based contrast agents.

U. Himmelreich, T. Geelen, C. Justicia and M. Hoehn
In vivo NMR laboratory, Max-Planck-Institute for Neurological Research Cologne, Germany

Background:
Gd-chelates and ultra-small paramagnetic iron oxide particles (USPIOs) are suitable for the visualization of deposits of cells *in vivo*. We have studied their suitability for the visualization of dendritic cells and the visualization of intracellular enzyme activity.

Methods:
Flt3+CD11b+progenitor cells and dendritic cells were isolated from mice. Labeling of cells was performed using USPIOs (endorem as well as sinerem) as well as Gd-DTPA. In addition, labeling was performed using a responsive contrast agent consiting of a Gd-DTPA chelate linked with two long fatty acid chains ($C_{17}H_{35}$) through ester bonds. This insoluble Gd-DTPA-FA complex can be activated by lipase activity and had a relaxivity of zero in the inactive state and 4.7 mM^{-1} s^{-1} after activation, respectively.

MRI: T1- and T2*-weighted MR images were acquired using a Bruker Biospin 7.0 Tesla small animal scanner equipped with an actively shielded gradient sets of 200 mT m^{-1} using 3D gradient echo sequences (FLASH) with TR=60ms (T1w) and 150ms (T2*w), TE=5ms(T1w) and 20ms (T2*w), 70º (T1w) 30º (T2*w) pulse, FOV= 3x3x1cm (animal model) and 4.5x4.5x1cm (agar phantoms), the isotropic spatial resolution was 78 μm for phantoms and 50 μm for animal experiments. For rf irradiation and signal detection custom-built coils were used. A 5-cm-diameter transmit-receive coil was used for agar phantoms and a 12-cm-diameter Helmholtz coil arrangement served for rf excitation with a 3.0 cm diameter surface coil for signal detection for animals. MR images were processed with the NIH software 'Image J'.

Animal model: 10,000-1,000,000 cells suspended in 2 □l were implanted in normal Wistar rats (n=4) into the border between the cortex and the corpus callosum (0.5 mm anterior, 3.0 mm lateral to bregma, 2.0 mm ventral from the dural surface) using sterotactic injection. Animals were imaged immediately after implantation and 4-14 days thereafter.

Results and Discussion:
Cell detectability was highest using USPIOs. The visualisation of cells with Gd-chelates depended on the route of uptake. Incubation of cells with Gd-chelates resulted in saturation of the R_1 relaxation rate for high concentrations of Gd_DTPA (>20mM). Electroporation of cell suspensions containing up to 100mM Gd resulted in stable labeling of all cell-lines and no saturation of R_1. Linking the Gd-DTPA complex to long aliphatic side chains results in a responsive contrast agent that can be activated by intracellular enzymes. We have tested this concept by using an ester link and activation of the chelate by intracellular lipase activity in dendritic cells. We were able to show that insoluble Gd-chelates are a suitable contrast agent for conditional activation by intracellular lipases. The chelate can easily be modified to be targeted by enzymes expressed during specific change of cell status. Such a system will then be suitable for functional cellular MR imaging. The concept was validated in animal models (ischemia in rats after MCAO).

Comparison of a CCD based and a fiber-based fluorescence tomography setups

Valentini G[1], Schulz R[2], Peter J[2], Semmler W[2], D'Andrea C[1], Cubeddu R[1]
[1]CNR-INFM and CNR-IFN, Dipartimento di Fisica, Politecnico di Milano, Milano, Italy; [2]Department of Medical Physics in Radiology, German Cancer Research Center (DKFZ), Heidelberg, Germany

Background: fluorescence mediated tomography (FMT) is a new promising technique aimed at localizing and quantifying selective probes *in vivo*, especially in small animals [1].
A typical fluorescence tomography set-up consists of many optical fibres located around the animal, in order to inject the excitation light and to collect the fluorescence emission. By using an appropriate theoretical model for photon migration inside biological tissues, the chromophore concentration inside the animal can be estimated from the comparison of experimental data with theoretical predictions. Recently, an alternative configuration for photon detection based on a CCD camera has been proposed by several authors [2].

Aim: The present work is intended to compare the performances for FMT of a fibre-based setup and a non-contact setup, exploiting the same number of detection points [3]. The comparison has been performed with respect to the quantification and localization of fluorescent inclusions in solid phantoms.

Methods: Two setups, baser either on detections fibres (57 fibres) or on a CCD (512 x 512 pixels) have been assembled, sharing most experimental devices. The light source was a laser diode emitting at 670nm, the phantom was a polyurethane cylinder (ø 4cm) with tissue like optical properties. The fluorescent inclusions were two hollow tubes (ø 4mm) filled with different concentrations of Cy5.5. The experimental data have been analyzed within a unified framework. In particular, a normalized Born approach has been used with a projection operator modelling the two detection methods.

Results:
While both methods gave a reconstructed value of the inclusions which are linearly dependent on dye concentration, the non-contact setup provided superior image quality. In particular, the centroid of the reconstructed inclusions was closer to the actual position of the Cy5.5 tubes, with all fluorochrome concentrations, and also the borders of the inclusions were better defined and more in agreement with the expected ones. It is worth noting that the comparison between the two imaging methods was performed using the same number of detection points, which correspond to the same computational effort. This demonstrate that the improvement did not come from an increase in detector numbers, which is a major argument in favour of CCD based setups, but was related to the non-contact method itself.

Conclusions:
We have peerformed a direct comparison between a fibre-based and a CCD based fluorescence tomography setups. Our study demonstrates that the non-contact detection system, beyond being simpler to assemble and to calibrate, gave a better reconstruction of fluorescent inclusions than the fibre based setup.

References:
[1] V. Ntziachristos et al; Molecular Imaging 1, 82 (2005)
[2] J. Ripoll et al; Phys. Rev. Lett. 91, 103901 (2003)
[3] Schulz et al; Optics Letters 31:769-771 (2006)

Molecular Imaging in Tissue and Cells by Computer-assisted Innovative Multimode Mass Spectrometry : COMPUTIS, a new European project

Coordinator email : serge.haan@cea.fr
Coordinator fax : +33 (0)1 69 08 95 29

Poster abstract: Introduction to the project

This project aims to develop new and improved technologies for **Molecular Imaging Mass Spectrometry** (**MIMS**), enabling innovative approaches in **functional genomics**, **proteomics** and **metabolomics**, as well as for investigation of **cells and tissues.**

Three objectives are considered as part of this proposal:
- Innovative **MS imaging instrumentation** through the application of novel desorption, ionisation and detection techniques,
- **Advanced diagnostic methods** for identifying diseases by study of molecular images,
- **Monitoring of therapeutic effects** on expression patterns of damaged and abnormal cells or tissues.

The proposed project is based on recent significant improvements in **desorption** and **ionisation** techniques such as **SIMS** (**S**econdary **I**on **M**ass **S**pectrometry) and **MALDI** (**M**atrix **A**ssisted **L**aser **D**esorption **I**onisation) associated with various mass analysers which offer an outstanding ability to **analyze organic molecules** as large as peptides or proteins at femtomole **sample amounts**.
These techniques are extrapolated to produce actual molecular images of flat specimen by mass spectrometry with a micrometric lateral resolution.

This project will provide **innovative analytical capabilities** for mapping a variety of biological compounds directly at the **tissue** or **cell level** by **superpositioning** information from different sources in the **same image.**
Thus **MIMS** is an extraordinary **new tool** which could lead to completely new analysis **concepts**.
In order to make it routinely accessible to users, it requires **appropriate instrumentation**, **sample preparation methodology** and **computerization** with high performance **massive data acquisition** and **processing.**

Application-driven developments of MIMS will be validated as part of this project by close **collaboration** of **pathologists**, **biologists**, **analytical chemists** and **informaticians**, to achieve the project objectives and lead to rapid **industrial** and clinical exploitation owing to the **active contribution** of the **SME** and **industrial** partners of the consortium.

Real time Bioluminescence Resonance Energy Transfer imaging in freely moving animals

Roncali E[1,2], Rogers KL[3], Picaud S[3], Boisgard R[1], Brûlet P[3] Maitrejean S[2], Tavitian B[1]

[1]*CEA, Service Hospitalier Frédéric Joliot ; Inserm, U 803, Imagerie de l'expression des gènes, Orsay, France.*

[2]*Biospace Mesures, France*

[3]*Unité d'Embryologie Moléculaire, CNRS URA 2578, Institut Pasteur, Paris, France*

Up to now, in vivo molecular imaging has been limited to anaesthetized or restrained animals and has not taken motion into account, although it is critically needed for behavioral studies in normal physiological conditions and dynamic signal transduction visualization.
In recent studies, the use of new Ca^{2+} sensitive Bioluminescence Resonance Energy Transfer (BRET) probes genetically encoded into transgenic animals has been demonstrated [1].
The millisecond time scale of these signaling pathways requires a device allowing real time optical imaging and providing a high time resolution in order to visualize bursts of calcium in whole living animals.

Here we present an upgrade of a photon counting system (Photon Imager) dedicated to bioluminescence, which allows to record simultaneously with a 40 ms time resolution the desired biological signal along with the video image of the animal. We use a special lighting, which does not disrupt the bioluminescence detection, and a beamsplitter to separate the bioluminescent signal from the one generated by the lighting. The video image is recorded by an additional CCD camera which is temporally synchronized with the intensified CCD camera dedicated to the bioluminescence.

We monitored local calcium transients in freely moving transgenic mice expressing the GFP-aequorin reporter protein and were able to correlate the bioluminescence signal taking place when calcium bursts occur to muscle contraction. The video movie and the bioluminescent sequence are co-registered at a video rate and a convenient exposure time can be chosen after the acquisition so that even very low bioluminescent signals can be detected.

The Video Imager system developed by Biospace Mesures enables bioluminescent signals in freely moving animals to be detected and spatially localized in the body.

For the first time an in vivo molecular modality provides the opportunity to perform non-invasive real time imaging in un-restrained or un-anaesthetized animals. Challenging studies like behavioral ones, and new applications of bioluminescent gene reporters are now greatly facilitated.

[1] Non-invasive *in vivo* imaging of Ca^{2+} signaling in live animals. Rogers KL[1], Picaud S[1], Roncali E[2], Boisgard R[2], Colasante C[1], Stinnakre J[1], Tavitian B[2], Brûlet P[1] (submitted)

LIST OF PARTICIPANTS

INDEX OF AUTHORS

A

B

C

D

H

I

J

K

L

M

N

O

P

Q

R

S